USE OF TIKHONOV REGULARIZATION IN

PRESSURE AND RATE TRANSIENT DERIVATIVE ANALYSIS FROM NOISY DATA

A Thesis

by

NATTAPON LORTONG

Submitted to the Office of Graduate and Professional Studies of
Texas A&M University
in partial fulfillment of the requirements for the degree of

MASTER OF SCIENCE

Chair of Committee,	Thomas A. Blasingame
Committee Members,	Peter Valkó
	Maria Barrufet
Head of Department,	Jeff Spath

December 2018

Major Subject: Petroleum Engineering

ABSTRACT

Use of the pressure derivative for pressure transient test analysis has been a crucial tool in the analysis of reservoir and well performance data since it was formally proposed by Bourdet, Ayoub, and Pirard in 1989. Despite the diagnostic advantage of using the pressure derivative for well test interpretation, the key drawback of the pressure derivative is its calculation. Bourdet et al. proposed a simple and very consistent numerical method to calculate the pressure derivative. This method is based on a weighted central-difference scheme. The so-called "Bourdet" algorithm is the most common pressure derivative calculation used in the petroleum literature. Even with its wide acceptance, the Bourdet pressure derivative calculation method has limitations, particularly for noisy data.

The goal of this work is to provide an alternate derivative calculation to the Bourdet method. The method we propose is Tikhonov Regularization. Tikhonov Regularization can be regarded as regression with the addition of a penalty term. The goal is to balance between goodness-of-fit and the roughness of fitted data to calculate a smooth derivative function from the result of regularization. In contrast to the Bourdet method, the regularization parameter can be calculated mathematically by generalized cross-validation and does not require manual manipulation from the analyst to determine the optimum regularization value.

This study includes the development and implementation of the Tikhonov Regularization method in order to calculate the pressure derivative using the MATLAB software program. We studied the effectiveness of the Tikhonov Regularization method for calculating the pressure derivative as compared to the Bourdet algorithm from this developed module. The effectiveness of derivative calculation is validated using both synthetic pressure data and field pressure data. We employ the

Root-Mean-Square (RMS) and Mean-Absolute-Error (MAE) as statistical measures of effectiveness.

Our results show that the Tikhonov Regularization method yields a significantly better derivative calculation than Bourdet method in all the cases in this study, particularly those cases with elevated levels of noise. Based on the results obtained in this study, we propose that the Tikhonov Regularization method should be used to calculate the pressure derivative for data cases exhibiting high levels of noise.

DEDICATION

To my father and mother who have always loved me unconditionally.

ACKNOWLEDGEMENTS

I would like to thank my advisor and committee chair, Dr. Tom Blasingame for guiding my studies at Texas A&M University. For his leadership throughout my time at the university, and for his extraordinary support when I was particularly challenged, I give my whole-hearted gratitude to Dr. Blasingame.

I would also like to thank Dr. Peter Valko and Dr. Maria Barrufet for their time and support to serve as the members of my committee. I would also like to extend my gratitude to Dr. David Craig for his support and the sharing the data from his work as these data provided a significant contribution to this research.

I also thank my graduate student colleagues, the faculty, and the staff at Texas A&M University for their contribution to make my time a great experience. I especially thank Ms. Eleanor Schuler for her support, assistance, and encouragement during my graduate studies.

Finally, I thank my family for their encouragement and continuous support — even when I am far away from home.

This work would not have been completed without the support of all of you. Thank you.

CONTRIBUTORS AND FUNDING SOURCES

This research was supervised by a thesis committee consisting of Dr. T. A Blasingame (advisor and committee chair), Dr. P. P. Valkó of the Department of Petroleum Engineering and Dr. M. A. Barrufet of the Departments of Petroleum and Chemical Engineering.

These graduate studies were supported by a scholarship from Chevron Thailand Exploration and Production Ltd.

The field data analyzed in this study were provided by Dr. David Craig of Reservoir Development Company/DFITpro.com.

All other work conducted for the dissertation was completed by the student independently.

TABLE OF CONTENTS

LIST OF FIGURES

LIST OF TABLES

TABLE Page

CHAPTER I

INTRODUCTION

1.1 Objectives

The overall objectives of this work are:

- To *validate* the applicability of computing the pressure derivative by use of a regularization method (in particular, the Tikhonov Regularization Method).
- To *compare* the results of computing the pressure derivative function using the Tikhonov Regularization Method as compared to the Bourdet pressure derivative method, specifically for different levels of noise in the raw data.
- To *apply* the Tikhonov Regularization Method to pressure transient test and rate transient (*i.e.*, production) data.

1.2 Statement of the Problem

1.2.1. Pressure Derivative

Reservoir pressure information has long been crucial for the diagnosis and analysis of well performance. Pressure data have been used to evaluate reservoir potential — which includes the amount of hydrocarbons in-place, the flow potential, and properties of the reservoir. Static pressure data (spot measurements) are used to estimate hydrocarbon volume in-place by material-balance methods. Dynamic (continuous) pressure data are used to assess reservoir properties; including properties such as permeability, skin, and reservoir boundaries.

Historically, pressure transient analysis methods relied on plots of pressure or pressure drop data as functions of time. Such methods include the classic Horner plot (Horner 1951) and various "type curves" (*e.g.*, Earlougher and Kersch 1974), but these methods suffer from the difficulty of

interpreting low resolution features in pressure and pressure drop data for the purpose of identifying specific flow regimes.

Bourdet, Ayoub, and Pirard (1989) formally proposed the pressure derivative to interpret and analyze pressure transient test data (instead of using pressure and pressure drop data). *The "pressure derivative" as used in reservoir engineering is the derivative of pressure with respect to natural logarithm of time or logarithm of superposition time.* The key advantage of the pressure derivative is ability to distinguish specific flow regimes, in general using the log-log plot. The major limitation of using the "pressure derivative" is the presence of data noise in the pressure data, where the effect of this noise is amplified by the differentiation process. The purpose of this work is to consider methods to develop a smooth pressure signal suitable for differentiation.

1.2.2. Bourdet Pressure Derivative Calculation

In order to utilize the pressure derivative plot, Bourdet et al. also proposed an algorithm to calculate pressure derivative from the base pressure (or pressure drop) data. The algorithm utilizes a simple weighted central difference derivative calculation which can be written mathematically as:

$$\left(\frac{dp}{dX}\right)_i = \frac{\left(\frac{\Delta p_1}{\Delta X_1}\right)\Delta X_2 + \left(\frac{\Delta p_2}{\Delta X_2}\right)\Delta X_1}{\Delta X_1 + \Delta X_2} \quad \text{.....(1)}$$

Bourdet algorithm is considered simple to implement but it has several limitation (Lane, Lee, and Watson 1991).

1. Bourdet et al. commented that the phenomena known as "end effects" can have a corruptive influence on the weighted difference formula (Eq. 1). This happens when calculating derivative at the data near starting or ending endpoints. A "pseudo-right" formulation is

proposed which uses the last point that meets the criteria $\Delta X_{1,2} \geq L$ to represent the interval at the end of data range.

2. The weighted difference pressure derivative calculation does not tolerate the presence of large "gaps" in the data function. Pressure data with large gaps often yield distorted pressure derivative functions that do not represent the underlying reservoir behavior.
3. Using a value of the spacing/smoothing factor (L) that is too small will yield a noisy derivative trend (the limit of a small value of L is a simple central difference), and the result of using an L-value that is too large is an "over-smoothed" pressure derivative function which does not give appropriate resolution to effects related to reservoir behavior.

The determination of an optimum L-value for the Bourdet derivative calculation is a practical challenge that has no simple solution. The most common range $0.1 < L < 0.3$ (where L is the fraction of a logarithm cycle) (Cheng, Lee, and McVay 2005), but the actual value used in analysis depends on the judgement of the analyst. Using a non-optimal L-value for the Bourdet derivative calculation can result in misleading shapes for pressure derivative curve, which in turn leads to the wrong interpretation of flow regimes.

To optimize the L-value, several strategies have been proposed. Cheng et al. (2005) suggested the use of the fast Fourier transform to evaluate pressure data in the frequency domain. We generally assume that the spectral energy of the mid- and high frequency ranges represents the noise in pressure data while the data in the low frequency range is the actual signature. In concept, the optimum L-value is that value which dampens the spectral energy in the mid- and high frequency ranges, yet has minimal impact on the low frequency range. However, there is no mathematical basis for how the noise can be fully suppressed, nor what level of noise is acceptable in the low frequency range. In short, the final judgement for the optimum L-value is at the discretion of the analyst.

1.2.3. Derivative Calculation by Tikhonov Regularization

The mathematical concept of regularization is the use of an additional term to optimize the solution — there are many classes of regularization in optimization problems. This research focuses on the method called *Tikhonov Regularization*. It is also known as "ridge regression" or "penalized least squares" (Stickel 2010).

In its simplest form, the regularization process can be viewed as regression with the addition of penalty term. Considering the normal regression concept, the goal is obtaining a fitted data trend with minimum deviation of the model to the measured data. This is called *goodness-of-fit*. Regularization adds the penalty term to the objective function for normal regression. In the case of Tikhonov regularization, this regularization or penalty term is *roughness*, where roughness is how smooth is the trend or, in other words, how fast the trend changes. Functions that have high roughness change rapidly when the independent variable changes. Mathematically, the rate of change is the derivative of function. Roughness in the Tikhonov regularization process is represented by a quadratic term in the derivative formulation. The derivative used in regularization can be of *any* order, but the most common formulation found in the literature is the second order derivative as this represents the curvature of the function.

Stickel (2010) demonstrates the mathematical formalization of Tikhonov regularization as follows: Goodness-of-fit is defined as:

$$\int_{x_1}^{x_N} [\hat{y}(x) - y(x)]^2 \, dx$$

Roughness is defined as:

$$\int_{x_1}^{x_N} \left[\hat{y}^d(x)\right]^2 dx$$

Where:

$$\hat{y}^d(x) = \frac{d^d \hat{y}}{dx^d}$$

Based on definition of the goodness-of-fit and roughness, the regularization objective function in linear algebra form is given as

$$Q = (\hat{\mathbf{y}} - \mathbf{y})^T \mathbf{B}(\hat{\mathbf{y}} - \mathbf{y}) + \lambda(\mathbf{D}\hat{\mathbf{y}})^T \tilde{\mathbf{B}}(\mathbf{D}\hat{\mathbf{y}})$$

Where $\mathbf{B}$ and $\tilde{\mathbf{B}}$ are the integration matrix. These matrices can be based on any integration rule in the literature such as the trapezoidal rule. The $\mathbf{D}$ matrix is the finite-difference differentiation matrix. The parameter λ is regularization parameter. This is the trade-off between goodness-of-fit and roughness when the analyst performs data analysis. The higher value of the regularization parameter (λ) yields a fitted data trend that is smoother. This is analogous to the L-parameter in the Bourdet derivative calculation. The goal in data analysis using Tikhonov regularization is to obtain the fitted data trend, $\hat{y}$, that minimizes Q for a given case of λ.

$\hat{\mathbf{y}}^*$ is defined as the fitted data trend that minimizes Q — thus we obtain:

$$\hat{\mathbf{y}}^* = \left(\mathbf{M}^T \mathbf{W}\mathbf{M} + \lambda \mathbf{D}^T \mathbf{U}\mathbf{D}\right)^{-1} \mathbf{M}^T \mathbf{W}\mathbf{y} \quad \text{.....(2)}$$

The derivative of fitted/smoothed data can be calculated using:

$$\frac{d\hat{\mathbf{y}}^*}{dx} = \mathbf{D}\hat{\mathbf{y}}^* \quad \text{.....(3)}$$

The detailed derivation of Tikhonov regularization procedure is found in Appendix A.

The result of the derivative calculation depends significantly on the regularization parameter. Selecting the optimum value of λ is critical to obtaining an appropriate and representative derivative calculation. There are many approaches that can be used to select the optimum value of λ — *e.g.,* trial and error (the same as for the Bourdet method) or something more statistically based such as generalized cross-validation (Eilers 2003, Lubansky et al. 2006, Stickel 2010).

For a given dataset of N pairs, the concept of this method is to calculate a smooth trend of data for specified λ. In each calculation, one of data points is removed from the calculation and the estimated for that data point is compared to the actual value. The summation of variance of each calculation for a given λ-value is obtained and defined as V_{GCV}. The λ-value that minimizes V_{GCV} is the optimum value for data smoothing by regularization (*i.e.*, λ_{opt}), derived from the generalized cross-validation process.

The direct calculation of λ_{opt} is an expensive calculation — however; there is analytical solution for determining $V_{GCV}(\lambda)$ based on Eq.4. (Eilers 2003, Lubansky et al. 2006, Stickel 2010).

$$V_{GCV}(\lambda_s) = \frac{\left(\mathbf{M}\hat{\mathbf{y}}^* - \mathbf{y}\right)^T \left(\mathbf{M}\hat{\mathbf{y}}^* - \mathbf{y}\right)/N}{\left[1 - tr(\mathbf{H})/N\right]^2} \quad \text{.....(4)}$$

Where:

$$\mathbf{H} = \mathbf{M}\left(\mathbf{M}^T\mathbf{W}\mathbf{M} + \lambda_s\delta^{-1}\mathbf{D}^T\mathbf{U}\mathbf{D}\right)^{-1}\mathbf{M}^T\mathbf{W}$$
$$\delta = \frac{tr\left(\mathbf{D}^T\mathbf{D}\right)}{N^{d+2}}$$
$$\lambda = \lambda_s\delta^{-1}$$

A few comments regarding Tikhonov regularization as compared to the Bourdet method:

1. The end effect in the Tikhonov regularization method is less than that observed for the Bourdet method as the Bourdet method requires a specified minimum distance in terms of a fraction of a log cycle, and the regularization approach does not have such limitations.

2. The Tikhonov regularization method utilizes a functional form to represent the smoothed data and as such, data "gaps" have less (or little) impact on the computed pressure and pressure derivative trends.

To our knowledge, the Tikhonov regularization method has not been reference or used in the petroleum engineering literature. One of the most common references for the use of the Tikhonov regularization method is in Chemistry where it is used to smooth, diagnose, and analyze experimental data. In our present work, we seek to validate/demonstrate the Tikhonov regularization method using pressure (and pressure drop) data for the purpose of diagnostic analysis of pressure transient data. As a process, we will compare results from the Bourdet and Tikhonov regularization methods. We also discuss the implementation of the Tikhonov regularization method in MATLAB.

1.3 Pressure Transient Basic Concept and Dimensionless Variables

The concept of pressure transient analysis and dimensionless variables are applied throughout this thesis. In fact, they are fundamental concept which requires the development of numerical analysis in this work. We summarize the background in this section for completeness.

1.3.1. Pressure Drawdown Test

The fundamental concept of pressure drawdown test is based on constant terminal rate solution. This solution describes how bottom hole flowing pressure of the well changes with time when the well is produced with constant rate. The situation of pressure drawdown test is illustrated in **Fig. 1**.

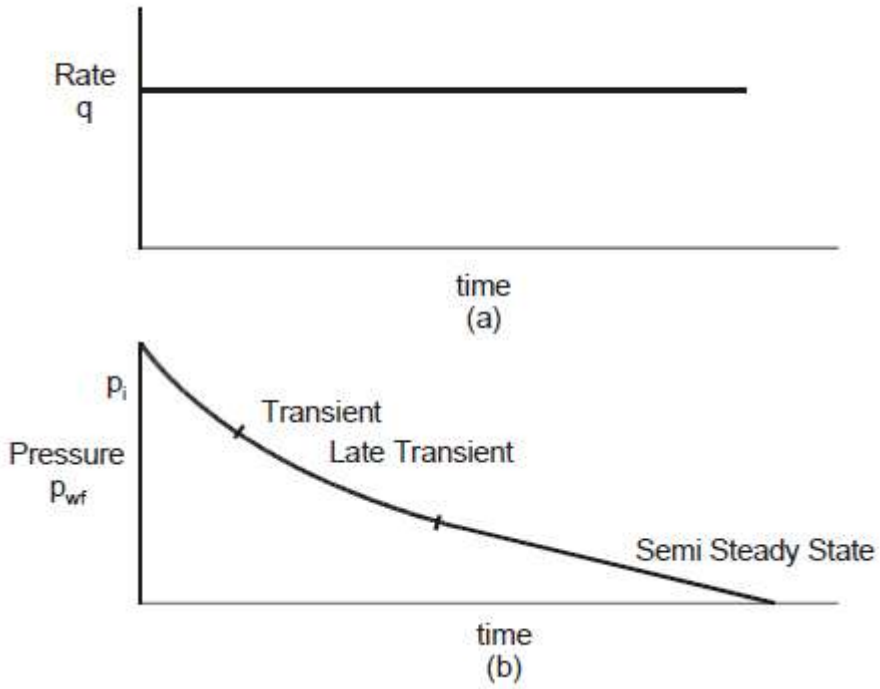

Fig. 1 — Pressure drawdown test; (a) constant production rate (b) Bottom hole Flowing pressure (Reprinted from Dake, 1978)

The mathematical detail behind constant production rate solution will be discussed in literature review section. Based on the plot of pressure with time, flow behavior can be divided into three periods which are transient flow, late transient flow and semi-steady state. Transient flow period is the duration that pressure response from the reservoir is not impacted from boundary condition. When boundary condition fully dominates the pressure response, the pressure response becomes semi-steady state meaning that the rate of pressure change is constant. With known analytical solution of pressure as function of time, the pressure measurement from pressure drawdown test can be used to analyze and obtain reservoir properties such as permeability.

1.3.2. Dimensionless Variables

Dimensionless variables are often used to express analytical solution in petroleum engineering literature due to its convenience. Unit of each variable has no impact in mathematical analysis

when dimensionless variable is used. The most common dimensionless variables found in petroleum engineering literature are following.

Dimensionless radius: r_D.

$$r_D = \frac{r}{r_w}$$

Dimensionless time: t_D.

$$t_D = \frac{kt}{\phi \mu c_t r_w^2}$$

Dimensionless pressure: p_D.

$$p_D = \frac{2\pi kh}{q\mu}\left(p_i - p\right)$$

The dimensionless variables presented here are general form with consistent units. The author notes that there are many forms of dimensionless variables in petroleum engineering literature. Some of dimensionless variable have constant factor multiplied to the group of variables to adjust for units such as field units. In addition, in some development, the definition of dimensionless variables can be changed corresponding to physical model such as in fracture well.

1.3.3. Superposition Theorem

Definition of superposition theorem can be described as any sum of individual solutions of a second order linear differential equation is also a solution of the equation (Dake 1978). Since reservoir fluid flow solution falls into this category, we can apply this theorem to solve fluid flow problem in reservoir. In practice, we can consider situation in **Fig. 2** as example. A well is produced at sequence of constant production rate. To determine bottomhole flowing pressure at

time t_n, we do not have to develop new flow solution to this specific problem. The superposition theorem can be applied to consider the well which is first produced at rate q_1 for duration t_n. After that, the well is produced at $q_2 - q_1$ for duration $t_n - t_1$. This method can be applied until the analysis reach last step of production rate. Then, the overall effect of production rate can be linearly summed to obtain bottomhole flowing pressure at time t_n.

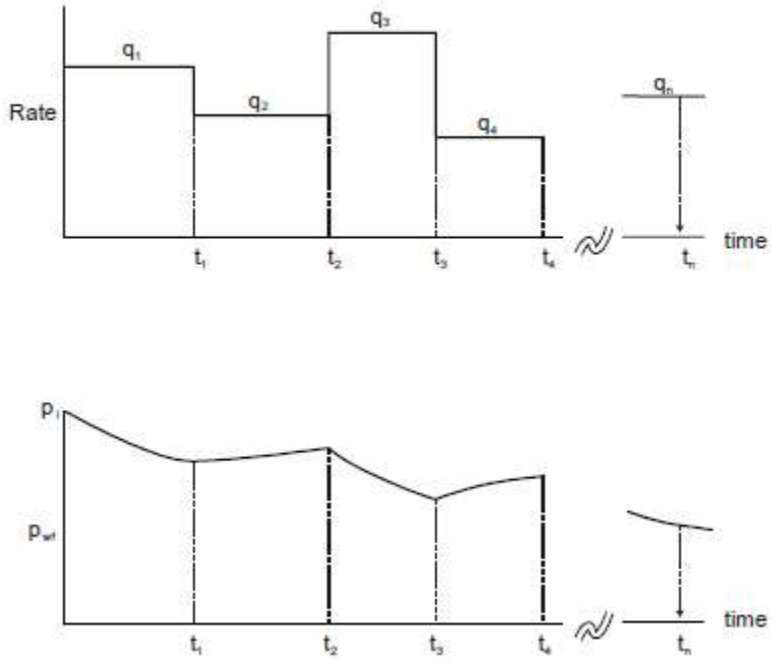

Fig. 2 — Production history of a well with multiple constant production rate and pressure and function of time (Reprinted from Dake, 1978)

1.3.4. Pressure Build Up Test

Pressure build up is likely to be most common pressure transient test method (Dake 1978). The production rate and pressure response of pressure build up test is illustrated in **Fig. 3**.

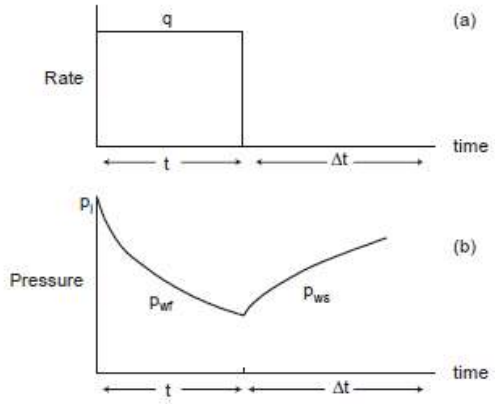

Fig. 3 — Pressure build up test; (a) production rate (b) Bottom hole pressure (Reprinted from Dake, 1978)

In pressure build up test, the well had been put on production for a period and then shut in. Pressure response during shut in period is used for reservoir properties analysis. Superposition theorem is applied in this case since the situation can be regarded as multiple production rate. When the well is shut in, production rate is zero.

CHAPTER II

LITERATURE REVIEW

The purpose of this chapter is to provide a brief concept of pressure transient analysis, pressure transient analysis development history including application of pressure derivative in the analysis, and available methods of pressure derivative calculation in petroleum engineering literature.

2.1 Pressure Transient Analysis History

Pressure transient testing involves the introduction of changes into the reservoirs via one or more wells and observe how the reservoirs react to the perturbation. Typically, the changes introduced into the system is production or injection rate and transient pressure is monitored. The result from the test is then matched with engineering model to interpret the desired result. Generally, the objectives of pressure transient test are determination of reservoir and well properties. These properties can be obtained quantitatively from the test. They include permeability or conductivity of the reservoir within the drainage area of the tested wells, average reservoir pressure, conditions of wellbore and near wellbore region (skin), and reservoir configuration within drainage area (shape and size).

Pressure transient analysis study field began in 1930s (Ramey 1982). Moore (1933) published the article about determination of reservoir permeability from pressure transient data. The article is considered one of the first publication in the field of pressure transient analysis.

Van Everdingen and Hurst (1949) published the article regarding the solution to diffusivity equation in Eq.55 for unsteady state flow in the reservoir.

$$\frac{\partial^2 p}{\partial r^2}+\frac{1}{r}\frac{\partial p}{\partial r}=\frac{\partial p}{\partial t} \quad \text{.....(5)}$$

The authors proposed the solutions for two inner boundary conditions in the article which are the constant terminal pressure case and the constant terminal rate case. In constant terminal pressure case, the pressure at inner boundary is assumed to be constant when time is more than zero and the solution seeks the rate as function of time. Constant terminal rate case, on the other hand, the fluid rate is assumed to be constant and the solution seeks pressure as function of time. For outer boundary conditions, the author considered the cases for infinite reservoir, constant pressure boundary, and no flow boundary.

With the help of Laplace transformation to solve the partial differential equation, the solutions for each case are obtained. For the case of constant terminal rate condition and infinite acting reservoir, the solution in is in Eq.6.

$$p_D\left(r_D,t_D\right)=\frac{2}{\pi}\int_0^{\infty}\frac{\left(1-e^{-u^2t_D}\right)\left[J_1(u)Y_0\left(ur_D\right)-J_0(u)Y_1(u)\right]}{u^2\left[J_1^2(u)+Y_1^2(u)\right]}du \quad \text{.....(6)}$$

With the assumption of line source inner boundary condition and large time approximation, Eq.6 can be simplified to be Eq.7 or Eq.8 where $r_D=1$.

$$p_D=-\frac{1}{2}Ei\left[-\frac{1}{4t_D}\right] \quad \text{.....(7)}$$

$$p_D=\frac{1}{2}\left[\log t_D+0.809007\right] \quad \text{.....(8)}$$

The original purpose of the article is estimating the water influx into reservoir for material balance calculation. However, Eq.8 shows that by plotting bottomhole pressure versus time when the well is produced at constant rate, straight line would be obtain on semi-log scale. Based on this trend, reservoir properties can be calculated. The application of this equation becomes the fundamental

knowledge in reservoir pressure transient analysis. The detail analysis of each solutions can be found in original article including the solutions for other cases.

Van Everdingen and Hurst also explored the concept which is later known as wellbore storage. They incoporated the effect of liquid produced from well annulus into pressure drawdown analsis. The term in Eq.999 describes the production rate that is impacted from liquid in annulus and is used to correct the production rate in pressure drawdown test where C is the volume of fluid unloaded from the annulus per unit bottomhole pressure per thickness of the reservoir.

$$q(\Delta t) = C\frac{d\Delta p}{dt} \quad \text{.....(9)}$$

Horner (1951) published the study relating to pressure build up analysis. The study indicates that build up pressure should be plot with logarithm of ratio of time. The ratio of time is defined as total producing duration plus shut in duration divided by shut in duration. The plot produces straight line and the slope can be related to reservoir permeability.

Van Everdingen (1953) introduced the concept of skin. Skin effect was defined as additional pressure drop in the vicinity area surrounding the wellbore due to a reduction in permeability. Permeability reduction can be a result of drilling, completion and production operations. This concept was used to explain additional pressure drop when the analysis such as pressure build up plot cannot explain the additional pressure drop around wellbore when the pressure trend is calculated from known reservoir properties. Pressure drop from skin is quantified in term of dimensionless pressure drop by Eq.10.

$$\Delta p_{skin} = \frac{141.2qB\mu}{kh}s \quad \text{.....(10)}$$

The literature of pressure transient analysis continued expanding during this point in time. However, the development was centered around the concept mentioned earlier. The analysis is mainly based on semi log straight line of pressure plot with function of time. The analytical equations were developed based on diffusivity equation, wellbore storage and skin concept to determined desired reservoir properties.

Despite its benefits, straight line plot has one major drawback which is the distortion of the plot from wellbore storage and skin effect. In some cases, the correct straight-line period cannot be identified or the information from early time in the test cannot be used. Type curve matching method for pressure transient analysis was developed to overcome this issue.

Ramey (1970) introduced the log-log type curve with the concept behind from definition of dimensionless time (t_D) and dimensionless pressure (p_D) in field unit.

$$t_D = \frac{0.00264kt}{\phi\mu c_t r_w^2} \quad \text{.....(11)}$$

$$p_D = \frac{kh\left(p_i - p_{wf}\right)}{141.2qB\mu} \quad \text{.....(12)}$$

By taking logarithm of dimensionless time and dimension pressure, we obtain

$$\log\left(t_D\right) = \log\left(\frac{0.00264k}{\phi\mu c_t r_w^2}\right) + \log\left(t\right) \quad \text{.....(13)}$$

$$\log\left(p_D\right) = \log\left(\frac{kh}{141.4qB\mu}\right) + \log\left(p_i - p_{wf}\right) \quad \text{.....(14)}$$

Eq.11 - 14 indicates that log-log plot of dimension pressure versus dimensionless time and plot of real pressure and time have the same shape with constant difference between two coordinates. The difference can be used to calculate reservoir properties.

There are many type curves developed in the literature, but they are all based on this concept. The factors that greatly impact the shape of type curve is wellbore storage and skin. Agarwal, Al-Hussainy, and Ramey (1970) established the log-log type curve between dimensionless pressure and dimensionless time. The curves are generated from analytical solution for constant rate drawdown test. Each curve represents one pair of dimensionless wellbore storage and skin factor. McKinley (1971) published type curve for pressure build up test. The curve is generated from finite different model combined with analytical solution. In this type curve, shut in time is plotted against pressure build up group which is defined as $\frac{5.61C\Delta p}{Bq}$. For each curve, the value is calculated for specific value of transmissivity group which is defined as $\frac{kh}{5.61\mu C}$. The skin factor is assumed to be zero for this type curve.

Earlougher et al. (1974) proposed the plot of type curve between $\frac{p_D C_D}{t_D}$ and $\frac{1}{0.000295}\frac{t_D}{C_D}$. The equations used for type curve generation are the same as Agarwal et al. However, they are plotted with different group of dimensionless variables. In addition, Earlougher et al. grouped the dimensionless wellbore storage and skin factor together as one dimensionless variable. Each curve is created for group of $C_D e^{2s}$. Since skin factor is in the form of dimensionless pressure, total dimensionless pressure is the linear sum of Eq. 8 and skin factor. Eq. 8 can be written as Eq. 15 to consider of pressure drop from skin. Therefore, each curve that has same value of $C_D e^{2s}$ can be group together based on Eq. 15.

$$p_D = \frac{1}{2}\left[\log\frac{t_D}{C_D} + 0.809007 + \ln\left(C_D e^{2s}\right)\right] \quad \text{.....(15)}$$

Gringarten et al. (1979) published the new type curve. It is plotted between p_D and $\frac{t_D}{C_D}$. The type curve is also calculated from the same analytical solution as Agarwal et al.'s. Each curve is also characterized by $C_D e^{2s}$.

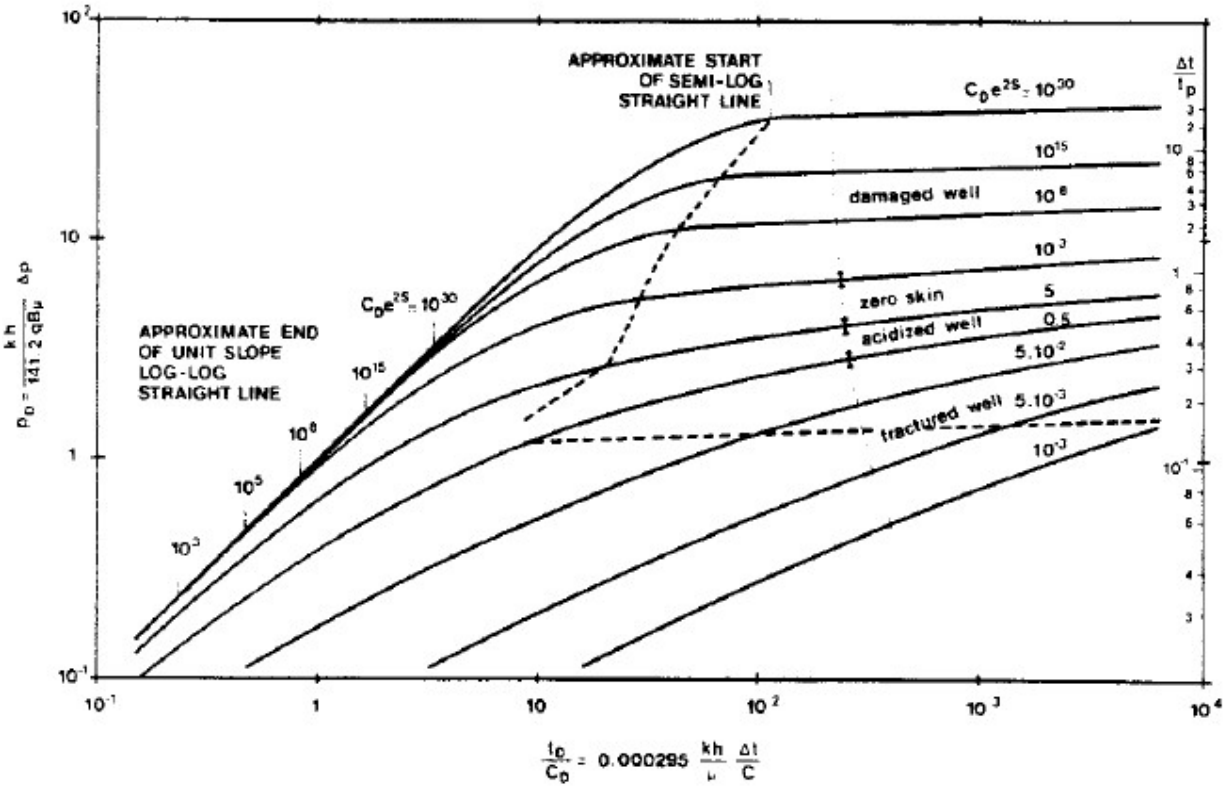

Fig. 4 — Type-curve for wellbore storage and skin effect (Reprinted from Gringarten et al., 1979)

Despite its benefit of analyzing short term well test by considering wellbore storage and skin effect, defining the correct portion of pressure plot to match with type curve is still challenging. Bourdet et al. (1989) published the new article recommending new interpretation method to use pressure derivative instead of pressure to analyze pressure transient test. Pressure derivative is a derivative

of pressure with respect to natural logarithm of time or superposition time. When pressure derivative is used to generate type curve, the signature of different flow regime is amplified. Thus, it is more convenient to match the pressure transient test result with type curve.

2.2 Pressure Derivative

Bourdet et al. (1989) defined pressure derivative as derivative of pressure with respect to natural logarithm of time or superposition time. In dimensionless term, it can be written as Eq.16 where p'_D is pressure derivative.

$$p'_D = \frac{dp_D}{d\ln t_D} = t_D \frac{dp_D}{dt_D} \quad \text{.....(16)}$$

Taking Eq. 8 as example for infinite acting reservoir case, the pressure derivative can be written as

$$p'_D = t_D \frac{d}{dt_D}\left[\frac{1}{2}\left[\log t_D + 0.809007\right]\right] = 0.5 \quad \text{.....(17)}$$

Eq. 17 shows that plot of pressure derivative on log-log scale result in constant value at 0.5 for infinite acting flow regime. Comparing to pressure plot on log-log scale, the infinite acting flow regime would be straight line. The beginning of straight line period on log-log plot is typically difficult to be identified. With the assist of pressure derivative plot, it is more convenient to identify the flow regime since it is constant value. Pressure derivative plot also exhibits unique characteristic for other flow regimes resulting from well and reservoir physical configuration. This leads to key benefit of applying both pressure and pressure derivative plots in pressure transient analysis to identify correct reservoir behavior.

Bourdet et al. (1989) also generated the new type curve based on pressure derivative plot. It is plotted between $\frac{t_D}{C_D}\frac{dp_D}{dt_D}$ which is pressure derivative and $\frac{t_D}{C_D}$. Each curve is also characterized by $C_D e^{2s}$. The type curve is shown in **Fig. 5**.

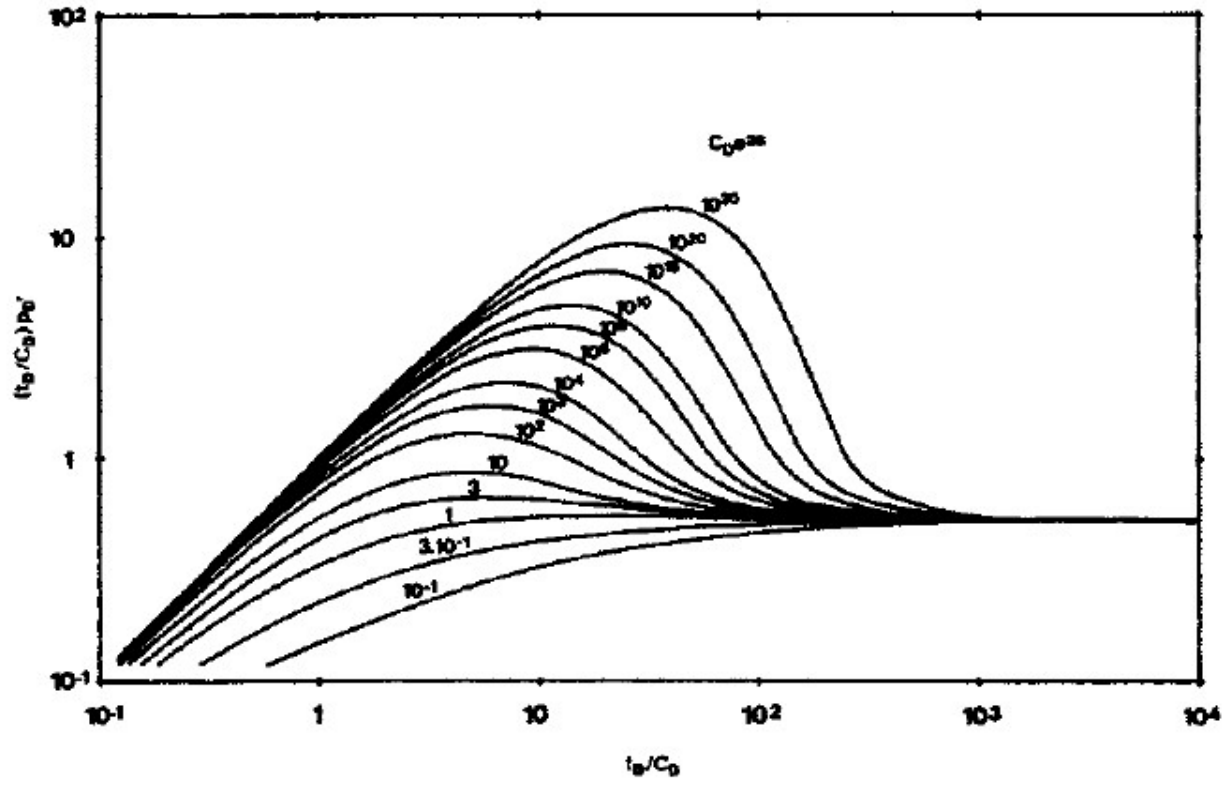

Fig. 5 — Derivative type curve for homogeneous reservoir (Reprinted from Bourdet et al., 1989)

2.3 Pressure Derivative Calculation

Pressure derivative has one main limitation which is the difficulty of derivative calculation from pressure measurement. The pressure measurement is always associated with noise. Differentiation process increases the noise to signal ratio. This can cause the challenge in analysis since it can distort the shape of pressure derivative plot.

Bourdet et al. also proposed an algorithm to calculate pressure derivative from pressure data. The algorithm utilizes central difference derivative calculation at point i and weighted average by distance of point i from X_1 and X_2 where X_1 is the point before X_i and X_2 is the point next to X_i. X_i represents natural logarithm of time function. This can be written mathematically in Eq. 1. which is re-written here.

$$\left(\frac{dp}{dX}\right)_i = \frac{\left(\frac{\Delta p_1}{\Delta X_1}\right)\Delta X_2 + \left(\frac{\Delta p_2}{\Delta X_2}\right)\Delta X_1}{\Delta X_1 + \Delta X_2}$$

Bourdet pointed out that when consecutive points are used for Eq. 1 calculation, derivative points become noisy and cannot be used for interpretation. It is proposed to consider the points further away from X_i with minimum distance of L. This can reduce noise effect to derivative calculation. Therefore, Eq. 1 is used for $\Delta X_{1,2} \geq L$. This method is illustrated in **Fig. 6**.

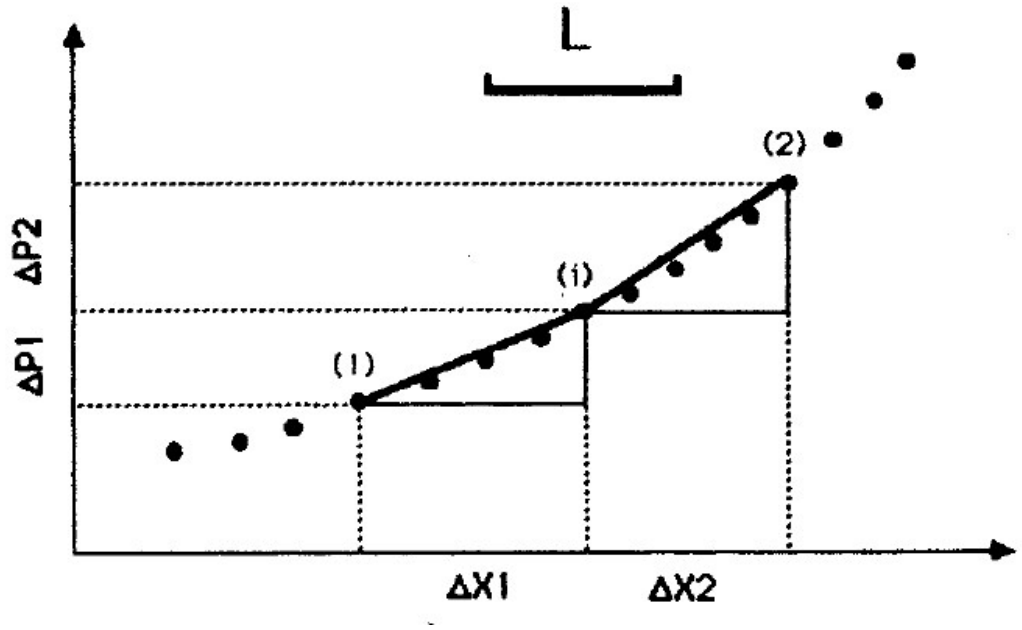

Fig. 6 — Bourdet differentiation algorithm (Reprinted from Bourdet et al., 1989)

Lane et al. (1991) proposed alternative method to calculate pressure derivative from measured pressure data. They pointed out that Bourdet algorithm is considered simple to implement but it has several limitations.

1. It is pointed out by Bourdet et al. for the phenomena called end effects. This happens when calculating derivative at the data near early time or late time that cannot satisfy $\Delta X_{1,2} \geq L$ condition. "Pseudo right" is used as a solution for end effect. It uses the last point that meet the criteria $\Delta X_{1,2} \geq L$ to represent the remaining interval closer to the end of data range.
2. The pressure derivative calculation considers only local value of data. This creates problem when there is missing data or data with wide gap. The shape such as peak of the trend can be distorted.
3. Pressure derivative calculated from this method can still be noisy even after high value of smoothing factor (L). If L value is increased too high, it can result in distorted shape of pressure derivative trend. Some characteristic necessary for analysis can be missing.

Lane et al. proposed to use spline approximation to calculate pressure derivative as alternative for Bourdet method. Spline is a combination of piecewise polynomial function with every two consecutive segments intersecting smoothly. The connected point between two segments is called knot. There are many classes of spline functions. The most common one is called B splines which are the combination of linearly independent spline element. For a defined domain $a \leq X \leq b$ with k interior knots at location $X = y_j$ for j = 1, 2, …k, the B splines function $S\left(X\right)$ can be defined in Eq. 18.

$$S\left(X\right) = \sum_{j=1}^{m+k} C_j B_j^m \left(X, \mathbf{y}\right) \quad \text{.....(18)}$$

Where m is order of B splines function, C_j is spline coefficient, and $\mathbf{y}$ is a vector containing locations of knots. The order of B splines depends on chosen degree of polynomial where order of the splines is one plus polynomial degree. B_j^m can be determined by specifying m and $\mathbf{y}$.

To fit splines function to measured pressure data, the order of splines function and locations of knots must be specified. Spline coefficient, C_j, can be determined from least square method represented in Eq. 19.

$$C_j^* = \underset{C_j}{\arg\min} \sum_{i=1}^{n_p} \left[p_i - S\left(X_i, C_j\right) \right]^2 \quad \text{.....(19)}$$

C_j^* is optimum value of spline coefficient that minimize the least square error between measured pressure data and splines fitted pressure function. n_p is number of pressure points available. Since order of splines and knot location and number must be specified to evaluate Eq. 19, finding absolute minimum of this equation is difficult and depends largely on initial guess.

Lane et al. recommended that quartic splines (m = 5) is appropriate for well test pressure data since second derivative of quartic spline is parabolic function which provides smoothness in type curve matching. The authors also provided algorithm to determine optimum knot locations and number. To find optimum knot locations and number, iterative evaluation of Eq. 19 is performed starting from one knot. The knots are added by one at a time. Statistical F test is applied to determine if knot adding should be stopped. The authors noted that using statistical F test is not mathematically rigorous, but it is sufficient for pressure derivative analysis. Two examples of pressure derivative analysis were evaluated by splines method and Bourdet method. The authors showed that splines method has better result for pressure derivative calculation.

Escobar, Navarrete, and Losada (2004) evaluated performance of different algorithms to calculate pressure derivative. The algorithms include Bourdet, Clark and Van Golf-Racht, Simons, Horne, Spline, and Polynomial. The article did not discuss any detail of each method used in evaluation. The authors applied each algorithm to calculate pressure derivative from synthetic data and noise based on eight different petroleum engineering solution. They concluded that Spline algorithm is the best method for pressure derivative calculation.

Cheng et al. (2005) studied the method to determine optimum window size to calculate pressure derivative by Bourdet method (L value). There is no common method to determined optimum L value for Bourdet pressure derivative calculation although it is standard method for pressure transient analysis. Analysts often use the range between 0.1 to 0.3 log cycle for the calculation. Cheng et al. proposed to use fast Fourier transform to evaluate pressure data in frequency domain to determine optimum level of smoothing. Fast Fourier transform of $x(t)$ that is function of time can be defined in Eq.20 and it can be inversed back from frequency domain to time domain by Eq. 21.

$$\tilde{x}(f) = \int_{-\infty}^{\infty} x(t) e^{-i2\pi ft} dt \quad \text{.....(20)}$$

$$x(t) = \int_{-\infty}^{\infty} \tilde{x}(f) e^{i2\pi ft} df \quad \text{.....(21)}$$

$\tilde{x}(f)$ is Fourier transform of $x(t)$. Since pressure data is measured as discrete points, Eq.20 and Eq. 21 must be modified for discrete data. Fourier transform for discrete data is shown in Eq. 22 and Inverse Fourier transform is shown in Eq. 23.

$$\tilde{x}(k\Delta f) = \Delta t \sum_{n=0}^{N-1} x(n\Delta t) e^{-i2\pi\Delta f n\Delta t} \quad \text{.....(22)}$$

$$x(n\Delta t) = \Delta f \sum_{n=0}^{N-1} \tilde{x}(k\Delta f) e^{i2\pi\Delta f n\Delta t} \quad \text{.....(23)}$$

In discrete Fourier transform equations, N is number of data points, n is time index ($n = 0,1,2,\ldots N-1$), k is frequency index ($k = 0,1,2,\ldots,N-1$), Δt is time interval between data points, and Δf is frequency interval ($\Delta f = 1/N\Delta t$). When data is transferred to frequency domain, they become complex number which can be represented as magnitude and phase in polar coordinate form.

Cheng et al. defined two parameters to determine optimum L value in frequency domain which are total energy factor (I_1) in Eq. 24 and low-frequency deviation factor (I_2) in Eq. 25.

$$I_1(L) = \sqrt{\sum_{j=0}^{N/2} \left[\left| \tilde{x}(f_j) \right|_L - \left| \tilde{x}(f_j) \right|_{L=0} \right]^2} \quad \text{.....(24)}$$

$$I_1(L) = \sqrt{\sum_{j=0}^{s} \left[\left| \tilde{x}(f_j) \right|_L - \left| \tilde{x}(f_j) \right|_{L=0} \right]^2} \quad \text{.....(25)}$$

$\left| \tilde{x}(f_j) \right|_L$ is magnitude of pressure derivative calculated by specified L value and transformed to frequency domain of frequency component j. $N/2$ is the Nyquist frequency which is the highest frequency component of the wave form. s is the frequency index that define low frequency location. This can be determined graphically to determine the frequency index that pressure derivative in frequency domain starts to oscillate.

Eq. 24 and Eq. 25 development is based on the concept that spectral energy of mid- and high frequency range representing the noise in pressure data while the value in low frequency range is actual information. The optimum L value is the value that damps the spectral energy in mid- and high frequency range the most with minimum impacts to low frequency range. Total spectral energy is represented by Eq. 24 and the impact to low frequency range is represented by Eq. 25. By calculating pressure derivative at various Bourdet Lvalues, the relationship between I_1, I_2 and L can be established. This is illustrated in **Fig. 7**. Analysts can determine optimum $L$by considering the value that significantly reduces total energy factor but not significantly increases low-frequency deviation factor.

Veneruso and Spath (2006) published the article regarding digital pressure derivative calculation. The concept of this method is fundamentally the same as Cheng et al.'s. Pressure derivative is transformed into frequency domain and filtered to determine useful information from noise component.

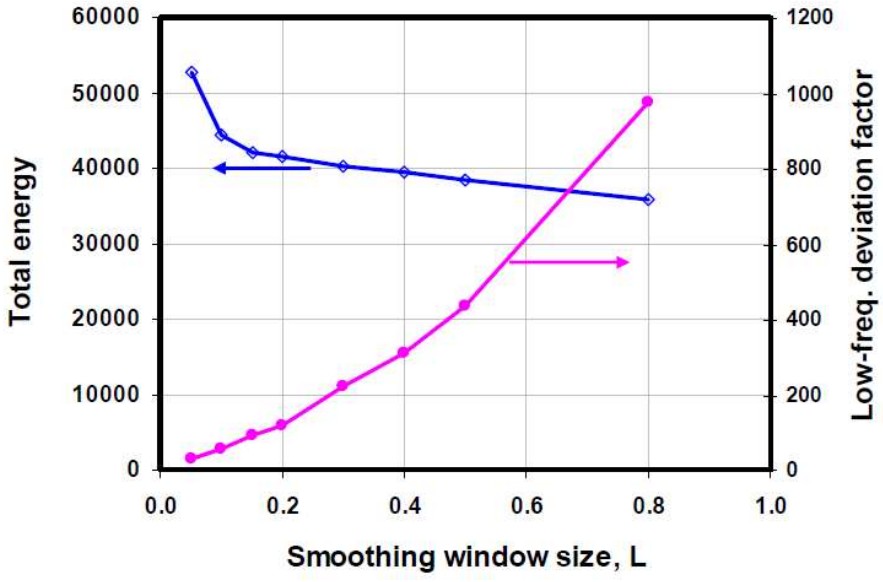

Fig. 7 — Optimum Bourdet Lvalue determination (Reprinted from Cheng et al., 2005)

2.4 Tikhonov Regularization

Eilers (2003) introduced new method to calculate smoothed trend from experimental data in Chemistry literature. His method was called discrete penalized least square method. The author proposed this method as alternative to Savitzy-Golay smoother (SGS) which is common method for data smoothing in Chemistry circle. Eilers described the algorithm to calculate smoothed data trend as the compromise between data fidelity and roughness of fitted data. Fidelity is how good the smoothed data fitted with experimental data. Roughness of fitted data is how smooth the curve is. The objective of penalized least square method is minimizing both values with specified factors to each term. The factors in the calculation can be determined by many methods including analyst judgement. Eilers proposed to use generalized cross-validation method to determine optimum value of these factors for smoothing. Although Eilers called this method penalized least square, it is conceptually the same as Tikhonov Regularization. To author of this work's knowledge, this was the first time Tikhonov Regularization introduced to scientific literature outside Statistics and Mathematics literature. Mathematical detail development of the algorithm will be discussed in next section.

Lubansky et al. (2006) published the article about computing derivative of experimental data. The authors proposed to use Tikhonov Regularization for derivative calculation. In this work, same mathematical concept is applied to interpret experimental data as in Eilers' work. However, Tikhonov Regularization application is extended from smoothing data trend to include derivative calculation. Lubansly et al. compared the result between derivative calculated from Tikhonov Regularization and Savitzy-Golay method with many data sets. The examples include both synthetic data and experimental data. They showed that Tikhonov Regularization can provide reliable derivative calculation.

Stickel (2010) published the article regarding data smoothing and derivative calculation by Tikhonov Regularization. He described regularization as regression with the addition of penalty term. Considering normal regression concept, the goal is obtaining the fitted data trend with minimum deviation of fitted data from measured data. This is called *goodness-of-fit* which is same as data fidelity described by Eilers. Regularization adds the penalty term to that objective of normal regression. In the case of Tikhonov regularization, this regularization or penalty term is *roughness*. Roughness is how smooth is the trend or, in other words, how fast the trend changes. Functions that have high roughness change rapidly when independent variable changes. Mathematically, the rate of change is derivative of function. Roughness in Tikhonov regularization is represented by quadratic term of derivative. The derivative used in this regularization can be any order but the most common found in literature is second order derivative since it represents the curvature of the function.

Stickel demonstrated the mathematical formalization of Tikhonov regularization per following.

Goodness-of-fit is defined as

$$\int_{x_1}^{x_N} \left[\hat{y}(x) - y(x)\right]^2 dx$$

Roughness is defined as

$$\int_{x_1}^{x_N} \left[\hat{y}^d(x)\right]^2 dx$$

where

$$\hat{y}^d(x) = \frac{d^d \hat{y}}{dx^d}$$

Based on definition of goodness-of-fit and roughness, the regularization objective function in linear algebra form as

$$Q = (\hat{\mathbf{y}} - \mathbf{y})^T \mathbf{B}(\hat{\mathbf{y}} - \mathbf{y}) + \lambda(\mathbf{D}\hat{\mathbf{y}})^T \tilde{\mathbf{B}}(\mathbf{D}\hat{\mathbf{y}})$$

$\mathbf{B}$ and $\tilde{\mathbf{B}}$ are integration matrix. They can be based on any integration rule in the literature such as trapezoidal rule. $\mathbf{D}$ is finite difference differentiation matrix. The parameter λ is regularization parameter. This is the trade-off between goodness-of-fit and roughness when the analyst performs data analysis. The higher value of regularization parameter would give the fitted data trend that is smoother. This is like L value in Bourdet derivative calculation. The goal in data analysis is to obtain the fitted data trend, $\hat{y}$, that minimize Q for a given case of λ. Note that this mathematical concept is the same as application in Eilers' and Lubansky et al.'s works.

Define $\hat{\mathbf{y}}^*$ as the fitted data trend that minimize Q and we obtain

$$\hat{\mathbf{y}}^* = \left(\mathbf{M}^T \mathbf{W}\mathbf{M} + \lambda \mathbf{D}^T \mathbf{U}\mathbf{D}\right)^{-1} \mathbf{M}^T \mathbf{W}\mathbf{y}$$

Then, the derivative of fitted smoothed data can be calculated from

$$\frac{d\hat{\mathbf{y}}^*}{dx} = \mathbf{D}\hat{\mathbf{y}}^*$$

The detail derivation of Tikhonov regularization can be found in Appendix A.

The result of derivative calculation depends greatly on regularization parameter. As you can observe that the regularization parameter is an analogy to L in Bourdet method. Selecting optimum value of λ is critical to obtain good result of derivative calculation. There are many methods to select optimum value of λ. This can be trial and error same as Bourdet method. However, the most common method to determine optimum regularization parameter is generalized cross-validation (Eilers 2003, Lubansky et al. 2006, Stickel 2010).

For the dataset of N pairs, the concept of this method is calculating N smooth trend of data for specified λ. In each calculation, one of data point is left out. The calculated data point at the left-out position is then compared to the actual left-out data. The summation of variance of each calculation for given λ is obtained and defined as V_{GCV}. The λ that minimizes V_{GCV} is the optimum value for data smoothing by regularization (λ_{opt}) based on generalized cross-validation.

The direct calculation of λ_{opt} is calculation expensive. However, there is analytical solution for determining $V_{GCV}(\lambda)$ based on Eq.4 which is rewritten below (Eilers 2003, Lubansky et al. 2006, Stickel 2010). The optimum λ is the one that minimize V_{GCV} which can be calculated numerically.

$$V_{GCV}(\lambda_s) = \frac{\left(\mathbf{M}\hat{\mathbf{y}}^* - \mathbf{y}\right)^T \left(\mathbf{M}\hat{\mathbf{y}}^* - \mathbf{y}\right)/N}{\left[1 - tr(\mathbf{H})/N\right]^2}$$

Where

$$\mathbf{H} = \mathbf{M}\left(\mathbf{M}^T\mathbf{W}\mathbf{M} + \lambda_s\delta^{-1}\mathbf{D}^T\mathbf{U}\mathbf{D}\right)^{-1}\mathbf{M}^T\mathbf{W}$$

$$\delta = \frac{tr\left(\mathbf{D}^T\mathbf{D}\right)}{N^{d+2}}$$

$$\lambda = \lambda_s\delta^{-1}$$

CHAPTER III

TIKHONOV REGULARIZATION IMPLEMENTATION AND VALIDATION

3.1 Implementation Work Flow

In this section, we present our workflow to implement Tikhonov regularization. The implementation is performed in MATLAB.

1. Data input into MATLAB. The input data includes independent and dependent variables from measurements. The only requirement is that the independent variable must be monotonic. Time-series analyses involves time as the independent variable and in physical processes, time is always increasing — hence this condition satisfies the regularization requirement. For this work, the spacing of independent variable (time) does not need to be equal (i.e., this approach permits unequally (even randomly) spaced measurements).
2. Differentiation matrix and anti-differentiation matrix construction. The differentiation matrix which is specified as D in the objective function is constructed based on a matrix of finite-differences. The input for the construction of matrix D is based on the independent variable vector obtained from step 1. The anti-differentiation matrix which is specified as B (and $\tilde{B}$) is also constructed from the independent variable vector. In this work, we apply the trapezoidal rule to create the anti-differentiation matrix. The mathematical detail for differentiation and antidifferentiation matrix is discussed in Appendix B.
3. Evaluation of the optimum regularization parameter. The evaluation is performed based on Eq. 4 and the objective of this evaluation is to find the value of λ which minimizes V_{GCV}. We use the built-in MATLAB function "fminbnd" to evaluate the optimum value of the regularization parameter.
4. Evaluation of Results. We apply Eq. 5 to evaluate a smoothed data trend from the original data. Using the smoothed data trend, we then calculate the derivative of data from differentiation matrix.

3.2 Validation Work Flow

The next objective is to validate the applicability of estimating the derivative function using the Tikhonov regularization method and comparing its effectiveness to the Bourdet method. We then provide the workflow to compare the Tikhonov regularization and Bourdet derivative methods. Our approach is straightforward — we first apply these methods to synthetic data where we add Gaussian error in various quantities to the exact solution. Once we are satisfied that the workflow is appropriate for synthetic data, we then apply this workflow to field data (short-term, high frequency pressure transient data and long-term, low frequency production data). This provides both a concept validation using the synthetic data and a practical application using the field data.

3.2.1. Synthetic Data Evaluation

In this section, we develop the following work flow to compare the performance of the Tikhonov regularization method and Bourdet pressure derivative calculation as applied to synthetic data (i.e., an exact/known solution where Gaussian data noise has been added).

1. Select analytical solutions computed the pressure and pressure derivative trends. The selected solutions include
    a. A vertical well in an infinite-acting reservoir with wellbore storage and skin (IARF)
    b. A vertical well in an infinite-acting without wellbore storage and skin in naturally fractured/dual porosity reservoir system (DUAL)
    c. A vertical well with a single vertical fracture having infinite fracture conductivity in an infinite-acting reservoir without wellbore storage and skin (HF).

    The analytical solutions used in this work are discussed in detail in Appendix C.
2. Add Gaussian (random) noise to the calculated analytical pressure trend. The noise has normal (Gaussian) distribution with standard deviations of 0.1%, 1.0%, and 5.0%.

3. Calculate pressure derivative from noisy synthetic pressure trends using the Tikhonov regularization and Bourdet methods. The regularization parameter is estimated using a generalized cross-validation method (as discussed above). Several values of the Bourdet L-parameter used to assess the most appropriate value for a given case. In this work, we have used L = 0.1, 0.2, 0.3, and 0.4.
4. Determine the statistical deviation of the numerically calculated pressure derivative ($y_{calculated}$) to analytical solution (y_{exact}). For this we use the standard measures of Root-Mean-Square (RMS) and Mean-Absolute-Error (MAE) to assess the "goodness-of-fit." RMS and MAE are defined per following where N is number of data points. Lower values of RMS and MAE imply better matches of calculated and exact results.

$$RMS = \sqrt{\sum_{N} \frac{\left(y_{calculated} - y_{exact}\right)^2}{N}}$$

$$MAE = \frac{100}{N} \sum_{N} \left| \frac{y_{calculated} - y_{exact}}{y_{exact}} \right| \%$$

3.2.2. Field Data Evaluation

In this section we elaborate on our strategy to assess the comparison of the Tikhonov regularization method to the Bourdet method for the purpose of estimating the derivative function of "field data" (*i.e.*, actual measurements). The key difference in this evaluation compared to our synthetic data evaluation is the fact that *we do not know the true derivative*, so we must rely more on the smoothness and shape of the derivative curves, as opposed to some sort of quantitative statistical measure. We recognize that considering "qualitative" factors such as "smoothness" and "shape" are subjective, but we believe that these factors are relevant, particularly in a practical sense.

Intuitively, we consider the Tikhonov regularization derivative function to be the "benchmark," and we then compare the Bourdet derivatives computed using various L-parameters to assess the "best" Bourdet derivative function. As comment, we find that we must use higher values of the L-parameter (*e.g.*, $L = 0.3$ or 0.4) for synthetic cases with high levels of noise and for the field data cases selected for this work. The pressure transient and production data analysis literature generally recommends $0.15 < L < 0.25$ for most field data cases, so our observation of the need for $0.30 < L < 0.4$ could be (and probably is) due to the high level of noise in our synthetic and field data cases.

Our methodology for the evaluation of the field data cases is as follows:

1. Select a particular set of field data, for this work we have:
    a. Pressure build-up test data
    b. Oscillating surface pressure data from pressure fall-off test
    c. Rate-transient (production) data for an oil well

    A library of all of the data used in this study can be found in Appendix D.
2. Calculate pressure derivative field data by the Tikhonov regularization method and the Bourdet method. As prescribed earlier in this work, the Tikhonov regularization parameter is calculated from the generalized cross-validation method. Bourdet L-values of 0.1, 0.2, 0.3, and 0.4 are used for the Bourdet derivative calculation.
3. Determine the optimum Bourdet L-parameter by using the RMS and MAE statistical measures, with the Tikhonov regularization derivative as the benchmark.

CHAPTER IV

EVALUATION RESULT

4.1 Synthetic Data Evaluation Result

4.1.1. A vertical well in an infinite-acting reservoir with wellbore storage and skin (IARF)

This case considers infinite-acting radial flow (IARF) with wellbore storage and zero skin effects as a test case. In particular, selected dimensionless wellbore storage case of $C_D = 1\text{x}10^4$ (which is on the lower end of the spectrum, but still provides all flow regimes of interest for our consideration (*i.e.*, wellbore storage domination, wellbore storage/transition, and infinite-acting radial flow)).

We have used the following cases of Gaussian noise — standard deviation of 0.1% (**Fig. 8**), 1.0% (**Fig. 9**), and 5.0% (**Fig. 10**). In each case we used both the Tikhonov regularization method (with λ-value indicated) and the Bourdet method (L-value indicated) value which provides the best RMS and MAE. For each case, the derivative computed using the Tikhonov regularization method yields the best results based on the RMS and MAE criteria (see **Tables 1 and 2**).

For the 0.1% noise case, both the Tikhonov regularization and Bourdet methods capture the important features in the pressure derivative trend — *i.e.*, the wellbore storage and infinite-acting radial flow regimes. In general, we observe that the derivative computed using the Bourdet algorithm exhibits more noise compared to the regularization method, and in particular; for 1.0% and 5.0% noise cases, the Bourdet method does not capture the infinite-acting radial flow regime (very noisy derivative). In comparison, the Tikhonov regularization method works well for all cases, clearly indicating the infinite-acting radial flow regime.

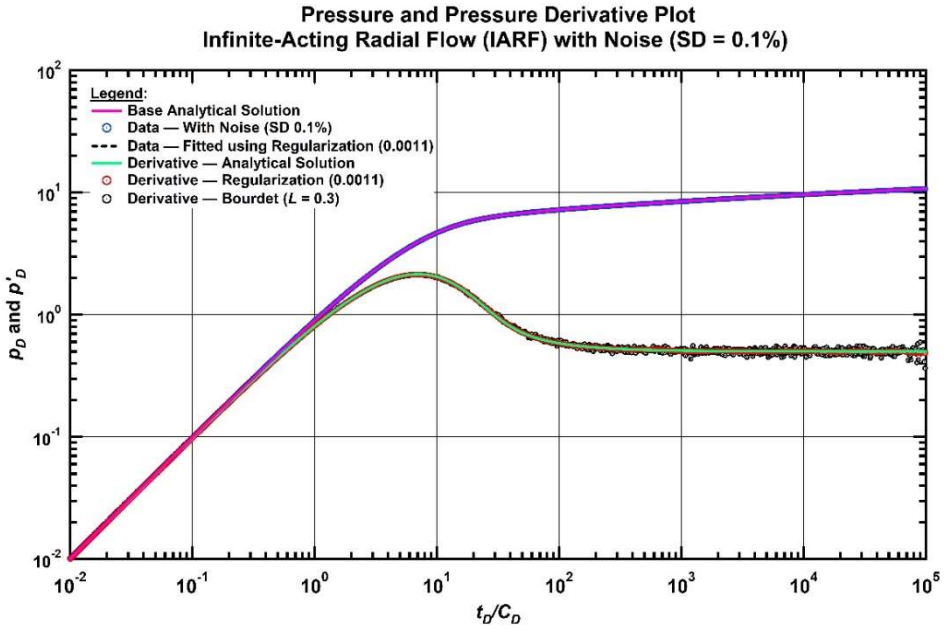

Fig. 8 — Pressure and pressure derivative plot for a vertical well in an infinite-acting reservoir with wellbore storage and skin case with noise (standard deviation — 0.1%).

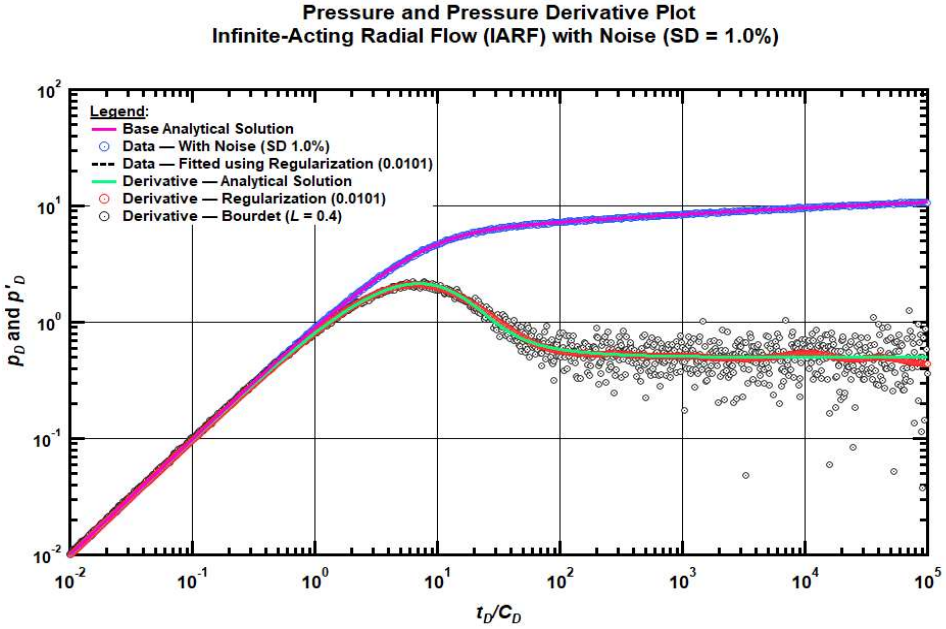

Fig. 9 — Pressure and pressure derivative plot for a vertical well in an infinite-acting reservoir with wellbore storage and skin case with noise (standard deviation — 1%).

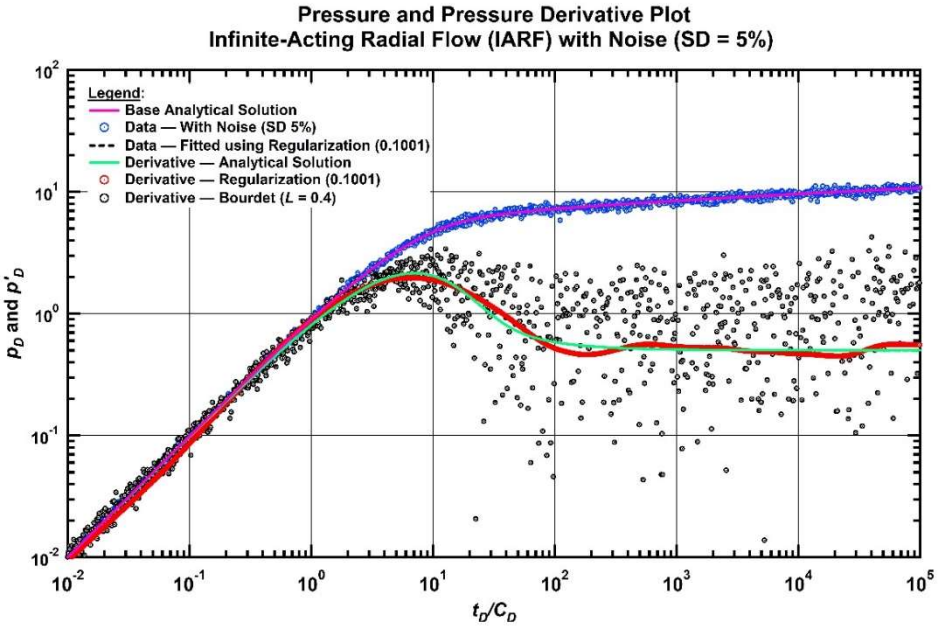

Fig. 10 — Pressure and pressure derivative plot for a vertical well in an infinite-acting reservoir with wellbore storage and skin case with noise (standard deviation — 5%).

4.1.2. A vertical well in an infinite-acting without wellbore storage and skin in naturally fractured/dual porosity reservoir system (DUAL)

This section considers the case of the naturally-fractured/dual porosity reservoir — specifically the case of pseudosteady-state interporosity flow — where the storativity parameter (ω) is 0.01 and the interporosity flow coefficient (λ_f) is 5×10^{-6}. These cases also consider the same levels of noise as previous cases with a standard deviation of noise at 0.1% (**Fig. 14**), 1.0% (**Fig. 15**), and 5.0% (**Fig. 16**). In each of these cases the best Bourdet *L*-value in terms of RMS and MAE is 0.4; and each case the Tikhonov regularization method yields the best results. The RMS and MAE results are summarized in **Tables 1 and 2**).

For both the 0.1% and 1.0% noise cases, both the Tikhonov regularization and Bourdet methods capture the "transition" between fracture-dominated flow and "system" flow observed for the naturally-fractured/dual porosity reservoir model. As would be expected due to the strong

character of the derivative in the "transition" regime, the derivative computed using the Bourdet method is significantly affected by data noise than the Tikhonov regularization method. In particular, for 1.0% noise case, the Bourdet pressure derivative signature is only "qualitatively" indicative of the dual porosity reservoir model, and for the 5.0% noise case, the Bourdet pressure derivative signature does not (even remotely) capture the shape of the dual porosity reservoir model. In fact, for the 5.0% noise case, the Bourdet pressure derivative could be misinterpreted as infinite-acting radial flow (*i.e.*, no naturally-fractured/dual porosity reservoir effects). By comparison, the pressure derivative obtained using the Tikhonov regularization method provides an acceptable level of clarity for all cases of data noise.

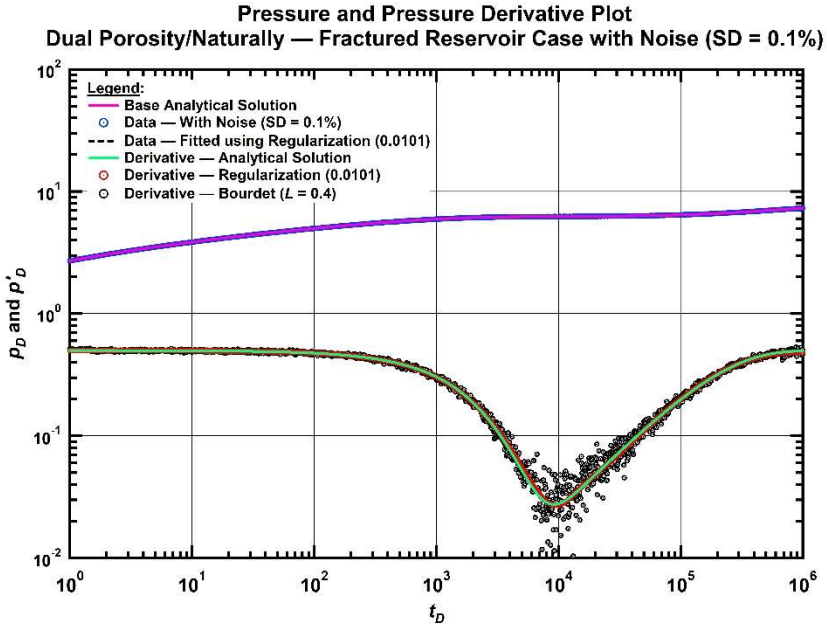

Fig. 11 — Pressure and pressure derivative plot for a vertical well in an infinite-acting without wellbore storage and skin in naturally fractured reservoir system case with noise (standard deviation at 0.1%).

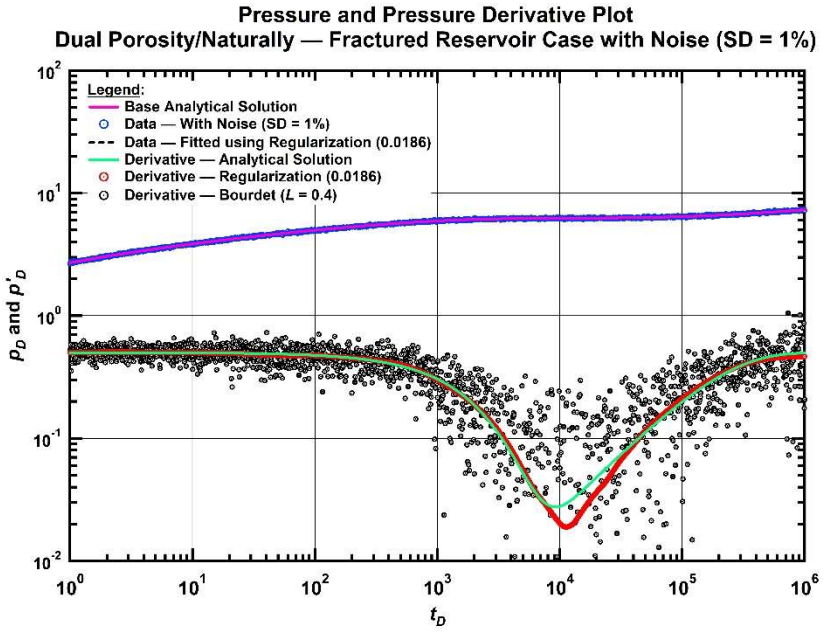

Fig. 12 — Pressure and pressure derivative plot for a vertical well in an infinite-acting without wellbore storage and skin in naturally fractured reservoir system case with noise (standard deviation at 1.0%).

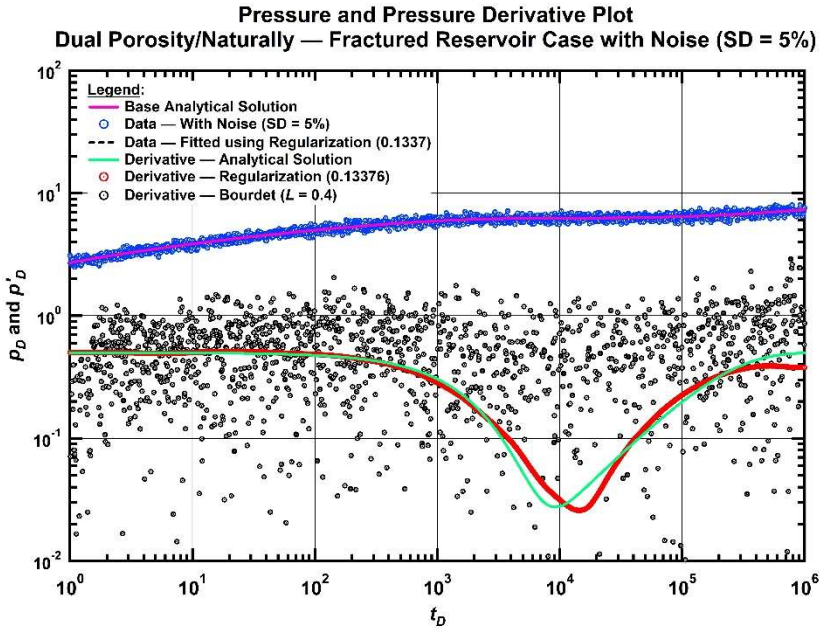

Fig. 13 — Pressure and pressure derivative plot for a vertical well in an infinite-acting without wellbore storage and skin in naturally fractured reservoir system case with noise (standard deviation at 1.0%).

4.1.3. A vertical well with a single vertical fracture having infinite fracture conductivity in an infinite-acting reservoir without wellbore storage and skin (HF).

The last analytical/synthetic case is that of a well with a single vertical fracture having infinite fracture conductivity in an infinite acting reservoir. This case is similar to the first case, but without wellbore storage and with a "negative" skin. There are 3 flow regimes — formation linear flow, transition, and infinite-acting radial flow. We again consider the 3 noise cases — i.e., the 0.1%, 1.0% and 5.0% standard deviation cases and the results for these cases are shown in **Figs. 14-16**, respectively. The Tikhonov regularization method yields the best performance for each case and in this case the "best" Bourdet *L*-parameter is 0.4. The RMS and MAE results are summarized in **Tables 1 and 2.**

Relative to the Bourdet algorithm, in all the cases we can observe the formation linear flow regime at early times, but for the 5.0% standard deviation noise case the Bourdet derivative signature is "qualitative" at best, particularly at early times. We can also observe the transition to radial flow in all cases, but again, the Bourdet derivative signature is challenging and begins to diverge for the 5.0% noise case. Lastly, for the infinite-acting radial flow cases we note that the Bourdet algorithm performs well for the 0.1% noise case, acceptably for the 1.0% noise case, but unacceptably for the 5.0% noise case.

In contrast, the Tikhonov regularization method produces excellent pressure derivative results for the 0.1 and 1.0% error cases, and very good/excellent results for the 5.0% cases. There can be no doubt that the Tikhonov regularization method holds significant promise as a diagnostic tool based on these synthetic cases.

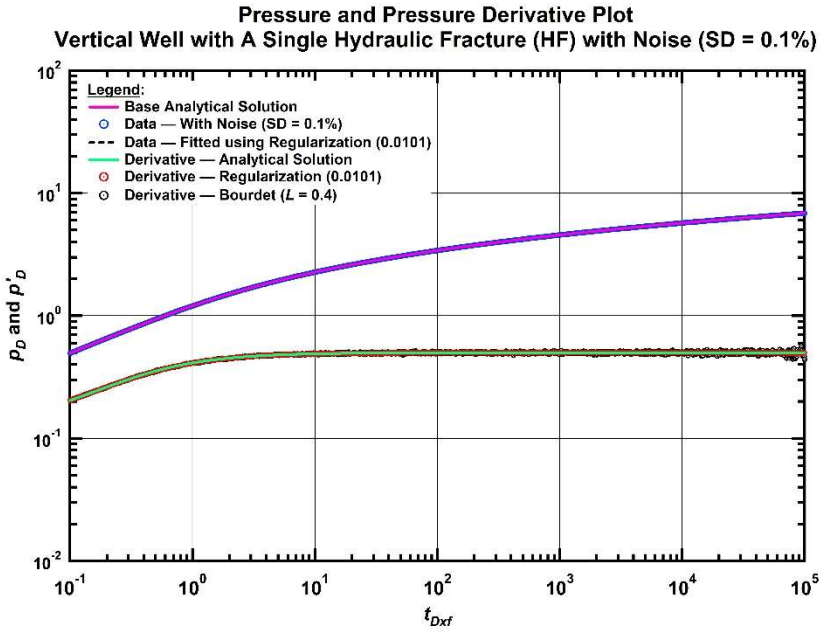

Fig. 14 — Pressure and pressure derivative plot for a hydraulically fractured vertical well with an infinite fracture conductivity in an infinite-acting reservoir without wellbore storage and skin case with noise standard deviation at 0.1%

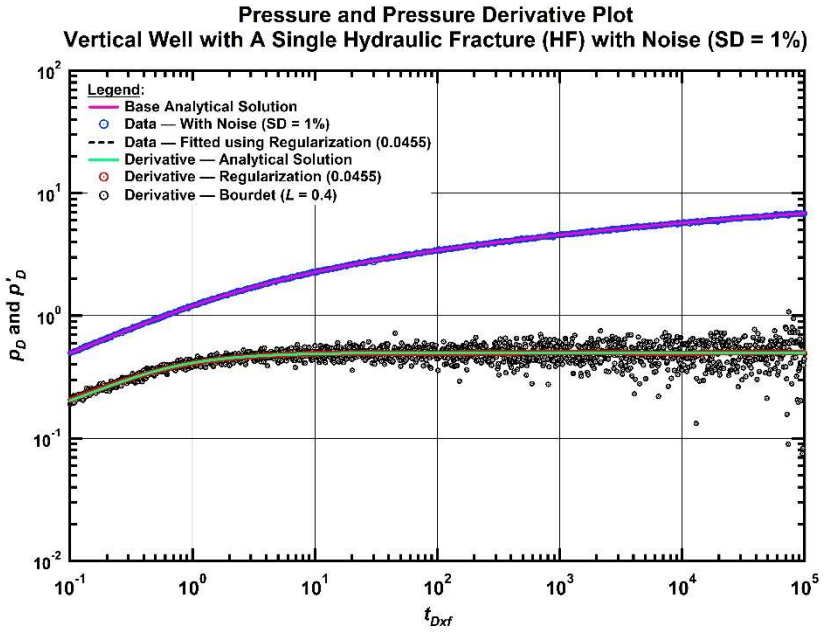

Fig. 15 — Pressure and pressure derivative plot for a hydraulically fractured vertical well with an infinite fracture conductivity in an infinite-acting reservoir without wellbore storage and skin case with noise standard deviation at 1.0%

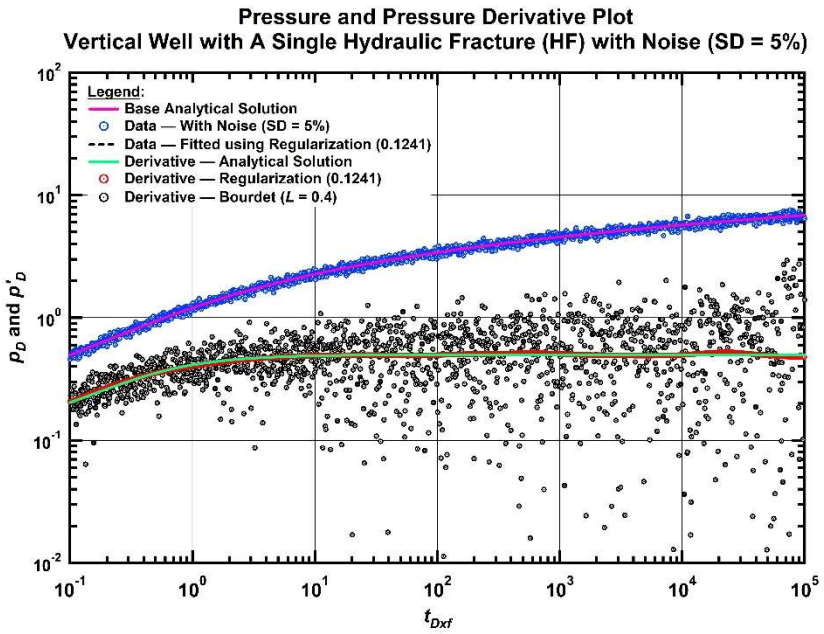

Fig. 16 — Pressure and pressure derivative plot for a hydraulically fractured vertical well with an infinite fracture conductivity in an infinite-acting reservoir without wellbore storage and skin case with noise standard deviation at 5.0%

As shown in **Figs. 8-16**, the Tikhonov regularization method for estimating the pressure derivative clearly outperforms the traditional Bourdet (weighted-difference) derivative method. It is certainly fair to state that for cases of low Gaussian noise, the Bourdet algorithm produces results which are comparable to the Tikhonov regularization method, and such performance ensures that the Bourdet algorithm should (and will) continue to be used. The question of implementation for a particular algorithm comes next — the Tikhonov regularization method is "self-optimizing," but the Bourdet algorithm must be optimized by the user. When the exact solution is known, as for the cases in this section, the Bourdet algorithm could be tested "statistically" (as we have done) to estimate the optimum Bourdet *L*-parameter. However; for applications to field data, the Bourdet *L*-parameter must be determined "qualitatively" from observations of the derivative trend for a given *L*-value.

Ultimately, the fact that there is no way to quantitatively optimize the Bourdet L-parameter in practice imposes a practical constraint on the Bourdet algorithm. As a conclusion, we must state that the Tikhonov regularization method is more robust and more rigorous in a statistical sense, and hence, should be the preferred derivative algorithm.

Table 1 — Root-Mean-Square (RMS) error estimated using the Bourdet and the Tikhonov Regularization pressure derivative calculations compared to the exact derivation solution

Solution	Noise SD (%)	Root-Mean-Square (RMS) Error					Regularization Parameter
		$L = 0.1$	$L = 0.2$	$L = 0.3$	$L = 0.4$	Regularization	
IARF	0.1	0.0381	0.0196	0.0143	0.0143	0.0025	0.0011
	1.0	0.3625	0.1791	0.1315	0.0975	0.0168	0.0101
	5.0	1.8500	0.9382	0.6300	0.4808	0.0518	0.1001
DUAL	0.1	0.0370	0.0194	0.0133	0.0104	0.0022	0.0101
	1.0	0.3663	0.1936	0.1309	0.0998	0.0088	0.0186
	5.0	1.9638	1.0805	0.7019	0.5499	0.0272	0.1337
HF	0.1	0.0268	0.0137	0.0099	0.0076	0.0019	0.0101
	1.0	0.2662	0.1350	0.0916	0.0718	0.0038	0.0455
	5.0	1.2498	0.6874	0.4620	0.3649	0.0091	0.1241

Table 2 — Mean Absolute Error (MAE) error estimated using the Bourdet and the Tikhonov Regularization pressure derivative calculations compared to the exact derivation solution

Solution	Noise SD (%)	Maximum Average Error (MAE) (percent)					Regularization Parameter
		$L = 0.1$	$L = 0.2$	$L = 0.3$	$L = 0.4$	Regularization	
IARF	0.1	3.5570	2.0548	2.0490	2.6197	0.4152	0.0011
	1.0	33.598	16.618	12.367	9.8347	2.0796	0.0101
	5.0	171.64	88.145	59.293	45.163	8.8911	0.1001
DUAL	0.1	21.728	10.905	7.4448	5.6734	0.7176	0.0101
	1.0	210.69	110.90	73.397	54.061	4.4667	0.0186
	5.0	1052.8	590.04	379.07	299.93	8.2279	0.1337
HF	0.1	3.6748	1.8320	1.3402	1.0842	0.4441	0.0101
	1.0	36.127	18.412	12.217	9.5205	1.0598	0.0455
	5.0	171.85	91.849	61.158	48.174	2.2892	0.1241

4.2 Field Data Evaluation Result

4.2.1. Data Case — Bourdet Pressure Build-Up Data

In this part, we obtain the data from the Bourdet et al. publication (Table 2 — SPE-12777). This is the case of a pressure build up for a fissured (naturally-fractured) reservoir. Superposition time is required to analyze pressure build up and it can be calculated in Eq. 26.

$$\ln t_{\text{sup}} = \frac{1}{q_n - q_{n-1}} \left[\sum_{i=1}^{n-1} \left(q_i - q_{i-1} \right) \ln \left[\sum_{j=1}^{n-1} \Delta t_j + \Delta t \right] \right] + \ln \Delta t \quad \text{.....(26)}$$

Where:

t_{sup} is superposition time

q_i is historical production rate,

Δt_j is historical production period for each production rate, and

Δt is shut in duration.

For this case, Bourdet et al. used L = 0.1 in the "Bourdet" derivative algorithm and presented the data derivative curve onto the "type curve" for a dual porosity reservoir system. Their work is shown in **Fig. 17** (which is Fig. 13 in their original publication). The model responses are represented by lines on **Fig. 17** and the data are presented as symbols.

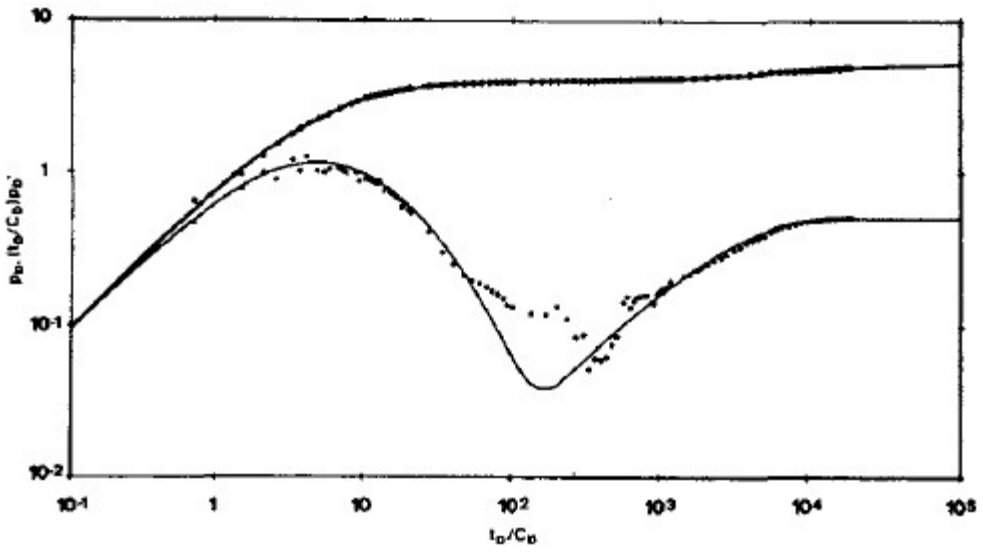

Fig. 17 — Bourdet pressure build up analysis in fissured reservoir (Reprinted from Bourdet et al., 1989)

In this work we use the Tikhonov regularization method for the calculation of the pressure derivative function (see **Fig. 18** with the Bourdet pressure derivative as shown on this plot for comparison). The Tikhonov regularization parameter value (0.0578) is obtained from generalized-cross-validation; and for comparison, we use the same *L*-parameter (0.1) as used in the original Bourdet publication.

In reviewing the derivative trends shown in **Fig. 18**, we observe that the "regularization" derivative is a bit "wavy" but we believe this is due to the spacing and sparsity of the data in the case given by Bourdet. We note that the regularization and Bourdet derivatives compare very well, and that the regularization derivative has a very strong signature at late times (total system radial flow). We also observe that the regularization derivative does not "dip" as lowly the pressure derivative from the Bourdet algorithm, but we also note a sparsity of data at these times so this deeper "dip" of the Bourdet derivative could be an artifact of sparse data in that region.

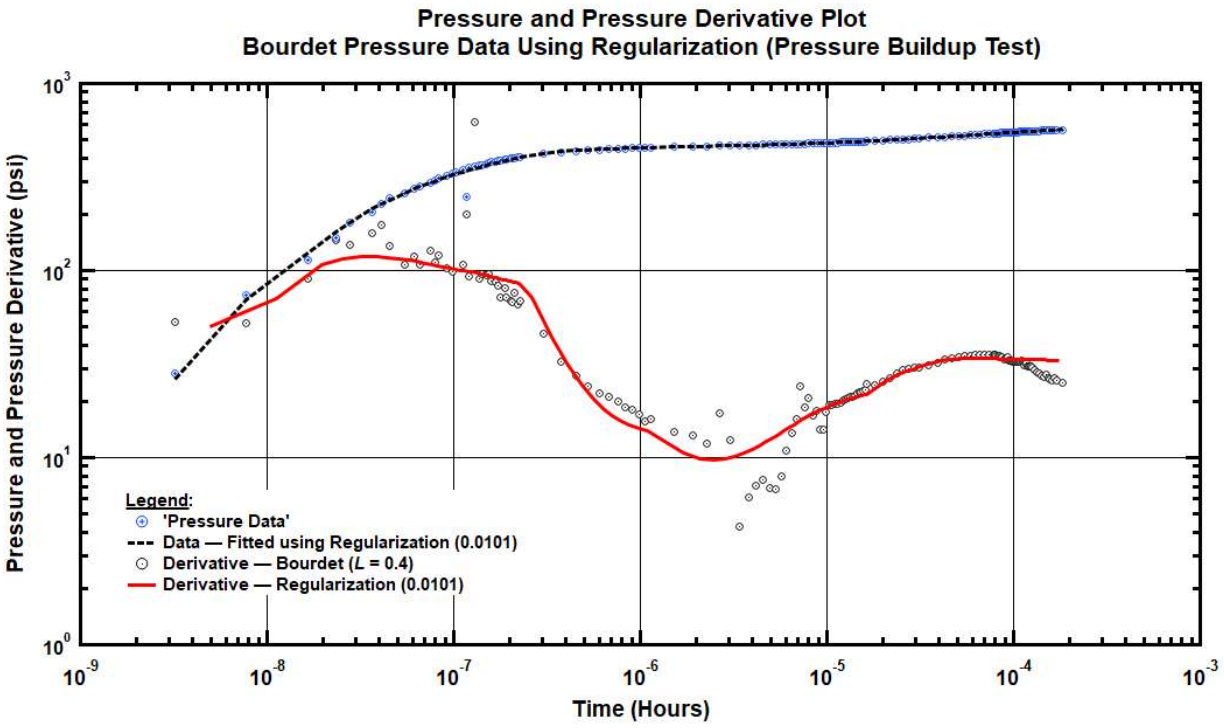

Fig. 18 — Bourdet pressure build up analysis in fissured reservoir using regularization

4.2.2. Data Case — Oscillating Surface Pressure Data from a Pressure Fall-Off Test

In this field data example, we consider the analysis of a pressure fall-off test with only surface pressure data where these data are impacted by atmospheric (surface) temperature change (these data are courtesy of Reservoir Development Company/ DFITpro.com and were provided by Dr. David Craig). The surface temperature affects the wellhead pressure gauge, resulting in oscillatory pressure measurements (the cycles of oscillation have a period of one day because of temperature changes during the day and night time).

As comment, such behavior is fairly common with surface pressure gauges, and the pressure derivative in such cases often amplifies these oscillations. The pressure trend for this case is shown in "full view" in **Fig. 19** and in a "zoom view" (of the oscillatory behavior) in **Fig. 20**.

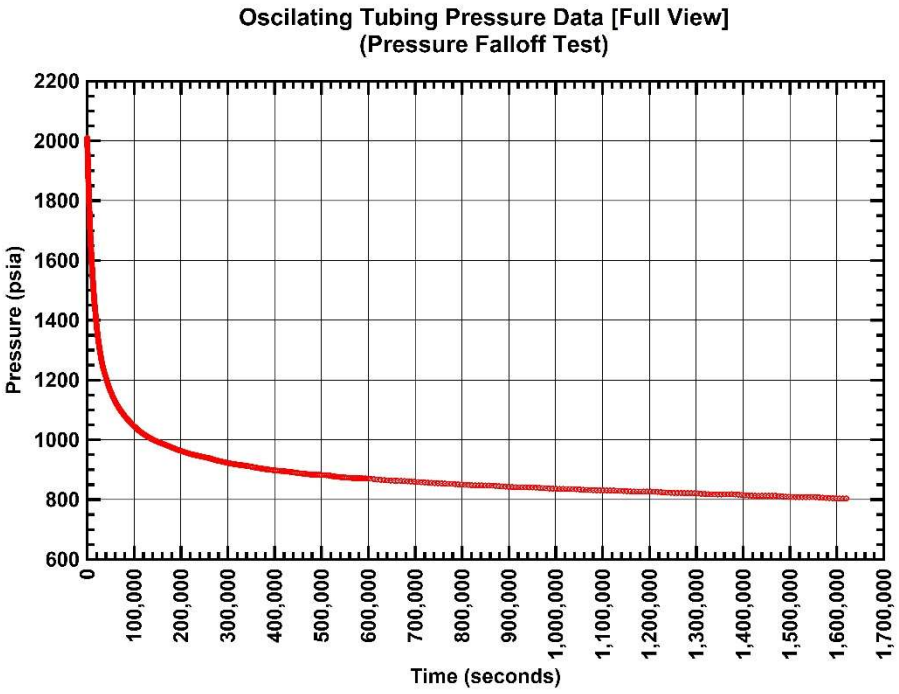

Fig. 19 — Oscillating surface pressure data from fall off test

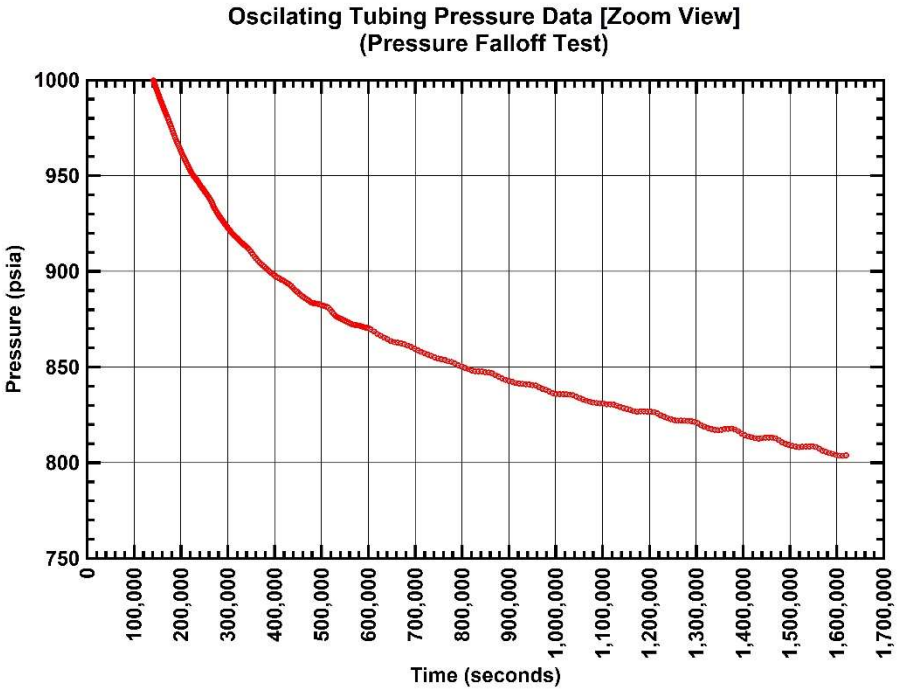

Fig. 20 — Oscillating surface pressure data from fall off test – late time

As with the other field data cases, we first compute the pressure derivatives using the Bourdet algorithm and again we test a range of the Bourdet "*L*-parameter" values (specifically we used *L* = 0.1, 0.2, 0.3, and 0.4; and we selected *L* = 0.4 as our final value based (qualitatively) on shape of the pressure derivative curve and as this value has the lowest RMS value compared to the Tikhonov regularization method). We then compute the pressure derivative using the Tikhonov regularization method (regularization parameter = 0.0101) and all of the pressure derivative trends are shown in **Fig. 21**. As comment, the derivatives computed using the Tikhonov regularization method and the Bourdet algorithm compare very well for this case, despite the temperature induced oscillations in the surface pressure data.

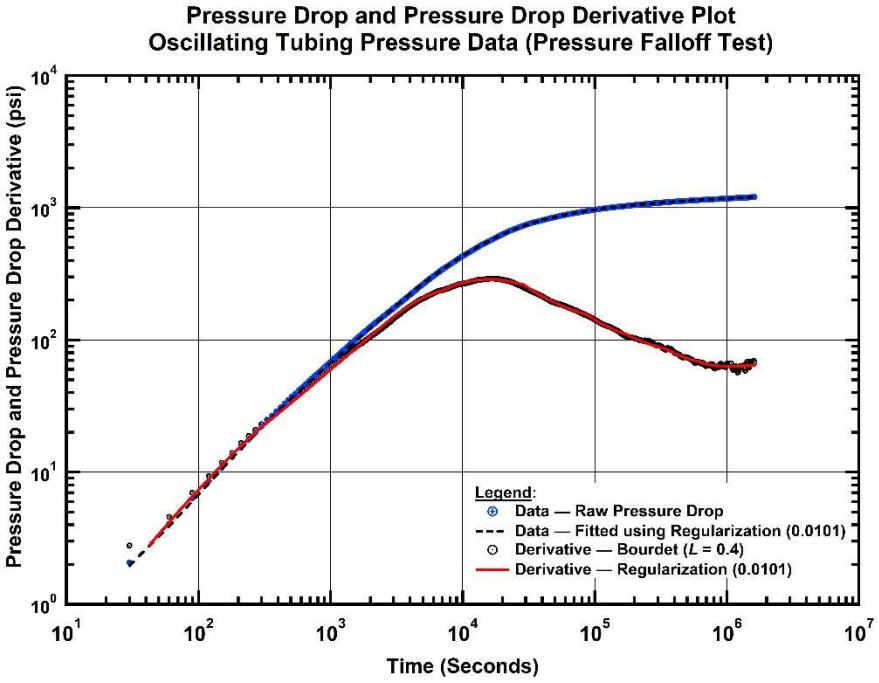

Fig. 21 — Pressure derivative from oscillating surface pressure data from fall off test

4.2.3. Rate Transient (Production) Data for an Oil Well

In this field data case we apply the Tikhonov regularization method and the Bourdet derivative algorithm to the production history of an oil well (these data are courtesy of Reservoir Development Company/DFITpro.com and were provided by Dr. David Craig). Historically, the analysis of production data is very challenging, particularly for the estimating derivative functions. As such, this case should be considered an extreme example for the calculation of the derivative function.

The data for this case consists of production rates and flowing pressures for an oil well with just under 2 years of production history (713 days). In this case we will use the rate normalized pressure drop (*i.e.*, $\Delta p/q$) instead of pressure to account for the variations in flowrate. The same procedures as in previous cases will also be used here — specifically the calculation of the pressure derivative function using the Tikhonov regularization method and the Bourdet derivative algorithm. The $\Delta p/q$ and $\Delta p/q$-derivative functions are plotted in **Fig. 22**. Similar to previous cases, the selected Bourdet L-parameter is 0.4 and the regularization parameter for Tikhonov regularization method is 0.0079.

In consideration of the relatively poor performance of the functions shown in **Fig. 22**, it was decided to attempt an "over-regularization" case (i.e., using a very high value of the regularization parameter), In **Fig. 23** we present the data and derivative functions computed using a regularization parameter value of 999.514.

In order to address the relatively poor performance of the derivative algorithms for this case, we manually removed the outlier data points — specifically those points on days 20, 21, 22, 23, 143, and 337. We then performed the derivative calculations for these data and the results are presented

in **Fig. 24**. In this case the Tikhonov regularization parameter is 0.0079 and the Bourdet L-parameter is 0.4. As can be seen in x, the performance of the derivative functions are significantly improved and are suitable for diagnostic analyses (*i.e.*, identification of flow regimes). The statistical measures for this case are: RMS = 4.112 psi/STBOD and MAE = 41.68%. As mentioned, this is an extreme case — production data are notoriously prone to data noise. Given the performance of the Tikhonov regularization method for this case, we believe that these results provide a proof, at least in concept, of the use of the Tikhonov regularization method to estimate derivative functions for cases with large/very large volumes of data noise.

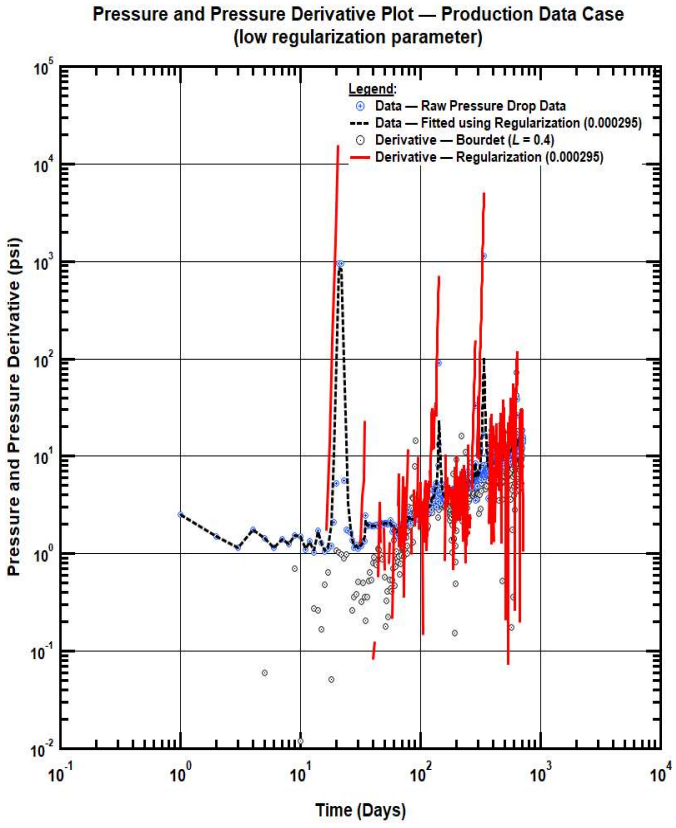

Fig. 22 — Rate transient analysis using a small value of the regularization parameter.

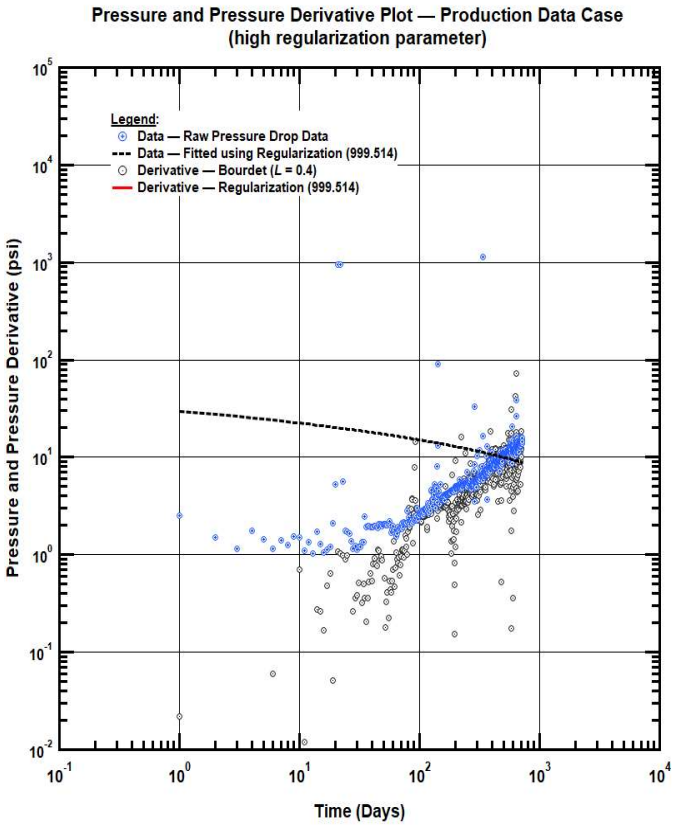

Fig. 23 — Rate transient analysis using a large value of the regularization parameter.

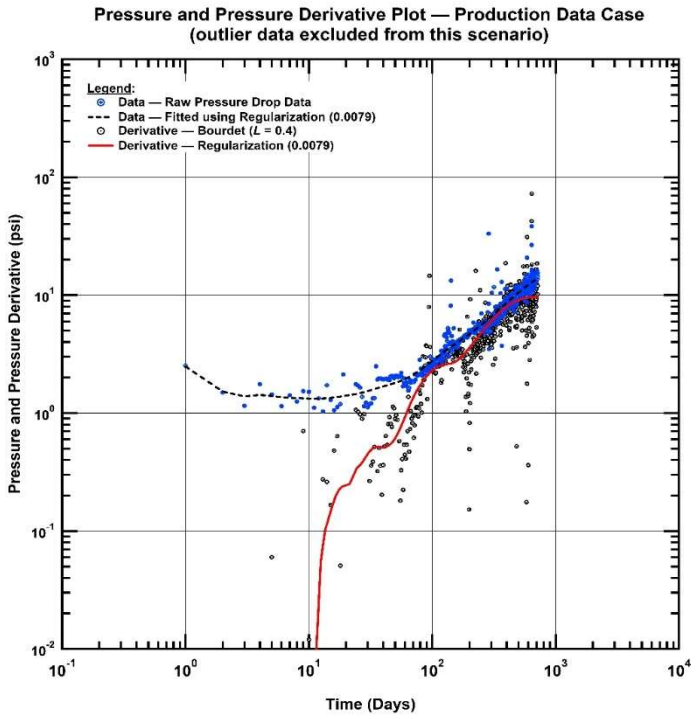

Fig. 24 — Rate transient analysis using data without outlier

CHAPTER V

SUMMARY, CONCLUSIONS, AND RECOMMENDATIONS FOR FUTURE EFFORT

5.1 Summary

In this work, we investigate the use of the Tikhonov Regularization method to estimate the derivative for noisy data using an application of this method developed in MATLAB. We note that our implementation of the Tikhonov Regularization method is based on the work of Eilers (2003), Lubansky et al. (2006), and Stickel (2010). The Tikhonov regularization provides a minimization of goodness-of-fit and roughness at the same time. The regularization objective function in linear algebra form can be written as:

$$Q = (\hat{\mathbf{y}} - \mathbf{y})^T \mathbf{B}(\hat{\mathbf{y}} - \mathbf{y}) + \lambda(\mathbf{D}\hat{\mathbf{y}})^T \tilde{\mathbf{B}}(\mathbf{D}\hat{\mathbf{y}})$$

By solving objective function, we obtain the fitted data trend as follows:

$$\hat{\mathbf{y}}^* = \left(\mathbf{M}^T \mathbf{W}\mathbf{M} + \lambda \mathbf{D}^T \mathbf{U}\mathbf{D}\right)^{-1} \mathbf{M}^T \mathbf{W}\mathbf{y}$$

For this work, the smoothness criteria is determined using an optimization process based on the generalized cross-validation method, which we believe provides the least bias for the Tikhonov Regularization method.

We demonstrate the Tikhonov Regularization method by using the exact solutions for several classic solutions in reservoir engineering (for simplicity, we have only considered the transient flow portion of these solutions). In particular, the case of a unfractured vertical well in an infinite-acting reservoir with wellbore storage and skin effects (*i.e.*, IARF), an unfractured vertical well in an infinite-acting reservoir without wellbore storage and skin effects in a naturally fractured/dual porosity reservoir system (*i.e.*, DUAL), and the case of a vertical well with a single (hydraulically

created) vertical fracture of infinite fracture conductivity in an infinite-acting reservoir without wellbore storage and skin effects (*i.e.*, HF).

For each solution we have generated a series of typical scenarios and have added Gaussian noise to these solutions as a means of testing the Tikhonov Regularization method and the Bourdet method to estimate the pressure derivative function from the analytical solutions with noise added. The "synthetic noise" has a (Gaussian) normal distribution with standard deviation at 0.1, 1.0 and 5.0 percent for each case. At low (0.1 percent) and medium (1.0 percent) noise levels, both the regularization method and the Bourdet method successfully extract the pressure derivative function (these results are compared to the analytical pressure derivative solution). However; we do note that for all cases, the Tikhonov Regularization method provides more robust (*i.e.,* accurate) estimates of the pressure derivative than the Bourdet method (which is the industry standard algorithm).

For the case with the highest level of noise in this work (*i.e.*, standard deviation = 5.0 percent), the Bourdet derivative method fails to yield the shape of pressure derivative response (much less accurate estimates). In contrast, the Tikhonov Regularization provides a remarkably accurate pressure derivative profile in terms of both "shape" and the accuracy of the computed derivative values.

We also implemented the Tikhonov regularization process on multiple field data cases. These cases include both pressure transient test and rate transient test. For pressure transient analysis, regularization has better performance comparing to Bourdet method. For the rate transient data case, we had to filter the outlying data points prior to calculating the pressure derivative in order to obtain a derivative trend that has the fidelity to provide a good diagnostic signature.

Given the results of our work, it would be tempting to simply give preference to the Tikhonov Regularization method — however; we believe that a comparative methodology that includes the Bourdet method will be useful for estimating the pressure derivative response. We have only considered the case of Gaussian (or normally distributed) noise, there could be cases of data bias and/or non-Gaussian types of noise which may adversely affect the utility of the Tikhonov Regularization method. It would not be an overstatement for us to comment that we are genuinely surprised at the robustness of the Tikhonov Regularization method, and to suggest that algorithms such as this should be routinely utilized for reservoir engineering applications.

5.2 Conclusions

The following conclusions have been derived in this work.

- The Tikhonov Regularization method is applicable to petroleum engineering applications. The method is proven using cases of synthetic and field data.
- The Tikhonov Regularization method has statistically better performance with regard to obtaining the pressure derivative function compared to Bourdet method especially for cases with high levels of data noise. The RMS and MAE statistical measures are used to assess the comparative performance of these algorithms.
- The Tikhonov Regularization method can be applied to pressure transient analysis and rate transient analysis. Practically-speaking, for pressure transient data there is typically not a high level of data noise. In the case of production data, elevated levels of noise (and outliers) are quite common. Outlier filtering is necessary for the interpretation of production data.

5.3 Recommendations for Future Effort

- Other classes of regularization such as total variation regularization (TVR) are possibly suited to this purpose. The primary limitation of the TVR method is the requirement for evenly-spaced data in order to calculate the pressure derivative function.
- Extension of testing of these algorithms to other types of noise is warranted. In particular, we have only considered Gaussian noise in our present work. Other types of data noise should be considered.

NOMENCLATURE

Field Variables (*Mathematics*)

C_j = spline coefficient

d = derivative order

f = frequency

i = data index

I_1 = total energy factor

I_2 = low-frequency deviation factor

L = minimum distance between derivative point for Bourdet pressure derivative

N = number of data pairs

Q = objective function

S = splines function

V_{GCV} = generalized cross-validation variance

x = independent variable

$\tilde{x}$ = Fourier transform of x

X = natural logarithm of time

y = dependent variable

$\hat{y}$ = smoothed dependent variable

$\hat{y}^*$ = smoothed dependent variable that minimize objective function (solution)

RMS = Root-Mean-Square

MAE = Mean-Absolute-Error

λ = regularization parameter

λ_{opt} = optimum regularization parameter

B, $\tilde{\mathbf{B}}$ = integral matrix

D = finite-difference matrix

f = independent variable matrix

M = mapping matrix

W = weighting matrix for goodness-of-fit

U = weighting matrix for roughness

Field Variables:

B = formation volume factor

C = wellbore storage coefficient

c_t = total system compressibility

h = pay thickness

k = permeability

p = pressure

p_i = initial reservoir pressure

p_{wf} = flowing bottom hole pressure

q = flow rate

r = radius

r_w = wellbore radius

s = skin

t = time

ϕ = porosity

μ = viscosity

IARF = Case of a vertical well in an infinite-acting reservoir with wellbore storage and skin

DUAL = Case of a vertical well in an infinite-acting without wellbore storage and skin in naturally fractured reservoir system

HF = Case of a hydraulically fractured vertical well with an infinite fracture conductivity in an infinite-acting reservoir without wellbore storage and skin

Dimensionless Variables:

C_D = dimensionless wellbore storage coefficient

p_D = dimensionless pressure

r_D = dimensionless radius

t_D = dimensionless time

Mathematical Functions:

Ei = Exponential integral

J_0 = Bessel function of the first kind of 0^{th} order

J_1 = Bessel function of the first kind of 1^{st} order

Y_0 = Bessel function of the second kind of 0^{th} order

Y_1 = Bessel function of the second kind of 1^{st} order

REFERENCES

Agarwal, R. G., Al-Hussainy, R. and Ramey, H. J., Jr. 1970. An Investigation of Wellbore Storage and Skin Effect in Unsteady Liquid Flow: I. Analytical Treatment. *SPEJ* (September 1970).

Bourdet, D., Ayoub, J. A. and Pirard, Y. M. 1989. Use of Pressure Derivative in Well Test Interpretation. *SPEFE* (June 1989) 293-302.

Cheng, Y., Lee, W. J. and McVay, D. A. 2005. Determination of Optimal Window Size in Pressure-Derivative Computation Using Frequency-Domain Constraints, paper SPE-96026-MS presented at the 2005 SPE Annual Technical Conference and Exhibition, Dallas, Texas, 9-12 October 2005.

Dake, L. P. 1978. *Fundamentals of Reservoir Engineering*, Elsevier Scientific Publishing Company (Reprint).

Earlougher, R. C., Jr. and Kersch, K. M. 1974. Analysis of Short-Time Transient Test Data By Type-Curve Matching. J. Pet. Tech. (July 1974) 793-800; 793-800; Trans., AIME, 257.

Eilers, P. H. 2003. A Perfect Smoother. *Analytical Chemistry* **75** (14) 3631-3636.

Escobar, F. H., Navarrete, J. M. and Losada, H. D. 2004. Evaluation of Pressure Derivative Algorithms for Well-Test Analysis, paper SPE-86936-MS presented at the 2004 SPE International Thermal Operations and Heavy Oil Symposium and Western Regional Meeting, Bakersfield, California, 16-18 March 2004.

Gringarten, A. C., Bourdet, D. P., Landel, P. A. et al. 1979. A Comparison Between Different Skin And Wellbore Storage Type-Curves For Early-Time Transient Analysis, paper presented at the SPE Annual Technical Conference and Exhibition, Las Vegas, Nevada.

Horner, D. R. 1951. Pressure Build-up in Wells, paper WPC-4135 presented at the Third World Pet. Cong., E.J. Brill, Leiden.

Lane, H. S., Lee, W. J. and Watson, A. T. 1991. An Algorithm for Determining Smooth, Continuous Pressure Derivatives From Well-Test Data. *SPEFE* (December 1991) 493-499.

Lubansky, A., Yeow, Y. L., Leong, Y. K. et al. 2006. A general method of computing the derivative of experimental data. *AIChE journal* **52** (1) 323-332.

McKinley, R. M. 1971. Wellbore Transmissibility from Afterflow-Dominated Pressure Buildup Data. *J. Pet. Tech.* (July 1971).

MATLAB, version R2016a 2016, The MathWorks Inc.

Moore, T. V., Schilthius, R.J., and Hurst, W. 1933. Determination of Pemleability From Field Data. *Bull., API 211*.

Ramey, H. J. 1982. Distinguished Transient Testing. **J. Pet. Technol., July, pp. 1407–1413**.

Ramey, H. J., Jr. 1970. Short-Time Well Test Data Interpretation in the Presence of Skin Effect and Wellbore Storage. *J. Pet. Tech.* (Feb. 1965) 223-233.

Stickel, J. J. 2010. Data smoothing and numerical differentiation by a regularization method. *Computers & chemical engineering* **34** (4) 467-475.

Van Everdingen, A. F. 1953. The Skin Effect and Its Influence on the Productive Capacity of a Well. *Journal of Petroleum Technology 5 (06):* 171-176.

Van Everdingen, A. F. and Hurst, W. 1949. The Application of the Laplace Transformation to Flow Problems in Reservoirs. *Trans. AIME (1949) 186,* 305-324.

Veneruso, A. F. and Spath, J. B. 2006. A Digital Pressure Derivative Technique for Pressure Transient Well Testing and Reservoir Characterization, paper SPE-103040-MS presented at

the 2006 SPE Annual Technical Conference and Exhibition, San Antonito, Texas, 24-27 September 2006.

APPENDIX A

DERIVATION OF TIKHONOV REGULARIZATION

The Tikhonov regularization method is derived in this Appendix:

Mathematical Formalism

Stickel (2010) provides the derivation of Tikhonov Regularization considering sequence of data pairs:

y_i for $i = 1,2,...,N$

x_i for $i = 1,2,...,N$

$x_i < x_{i+1}$

We assume that there exists a function $y(x)$ that exactly describes the relationship between x and y. The goal of this analysis is to estimate $y(x)$ from available data where we define $\hat{y}(x)$ as a smooth approximation of $y(x)$. For this work, the goodness-of-fit can be defined as prescribed in Eq. A.1.

$$\int_{x_1}^{x_N} [\hat{y}(x) - y(x)]^2 \, dx \quad \text{.....(A.1)}$$

The "roughness" term is defined as shown in Eq. A.2.

$$\int_{x_1}^{x_N} [\hat{y}^d(x)]^2 \, dx \quad \text{.....(A.2)}$$

where

$$\hat{y}^d(x) = \frac{d^d \hat{y}}{dx^d}$$

The "roughness" term indicates how smooth the data trend $\hat{y}(x)$ would be — in theory, a second derivative provides the curvature of the trend. By limiting the roughness value to a small value, the fitted curve should be smooth. In the regularization process, the objective is to minimize both the goodness-of-fit and the roughness simultaneously. Such a condition can be achieved with compromise between the goodness-of-fit and the roughness. To determine the optimum solution, weighting factors must be used. The objective function for regularization ($Q(\hat{y})$) is defined by Eq. A.3.

$$Q(\hat{y}) = \int_{x_1}^{x_N} [\hat{y}(x) - y(x)]^2 \, dx + \lambda \int_{x_1}^{x_N} [\hat{y}^d(x)]^2 \, dx \quad \text{.....(A.3)}$$

λ is the weighting factor multiplied by the roughness term — and λ is called the regularization parameter. The smaller the value of the regularization parameter yields a smooth trend $\hat{y}(x)$ that is closer to the data function $y(x)$, while larger λ-values yield $\hat{y}(x)$ trends that are very smooth, but these trends can (and likely will) lie far from the data function trend, $y(x)$.

The solution of desired smooth trend ($\hat{y}(x)$) is one that minimizes $Q(\hat{y})$ for a given λ-value, this trend is defined as $\hat{y}^*$and is obtained as follows:

$$\hat{y}^* = \underset{\hat{y}}{\arg\min}\, Q(\hat{y}) \quad \text{.....(A.4)}$$

As this data analysis procedure involves discrete data points, Eqs. A.1 to A.4 can be rewritten into a linear algebra (*i.e.,* matrix) format. The derivative and integral of any function $\mathbf{f}$ in the form of column vector can be numerically approximated by the following expressions:

$$\mathbf{f}^{(d)} \approx \mathbf{D}^{(d)}\mathbf{f}$$

$$\int_{x_1}^{x_N} |f(x)|^2 \, dx \approx \mathbf{f}^T \mathbf{B} \mathbf{f}$$

The matrix $\mathbf{D}^{(d)}$ is a finite-difference approximation for derivatives of the order *d,* and the $\mathbf{B}$ term is the integral matrix. Both $\mathbf{D}^{(d)}$ and $\mathbf{B}$ can be developed using any numerical approximation rules. To smooth the data trend, simple forward or backward differences (for the derivatives) and the trapezoidal rule (for the integrals) are sufficient. The detail of these numerical methods can be found in **Appendix B**. Based on numerical approximation, Eq. A.3 can be written as

$$Q = (\hat{\mathbf{y}} - \mathbf{y})^T \mathbf{B} (\hat{\mathbf{y}} - \mathbf{y}) + \lambda (\mathbf{D}\hat{\mathbf{y}})^T \tilde{\mathbf{B}} (\mathbf{D}\hat{\mathbf{y}}) \quad \text{.....(A.5)}$$

The matrix $\mathbf{D}$ can be any order but the superscript (d) is dropped out for convenience. $\mathbf{D}\hat{\mathbf{y}}$ has the size of $N - d \; x \; 1$. Thus $\tilde{\mathbf{B}}$ must have the dimension of $N - d \; x \; N - d$. In writing Eq. A.5, there is no requirement that the x-values must be equally-spaced. However, the values of x must be in monotonic order.

In some cases, the analyst may wish to process the data prior to performing regression. This can happen when there are too many or too few data points. The original data set of N pairs can be mapped to $\widehat{N}$ pairs of processed data. This can be performed by any interpolation or extrapolation method. In linear algebra form, the mapping matrix $\boldsymbol{M}$ can be multiplied by $\hat{y}$ to map the values to desired y points. This is written as:

$$Q = (\mathbf{M}\hat{\mathbf{y}} - \mathbf{y})^T \mathbf{B} (\mathbf{M}\hat{\mathbf{y}} - \mathbf{y}) + \lambda (\mathbf{D}\hat{\mathbf{y}})^T \tilde{\mathbf{B}} (\mathbf{D}\hat{\mathbf{y}}) \quad \text{.....(A.6)}$$

In addition to data mapping, some cases will require different weighting in different sections of a given data trend. For example, the trend requires better goodness-of-fit at low values of x but it

requires smoother curve at large values of x. This can be achieved by modifying matrix $\mathbf{B}$ and $\tilde{\mathbf{B}}$ to have different weighting at different values of x. Hence the objective function can be written in general form as

$$Q = (\mathbf{M}\hat{\mathbf{y}} - \mathbf{y})^T \mathbf{W}(\mathbf{M}\hat{\mathbf{y}} - \mathbf{y}) + \lambda(\mathbf{D}\hat{\mathbf{y}})^T \mathbf{U}(\mathbf{D}\hat{\mathbf{y}}) \quad \text{.....(A.7)}$$

where $\mathbf{W}$ and $\mathbf{U}$ are modified $\mathbf{B}$ and $\tilde{\mathbf{B}}$ matrices used to provide variable data weighting. When there is no data mapping or data weighting requirements, $\boldsymbol{M = I, W = B, and\ U = \tilde{B}}$, and Eq. A.7 simply reduces to Eq. A.5.

Analytical Solution

The objective is to find $\hat{y}^*$ such that Q in Eq. A.7 minimized. This can be achieved by taking the derivative of Q with respect to $\hat{y}$ and finding $\hat{y} = \hat{y}^*$ such that $\frac{dQ}{d\hat{y}}$ equals zero.

From Eq. A.7, we obtain:

$$\begin{aligned}\frac{dQ}{d\hat{y}} &= \frac{d}{d\hat{y}}\left[(\mathbf{M}\hat{\mathbf{y}} - \mathbf{y})^T \mathbf{W}(\mathbf{M}\hat{\mathbf{y}} - \mathbf{y}) + \lambda(\mathbf{D}\hat{\mathbf{y}})^T \mathbf{U}(\mathbf{D}\hat{\mathbf{y}})\right] \\ &= 2\mathbf{M}^T \mathbf{W}(\mathbf{M}\hat{\mathbf{y}} - \mathbf{y}) + 2\lambda \mathbf{D}^T \mathbf{U}\mathbf{D}\hat{\mathbf{y}}\end{aligned}$$

Setting $\frac{dQ}{d\hat{y}} = 0$ for $\hat{y} = \hat{y}^*$, we have:

$$\begin{aligned}2\mathbf{M}^T \mathbf{W}(\mathbf{M}\hat{\mathbf{y}}^* - \mathbf{y}) + 2\lambda \mathbf{D}^T \mathbf{U}\mathbf{D}\hat{\mathbf{y}}^* &= 0 \\ (\mathbf{M}^T \mathbf{W}\mathbf{M} + \lambda \mathbf{D}^T \mathbf{U}\mathbf{D})\hat{\mathbf{y}}^* &= \mathbf{M}^T \mathbf{W}\mathbf{y}\end{aligned}$$

$$\hat{\mathbf{y}}^* = (\mathbf{M}^T \mathbf{W}\mathbf{M} + \lambda \mathbf{D}^T \mathbf{U}\mathbf{D})^{-1} \mathbf{M}^T \mathbf{W}\mathbf{y} \quad \text{.....(A.8)}$$

Generalized Cross-Validation

As one can suspect, determining the regularization parameter (λ) is one of the key challenges for data smoothing. The optimal λ-value can, and obviously should vary between different data sets. The order of the regularization parameter can range from 10^{-10} to 10^{10} (Leong Yeow, C. Ko, and P. P. Tang 2000, Lubansky et al. 2006, Stickel 2010). Choosing the appropriate regularization parameter can be achieved by several methods (Boyd and Vandenberghe 2003, Eilers 2003, Lubansky et al. 2006, Stickel 2010, Wang, Jia, and Cheng 2002). The most basic approach is simple trial and error. The value of regularization parameter (λ) can be changed until the desired trend is obtained. However, this approach has two significant disadvantages. First, the process of trial and error is tedious, and the result of the desired trend is subjective. The second disadvantage is that trial and error can result in bias.

Another approach could be for the analyst to introduce a mathematically controlled process to determine λ such as something that optimizes the standard deviation of $\hat{y} - y$ — e.g., the optimum λ should yield the minimum value of the standard deviation. For reference, the most common method for determining regularization parameter is generalized cross-validation. Generalized cross-validation is based on "leaving-out-one" principle (Wahba 1990). The concept of this method is calculating N smooth trend of data for specified λ. In each calculation, a single data point is removed and the calculated data point at the omitted position is then compared to the actual removed/omitted data point. The summation of variance of each calculation for given λ is obtained and defined as V_{GCV}. The λ-value that minimizes V_{GCV} is the optimum value for data smoothing by regularization (λ_{opt}) based on generalized cross-validation.

$$\lambda_{opt} = \underset{\lambda}{\arg\min} \left[V_{GCV}(\lambda) \right] \quad \text{(A.9)}$$

The direct calculation of λ_{opt} can be tedious. However, there is an analytical solution for determining $V_{GCV}(\lambda)$ based on Eq. A.10 (Eilers 2003, Lubansky et al. 2006, Stickel 2010).

$$V_{GCV}(\lambda_s) = \frac{\left(\mathbf{M}\hat{\mathbf{y}}^* - \mathbf{y}\right)^T \left(\mathbf{M}\hat{\mathbf{y}}^* - \mathbf{y}\right)/N}{\left[1 - tr(\mathbf{H})/N\right]^2} \quad \text{.....(A.10)}$$

Where:

$$\mathbf{H} = \mathbf{M}\left(\mathbf{M}^T\mathbf{W}\mathbf{M} + \lambda_s\delta^{-1}\mathbf{D}^T\mathbf{U}\mathbf{D}\right)^{-1}\mathbf{M}^T\mathbf{W}$$

$$\delta = \frac{tr\left(\mathbf{D}^T\mathbf{D}\right)}{N^{d+2}}$$

$$\lambda = \lambda_s\delta^{-1}$$

Combining Eq. A.9 and A.10, the value of λ_{opt} can be calculated numerically.

References

Boyd, S. and Vandenberghe, L. 2003. *Convex Optimization*. Cambridge, U.K, Cambridge University Press. (Reprint).

Eilers, P. H. 2003. A perfect smoother. *Analytical chemistry* **75** (14) 3631-3636.

Leong Yeow, Y., C. Ko, W. and P. P. Tang, P. 2000. Solving the Inverse Problem of Couette Viscometry by Tikhonov Regularization. *Journal of Rheology* **44** (6), 1335-1351.

Lubansky, A., Yeow, Y. L., Leong, Y. K. et al. 2006. A general method of computing the derivative of experimental data. *AIChE journal* **52** (1) 323-332.

Stickel, J. J. 2010. Data smoothing and numerical differentiation by a regularization method. *Computers & chemical engineering* **34** (4) 467-475.

Wahba, G. 1990. *Spline Models for Observational Data*: Spline Models for Observational Data, PA:SIAM (Reprint).

Wang, Y. B., Jia, X. Z. and Cheng, J. 2002. A numerical differentiation method and its application to reconstruction of discontinuity. *Inverse Problems* **18** (6) 1461-1476.

Nomenclature

d = derivative order

i = data index

N = number of data pairs

Q = objective function

V_{GCV} = generalized cross-validation variance

x = independent variable

y = dependent variable

$\hat{y}$ = smoothed dependent variable

$\hat{y}^*$ = smoothed dependent variable that minimize objective function (solution)

λ = regularization parameter

λ_{opt} = optimum regularization parameter

$\mathbf{B}$, $\widetilde{\mathbf{B}}$ = integral matrix

$\mathbf{D}^{(d)}$ = finite-difference matrix

$\mathbf{f}$ = independent variable matrix

$\mathbf{M}$ = mapping matrix

$\mathbf{W}$ = weighting matrix for goodness-of-fit

$\mathbf{U}$ = weighting matrix for roughness

APPENDIX B

NUMERICAL DERIVATIVE AND INTEGRAL FORMULATIONS

The formulas for numerical derivatives and integrals are presented below:

Numerical Derivatives

Given the set of pair of data per following

f_i for $i = 1,2,...,N$

x_i for $i = 1,2,...,N$

$x_i < x_{i+1}$

Numerical derivatives can be calculated by finite-difference method in Eq. B.1.

$$f'(x_i) \approx f_i' = \frac{-f_{i-1} + f_i}{-x_{i-1} + x_i} \quad \text{..... (B.1)}$$

In matrix notation forms, Eq. B.1 can be shown as

$$\begin{bmatrix} f_1' \\ \vdots \\ f_{N-1}' \end{bmatrix} = \begin{bmatrix} (-x_1 + x_2)^{-1} & 0 & & \\ 0 & (-x_2 + x_3)^{-1} & 0 & \vdots \\ \vdots & & \ddots & \\ 0 & \cdots & 0 & (-x_{N-1} + x_N)^{-1} \end{bmatrix} \begin{bmatrix} -1 & 1 & 0 & \cdots & \\ 0 & -1 & 1 & 0 & \vdots \\ & & \ddots & \ddots & \\ 0 & \cdots & 0 & -1 & 1 \end{bmatrix} \begin{bmatrix} f_1 \\ \vdots \\ f_N \end{bmatrix}$$

$$\mathbf{f}' = \mathbf{V}^{(1)}\hat{\mathbf{D}}^{(1)}\mathbf{f}$$

$$\mathbf{f}' = \mathbf{D}^{(1)}\mathbf{f}$$

Apply Eq. B.1 again for second derivative, obtain

$$f''(x_i) \approx f_i'' = 2\left[\frac{-f_{i-1}' + f_i'}{-x_{i-1} + x_{i+1}}\right]$$

In matrix notation forms, obtain

$$\begin{bmatrix} f_2'' \\ \vdots \\ f_{N-1}'' \end{bmatrix} = \begin{bmatrix} (-x_1+x_3)^{-1} & 0 & & \\ 0 & (-x_2+x_4)^{-1} & 0 & \vdots \\ \vdots & & \ddots & \\ 0 & \cdots & 0 & (-x_{N-2}+x_N)^{-1} \end{bmatrix} \begin{bmatrix} -1 & 1 & 0 & \cdots & \\ 0 & -1 & 1 & 0 & \vdots \\ & & \ddots & \ddots & \\ 0 & \cdots & 0 & -1 & 1 \end{bmatrix} \begin{bmatrix} f_1' \\ \vdots \\ f_{N-1}' \end{bmatrix}$$

$$\mathbf{f}'' = 2\mathbf{V}^{(2)}\hat{\mathbf{D}}^{(1)}\mathbf{f}' = 2\mathbf{V}^{(2)}\hat{\mathbf{D}}^{(1)}\mathbf{D}^{(1)}\mathbf{f}$$

$$\mathbf{f}'' = \mathbf{D}^{(2)}\mathbf{f}$$

By repeating the same steps, we obtain

$$f^{(d)}(x_i) \approx f_i^{(d)} = d\left[\frac{-f_{i-1}^{(d-1)} + f_i^{(d-1)}}{-x_{i-\left\lceil \frac{d}{2} \right\rceil} + x_{i+\left\lfloor \frac{d}{2} \right\rfloor}}\right] \quad \text{..... (B.2)}$$

where $\lceil \cdot \rceil$ and $\lfloor \cdot \rfloor$ are ceiling and flooring operations.

In matrix notation form, we obtain

$$\mathbf{f}^{(d)} = d\mathbf{V}^{(d)}\hat{\mathbf{D}}^{(1)}\mathbf{f}^{d-1} = d\mathbf{V}^{(d)}\hat{\mathbf{D}}^{(1)}\mathbf{D}^{(d-1)}\mathbf{f}$$

$$\mathbf{f}^{(d)} = \mathbf{D}^{(d)}\mathbf{f} \quad \text{..... (B.3)}$$

where $\mathbf{f} \in \Re^N$ and $\mathbf{f}^{(d)} \in \Re^{N-d}$.

Numerical Integrals

Given the set of pair of data per following

f_i for $i = 1,2,...,N$

x_i for $i = 1,2,...,N$

$x_i < x_{i+1}$

By trapezoidal rule, we obtain

$$\int_{x_1}^{x_N} |f(x)|^2 dx \approx \frac{1}{2}(-x_1 + x_2) f_1^2 + \frac{1}{2}\sum_{i=2}^{N-1}(-x_{i-1} + x_{i+1}) f_i^2 + \frac{1}{2}(-x_{N-1} + x_N) f_N^2$$

$$= \frac{1}{2}\begin{bmatrix} f_1 \\ \vdots \\ f_N \end{bmatrix}^T \begin{bmatrix} (-x_1 + x_2) & 0 & & & \\ 0 & (-x_1 + x_3) & 0 & \vdots & \vdots \\ \vdots & & \ddots & (-x_{N-2} + x_N) & \\ 0 & \cdots & 0 & 0 & (-x_{N-1} + x_N) \end{bmatrix} \begin{bmatrix} f_1 \\ \vdots \\ f_N \end{bmatrix}$$

$$\int_{x_1}^{x_N} |f(x)|^2 dx \approx \mathbf{f}^T \mathbf{B} \mathbf{f} \quad \text{..... (B.4)}$$

Note that the ½ factor is included in $\mathbf{B}$.

References

Stickel, J. J. 2010. Data smoothing and numerical differentiation by a regularization method. *Computers & chemical engineering* **34** (4) 467-475.

Nomenclature

d	=	derivative order
f	=	dependent variable
x	=	independent variable
$\mathbf{B}$	=	integral matrix
$\mathbf{D}^{(d)}$	=	finite-difference matrix
$\mathbf{f}$	=	independent variable matrix
$\mathbf{f}^{(d)}$	=	derivative of order d^{th} of independent variable matrix
$\mathbf{V}^{(d)}$	=	finite-difference matrix

APPENDIX C

TRANSIENT FLOW SOLUTIONS USED IN THIS STUDY

The constant rate transient flow solutions used in this this study are summarized below.

Vertical Well — Infinite-Acting Reservoir:

(With wellbore storage and skin effects (IARF))

$$P_D(t_D) = \frac{4}{\pi^2}\int_0^\infty \frac{\left(1-e^{-u^2 t_D}\right)du}{u^3\left\{\left[uC_D J_0(u)-\left(1-C_D su^2\right)J_1(u)\right]^2+\left[uC_D Y_0(u)-\left(1-C_D su^2\right)Y_1(u)\right]^2\right\}} \quad \text{..... (C.1)}$$

$$P_{Dd} = \frac{4t_D}{\pi^2}\int_0^\infty \frac{e^{-u^2 t_D}du}{u\left\{\left[uC_D J_0(u)-\left(1-C_D su^2\right)J_1(u)\right]^2+\left[uC_D Y_0(u)-\left(1-C_D su^2\right)Y_1(u)\right]^2\right\}} \quad \text{..... (C.2)}$$

Where the dimensionless variables for this case are defined in terms of field units as:

$$t_D = 2.637x10^{-4}\frac{kt}{\phi c_t \mu . r_w^2} \qquad P_D = \frac{1}{141.2}\frac{kh}{qB\mu}\left(p_i - p_{wf}\right) \qquad C_D = \frac{0.8936C}{\phi c_t h r_w^2}$$

Vertical Well — Infinite-Acting, Naturally-Fractured/Dual Porosity Reservoir:

(No wellbore storage or skin effects (dual porosity - DUAL))

$$P_D(t_D) = \frac{1}{2}\ln\left[\frac{4}{e^\gamma}t_D\right] - \frac{1}{2}E_1\left[\frac{\lambda_f}{\omega(1-\omega)}t_D\right] + \frac{1}{2}E_1\left[\frac{\lambda_f}{(1-\omega)}t_D\right] \quad \text{..... (C.3)}$$

$$P_{Dd} = \frac{1}{2} + \frac{1}{2}\exp\left[\frac{-\lambda_f}{\omega(1-\omega)}t_D\right] - \frac{1}{2}\exp\left[\frac{-\lambda_f}{(1-\omega)}t_D\right] \quad \text{..... (C.4)}$$

Where the dimensionless variables for this case are defined in terms of field units as:

$$t_D = 2.637x10^{-4}\frac{kt}{\left(\phi_{fb}c_{tfb} + \phi_{ma}c_{ma}\right)\mu . r_w^2} \qquad P_D = \frac{1}{141.2}\frac{kh}{qB\mu}\left(p_i - p_{wf}\right)$$

$$\omega = \frac{\phi_{fb} c_{tfb}}{\phi_{fb} c_{tfb} + \phi_{ma} c_{ma}} \qquad \lambda_f = 12 \frac{r_w^2}{h_{ma}^2} \frac{k_{ma}}{k_{fb}}$$

Vertical Well with an Infinite Conductivity Vertical Fracture — Infinite-Acting Reservoir:

(No wellbore storage or skin effects (HF))

$$P_D\left(t_{Df}\right) = \frac{\sqrt{\pi t_{Dxf}}}{2}\left[erf\left[\frac{1-x_D}{2\sqrt{t_{Dxf}}}\right] + erf\left[\frac{1+x_D}{2\sqrt{t_{Dxf}}}\right] + \frac{\left(1-x_D\right)}{4} E_1\left[\frac{\left(1-x_D\right)^2}{4t_{Dxf}}\right] + \frac{\left(1+x_D\right)}{4} E_1\left[\frac{\left(1+x_D\right)^2}{4t_{Dxf}}\right]\right] \quad \text{..... (C.5)}$$

$$P_{Dd}\left(t_{Df}\right) = \frac{\sqrt{\pi t_{Dxf}}}{4}\left[erf\left[\frac{1-x_D}{2\sqrt{t_{Dxf}}}\right] + erf\left[\frac{1+x_D}{2\sqrt{t_{Dxf}}}\right]\right] \quad \text{..... (C.6)}$$

Where the dimensionless variables for this case are defined in terms of field units as:

$$t_{Dxf} = 2.637x10^{-4} \frac{kt}{\phi c_t \mu . x_f^2} \qquad P_D = \frac{1}{141.2} \frac{kh}{qB\mu}\left(p_i - p_{wf}\right) \qquad x_D = \frac{x}{x_f}$$

(x_D=0 for uniform-flux and x_D=0.732 for infinite conductivity)

References

Agarwal, R. G., Al-Hussainy, R. and Ramey, H. J., Jr. 1970. An Investigation of Wellbore Storage and Skin Effect in Unsteady Liquid Flow: I. Analytical Treatment. *SPEJ* (September 1970).

Cinco-Ley, H. and Samaniego-V, F. 1981. Transient Pressure Analysis for Fractured Wells. *JPT* (September 1981) 1749.

Warren, J. E. and Root, P. J. 1963. The Behavior of Naturally Fractured Reservoirs. *SPEJ* (September 1963) 245-55; Trans., AIME, 228.

APPENDIX D

SUMMARY OF FIELD DATA USED IN THIS STUDY

In this appendix, we summarize the data that we use in field data evaluation. There are three cases

a. Bourdet pressure build up data
b. Oscillating surface pressure data from fall off test
c. Rate transient data for oil well

For Bourdet pressure build up data, we use the data from Table 2 in SPE-12777-PA article (Bourdet et al. 1989). Since it can be found in original publication, we will not show the data in this work. For oscillating surface pressure data from fall off test case, the data is obtained from pressure gauge which has 1 second frequency. Publishing all the data here is not possible due to number of data points. It will be provided as separate data file attached to this thesis.

The last case of rate transient data for oil well consists of production data for 713 days. This data is courtesy of Reservoir Development Company/DFITpro.com and provided by Dr. David P. Craig. It is shown in **Table D. 1**.

Table D. 1 — Rate transient data for oil well

Time (days)	Production rate (STB/d)	Flowing pressure (psi)	Time (days)	Production rate (STB/d)	Flowing pressure (psi)
0	475.0759	3394.2058	357	176.0707	2914.0441
1	412.5517	3359.6605	358	146.8300	2877.5676
2	526.5517	3611.7370	359	218.2652	2973.4417
3	638.0690	3664.8700	360	206.0666	2890.4483
4	444.4138	3617.1284	361	211.7866	2875.0133
5	548.2759	3612.3887	362	218.7734	2910.7790
6	685.6552	3614.7671	363	219.2331	2868.9953
7	552.4138	3618.4917	364	209.6910	2872.2639
8	628.1379	3614.8697	365	115.9186	2898.8601
9	496.1379	3637.1077	366	317.9745	3217.9806
10	485.7931	3664.1574	367	213.7845	2940.6430
11	663.3103	3663.9225	368	198.0569	2953.1207
12	549.1034	3668.4727	369	199.4121	2980.6498
13	711.7241	3665.4194	370	207.8435	3039.0205

Time (days)	Production rate (STB/d)	Flowing pressure (psi)	Time (days)	Production rate (STB/d)	Flowing pressure (psi)
14	482.8965	3568.6268	371	193.6510	3045.7587
15	648.8276	3562.5784	372	196.7293	2836.9302
16	788.6897	3566.7850	373	196.2541	3030.4818
17	783.7241	3520.4028	374	189.2672	3050.1509
18	758.4828	3494.9050	375	193.3079	2911.2032
19	438.2414	3468.7497	376	204.4797	2893.5192
20	179.5862	3458.2458	377	199.3735	2852.8253
21	1.0000	3456.1237	378	206.4876	2868.8626
22	1.0000	3455.0434	379	197.4121	2850.4021
23	168.5517	3455.0434	380	188.6797	2758.4696
24	461.4483	3587.7315	381	188.2648	2900.8120
25	451.3103	3627.9435	382	185.1248	3063.3280
26	477.4138	3614.5602	383	193.2028	2878.8449
27	590.6207	3588.7940	384	177.2745	2884.7722
28	722.4483	3574.3176	385	193.5434	3055.6333
29	711.3448	3528.4283	386	166.3624	2869.1474
30	811.7931	3489.5805	387	154.3883	3152.3039
31	824.9310	3415.7532	388	189.5517	3037.6935
32	825.6552	3400.9882	389	132.3710	2906.4172
33	757.8966	3386.8149	390	184.5945	2938.3489
34	779.2759	3355.1602	391	159.3214	2934.0004
35	422.6897	3346.7205	392	186.4314	2917.7425
36	525.3103	3391.0053	393	190.0193	2861.2412
37	513.1724	3389.2206	394	173.3465	3045.5384
38	513.7931	3388.9322	395	169.5910	2907.6350
39	511.0690	3407.2011	396	184.6645	2895.6994
40	506.7586	3418.2914	397	189.2545	2895.4039
41	509.1034	3411.0925	398	172.9666	2909.2160
42	509.6552	3407.0910	399	185.6979	2892.5880
43	512.2069	3398.9912	400	177.3741	3021.9652
44	517.7586	3411.2200	401	183.9328	2858.2197
45	519.2414	3412.3651	402	138.7179	2830.2750
46	478.5862	3422.5402	403	178.1910	2879.9845
47	481.7586	3402.3372	404	184.6283	2921.3348
48	481.1724	3426.7446	405	180.9635	2795.0110
49	490.0690	3431.8010	406	159.1372	2865.6137
50	486.4483	3395.4969	407	187.2400	2875.1683
51	483.3103	3396.4290	408	180.1438	2886.2197
52	466.8966	3434.8906	409	162.1259	2858.5988
53	486.3448	3418.3037	410	182.4741	2883.7126
54	486.0345	3417.7221	411	180.3090	2892.3412
55	465.6207	3450.1594	412	180.0148	3020.1632
56	439.0345	3438.5542	413	174.4969	2830.2301
57	459.9655	3474.4811	414	179.1255	2864.9574
58	543.0345	3484.0481	415	178.0107	3020.6075
59	510.9310	3478.8727	416	179.3693	2970.3937
60	464.7586	3487.2238	417	170.3607	2826.1414
61	507.6207	3500.3682	418	180.1379	2967.2819
62	497.7931	3497.2814	419	179.0938	2788.1901
63	554.4138	3478.8103	420	180.3331	2929.5059
64	574.0690	3510.5728	421	189.5817	2919.4952
65	546.6897	3504.9900	422	169.8621	3006.5227
66	477.4138	3489.0984	423	174.8690	2840.1620
67	554.0690	3398.2546	424	162.9969	2995.8684
68	542.5172	3388.9105	425	179.9069	2990.0365

Time (days)	Production rate (STB/d)	Flowing pressure (psi)	Time (days)	Production rate (STB/d)	Flowing pressure (psi)
69	509.4138	3454.5320	426	173.5266	2772.8794
70	496.4138	3469.9572	427	166.5397	2849.8835
71	509.7586	3463.5741	428	174.9479	2840.7067
72	461.0690	3419.2746	429	169.4886	2859.7109
73	509.0690	3425.2745	430	171.1907	2842.6060
74	449.4483	3434.4675	431	183.0341	2845.0732
75	473.7241	3411.8432	432	172.4469	2884.7639
76	499.2759	3364.7025	433	160.0624	2865.9842
77	478.6897	3387.5942	434	168.6424	2878.2163
78	480.7241	3390.1698	435	162.7876	2865.1155
79	351.9655	3405.4273	436	154.9928	2818.8318
80	466.9310	3398.7916	437	172.1990	2827.1578
81	429.5862	3373.6820	438	140.9235	2970.3266
82	472.7586	3354.6308	439	161.2169	2905.7823
83	502.4483	3357.5804	440	174.6869	2840.8840
84	452.4483	3385.6391	441	173.4669	2858.7697
85	455.1379	3383.5114	442	176.3200	2884.1945
86	454.9310	3352.1242	443	168.9569	2863.2246
87	490.7931	3358.2064	444	199.2910	2807.3358
88	463.3103	3370.1574	445	179.3100	2807.6934
89	435.4483	3362.4451	446	173.3834	2746.4421
90	451.1379	3363.8815	447	177.8845	2938.6481
91	417.5862	3363.1972	448	181.0455	2811.9901
92	453.7241	3373.6602	449	207.1448	2775.3436
93	447.5862	3338.9052	450	200.1286	2804.7503
94	419.7586	3350.9486	451	175.0803	2928.7077
95	464.5862	3349.3584	452	189.3997	2811.4879
96	347.6552	3353.3431	453	192.8176	2822.5234
97	453.1724	3355.1016	454	195.6183	2879.8641
98	428.3448	3332.8059	455	172.9917	2770.4915
99	418.0000	3353.5909	456	169.1421	2769.9900
100	423.0345	3250.8812	457	165.0272	2830.2274
101	419.5172	3289.5568	458	192.9652	2802.5053
102	417.8276	3304.7088	459	177.1959	2790.0870
103	415.4828	3281.3317	460	185.6962	2789.9017
104	391.5862	3292.4493	461	177.6072	2806.8242
105	389.7241	3314.3076	462	189.8790	2798.4417
106	412.8621	3348.7691	463	164.2524	2811.0789
107	376.3448	3337.0458	464	156.7100	2795.0140
108	394.5172	3350.5463	465	192.4369	2744.5555
109	382.3448	3343.7883	466	207.3438	2914.9706
110	360.6552	3336.4550	467	150.4014	2813.0508
111	388.8276	3283.2872	468	142.4807	2740.7520
112	381.1379	3269.5981	469	179.0997	2808.8210
113	375.1379	3322.2274	470	173.4435	2783.9712
114	376.4483	3284.5666	471	175.0386	2797.8115
115	377.2759	3336.3448	472	182.7938	2853.4094
116	363.2759	3291.7110	473	178.1776	2797.2154
117	369.0690	3308.7069	474	160.5710	2750.8740
118	340.2069	3256.0320	475	183.1469	2763.4283
119	407.7241	3297.1367	476	169.6872	2800.2514
120	347.1034	3291.2800	477	168.2721	2779.7677
121	378.1034	3271.8816	478	184.6172	2784.4290
122	373.5862	3247.0617	479	168.7707	2827.1302
123	396.9310	3272.3575	480	171.0238	2804.1797

Time (days)	Production rate (STB/d)	Flowing pressure (psi)	Time (days)	Production rate (STB/d)	Flowing pressure (psi)
124	337.1379	3252.4957	481	154.6083	2787.9622
125	257.0345	3237.1915	482	186.7693	2874.6521
126	246.4828	3255.2386	483	165.7462	2837.0824
127	302.6024	3282.5020	484	156.0869	2812.4343
128	357.7638	3264.5339	485	178.5545	2850.9786
129	321.7828	3253.1473	486	169.1400	2762.6896
130	311.1379	3246.2544	487	172.5993	2765.5031
131	267.2234	3225.2858	488	187.2490	2693.1277
132	280.6683	3252.1542	489	147.8562	2797.6145
133	246.8376	3214.1203	490	156.7697	2794.8460
134	223.9972	3223.2873	491	158.2755	2700.4445
135	227.8428	3268.1727	492	147.3138	2870.7238
136	398.2307	3189.7902	493	153.7310	2876.4466
137	243.9528	3231.3613	494	165.3283	2777.6161
138	310.9886	3213.9462	495	135.8169	2783.3449
139	295.4866	3243.1748	496	154.8145	2795.9069
140	338.3562	3226.6635	497	153.1290	2732.4956
141	144.3759	3226.5504	498	153.5903	2774.2193
142	89.9603	3204.8572	499	152.6903	2800.0473
143	13.2359	3194.5592	500	148.8879	2711.1751
144	267.6617	3197.7909	501	151.2631	2817.9854
145	298.4359	3191.4937	502	149.1259	2767.5412
146	367.5227	3190.0959	503	150.5035	2776.8662
147	309.1493	3166.0412	504	149.4966	2830.5008
148	314.6983	3195.6183	505	145.9983	2762.1405
149	232.0524	3182.7970	506	152.9224	2777.5411
150	336.9466	3169.6207	507	140.0217	2841.3793
151	309.8965	3171.8912	508	152.7972	2865.5290
152	306.0528	3169.7055	509	142.2662	2833.4412
153	325.2221	3203.1157	510	138.7117	2809.9825
154	318.2155	3189.6033	511	150.0334	2772.4471
155	321.1397	3175.5399	512	144.6728	2789.1495
156	318.9338	3173.9523	513	142.5710	2795.1733
157	315.6283	3187.1732	514	140.3748	2824.5788
158	324.2507	3171.4237	515	152.7172	2855.8446
159	333.7734	3202.4870	516	150.2541	2893.8793
160	332.8862	3193.5765	517	147.9448	2719.6906
161	324.8859	3215.9974	518	145.4100	2769.0209
162	301.3224	3158.9062	519	138.0876	2813.6354
163	303.0452	3158.5251	520	137.2238	2807.0239
164	307.8652	3169.9420	521	136.6472	2883.2328
165	308.1059	3187.4614	522	138.1341	2902.4813
166	300.7783	3139.7927	523	135.7841	2763.2075
167	305.2576	3148.5177	524	139.8417	2774.8715
168	302.8214	3162.8852	525	140.8297	2926.2930
169	300.5110	3168.6583	526	138.8790	2797.6992
170	303.0703	3132.4566	527	144.5993	2801.3048
171	302.8914	3156.5712	528	162.7172	2714.8404
172	305.9148	3127.4936	529	158.0793	2803.1746
173	289.3052	3160.5688	530	162.3290	2724.8002
174	295.5117	3149.8443	531	158.6541	2787.9893
175	294.2645	3155.0610	532	161.4717	2891.6162
176	292.3945	3134.6869	533	154.9514	2684.1015
177	295.2914	3132.9201	534	160.2465	2718.9190
178	288.7038	3145.4040	535	162.9872	2875.0680

Time (days)	Production rate (STB/d)	Flowing pressure (psi)	Time (days)	Production rate (STB/d)	Flowing pressure (psi)
179	289.4641	3130.0687	536	155.6969	2740.7695
180	285.7710	3142.5198	537	156.5855	2895.7743
181	281.6583	3136.8845	538	158.1507	2813.0405
182	290.6614	3134.3836	539	148.4945	2803.7178
183	282.5307	3130.3323	540	145.6807	2745.1793
184	279.5334	3133.3498	541	139.0583	2748.6578
185	286.2690	3119.3499	542	143.8283	2874.6251
186	277.7210	3117.9363	543	146.5024	2807.5478
187	284.0607	3096.1652	544	143.7400	2722.2314
188	282.7714	3130.8116	545	147.5652	2897.5339
189	279.6907	3130.4467	546	155.6962	2726.6892
190	277.2483	3113.8835	547	146.7100	2806.1420
191	286.3845	3125.9432	548	153.3507	2757.7922
192	290.2610	3133.9871	549	145.8869	2751.8896
193	282.2138	3148.1212	550	152.5652	2728.8919
194	268.0941	3136.7192	551	138.9314	2885.1322
195	271.7241	3122.7809	552	147.2862	2728.8259
196	274.9366	3122.8334	553	143.8724	2745.6379
197	271.6200	3135.5646	554	148.9862	2860.3141
198	275.8583	3142.4878	555	143.1997	2740.9733
199	256.0145	3106.4974	556	139.1831	2894.6037
200	261.7914	3097.4905	557	143.4345	2740.5327
201	266.1583	3099.4321	558	144.7493	2739.5206
202	270.2576	3105.4213	559	124.5186	2739.5328
203	266.1145	3095.0087	560	145.8152	2761.4461
204	267.0648	3121.5937	561	141.0955	2761.6354
205	259.1807	3107.7623	562	141.1134	2759.2613
206	269.3793	3101.0220	563	143.1593	2896.3367
207	264.6255	3115.7044	564	144.6338	2774.8283
208	261.5834	3117.1508	565	169.5276	2891.1210
209	255.3552	3097.1010	566	130.2172	2761.8808
210	255.7455	3126.5546	567	120.3617	2791.7656
211	258.2352	3079.0931	568	117.8966	2761.1878
212	255.5445	3098.3349	569	133.5628	2874.3253
213	257.2159	3090.9668	570	141.5383	2750.3036
214	263.7859	3098.6663	571	131.0679	2772.8211
215	260.7610	3118.5314	572	147.5466	2719.5139
216	221.7055	3105.3446	573	136.8738	2720.3701
217	256.1721	3094.1100	574	135.8810	2720.2692
218	257.1345	3100.5123	575	143.6721	2718.8593
219	265.8097	3103.7789	576	148.8021	2727.5829
220	271.3497	3102.6307	577	127.1786	2727.6315
221	250.3107	3104.1035	578	143.4162	2741.4812
222	270.1697	3111.8377	579	159.4917	2717.7542
223	243.8007	3100.9449	580	125.7531	2727.0446
224	245.8024	3085.1022	581	146.2072	2740.2939
225	265.0772	3113.8705	582	126.1245	2710.7645
226	252.2097	3100.6379	583	151.2634	2747.5532
227	249.2410	3089.2938	584	150.3624	2738.8900
228	248.7990	3090.6461	585	134.9914	2756.8873
229	255.3214	3076.6789	586	189.4779	2756.7428
230	252.0407	3101.8933	587	80.9824	2719.5421
231	240.0328	3074.8623	588	111.9021	2725.0159
232	248.7279	3086.4450	589	126.8117	2740.3089
233	251.1110	3076.4441	590	125.6262	2738.9024

Time (days)	Production rate (STB/d)	Flowing pressure (psi)	Time (days)	Production rate (STB/d)	Flowing pressure (psi)
234	238.3472	3056.3395	591	128.2917	2751.4015
235	239.7234	3057.7951	592	125.9452	2744.8735
236	249.6217	3067.0076	593	158.3914	2744.8537
237	251.9090	3040.2570	594	127.0217	2750.3064
238	237.2186	3055.7707	595	123.6962	2750.0133
239	249.1404	3069.7713	596	131.9700	2715.7091
240	244.9283	3093.0850	597	125.5948	2746.0799
241	242.5645	3098.1522	598	130.6548	2926.7503
242	247.4983	3062.2755	599	136.3238	2742.7985
243	240.3748	3073.2850	600	144.9907	2738.4006
244	253.3645	3065.8569	601	132.9338	2942.1921
245	243.3252	3069.5212	602	143.9565	2942.0816
246	244.7404	3074.0423	603	143.8493	2724.4263
247	244.3552	3068.8239	604	144.8972	2728.1776
248	236.9752	3068.2390	605	119.0441	2778.5826
249	271.6790	3060.5741	606	113.0200	2725.3864
250	190.3469	3069.6689	607	137.2659	2799.6937
251	241.5017	3088.9487	608	138.3234	2799.8913
252	254.4000	3084.1360	609	126.9414	2794.5210
253	241.6186	3050.9124	610	139.2641	2773.9795
254	234.1248	3061.9171	611	137.8824	2793.0188
255	247.8448	3057.3928	612	129.7724	2869.7100
256	238.4362	3070.4930	613	132.1224	2748.0441
257	241.1183	3047.7873	614	124.8431	2746.0812
258	241.1972	3062.0223	615	133.7914	2792.1899
259	238.3310	3057.3650	616	130.0521	2740.8319
260	231.2224	3044.4086	617	144.6779	2932.7373
261	236.3079	3055.1357	618	131.1314	2924.3624
262	236.1252	3046.2436	619	131.1438	2930.8821
263	233.1321	3055.0908	620	128.9838	2922.0189
264	230.2110	3045.3864	621	132.1941	2922.0007
265	239.4100	3035.9161	622	130.5224	2881.7927
266	223.7997	3052.5709	623	124.4445	2881.7788
267	289.0648	3043.1653	624	122.6459	2777.3495
268	299.9028	2983.8796	625	120.7338	2777.3348
269	283.9672	2983.5791	626	124.6600	2864.7831
270	281.8159	2968.0727	627	123.3007	2864.8149
271	276.4234	2984.2383	628	123.9341	2939.0879
272	276.4955	2958.9894	629	130.0928	2942.1284
273	269.9607	2963.5320	630	128.2545	2942.1802
274	270.8183	2961.6952	631	122.0976	2921.9945
275	271.2366	2958.3268	632	121.1879	2889.4048
276	272.4548	2954.1373	633	121.7117	2889.3975
277	271.6076	2959.6337	634	124.2866	2766.3370
278	261.1859	2967.0751	635	120.9366	2794.9929
279	256.3259	2959.1154	636	132.7103	2799.9886
280	270.1921	2948.6799	637	112.3724	2788.2843
281	260.7334	2971.8298	638	60.5276	2788.1215
282	200.1659	2966.3387	639	42.0231	2787.8326
283	280.0903	2980.6762	640	93.1114	2866.9490
284	276.1972	2941.9137	641	119.3576	2871.9428
285	254.6221	2951.2973	642	122.3083	2991.9641
286	43.3145	2958.9114	643	136.4162	2974.6305
287	211.1965	2617.5423	644	94.8269	2974.7489
288	243.8490	3013.6697	645	108.6652	2947.6350

Time (days)	Production rate (STB/d)	Flowing pressure (psi)	Time (days)	Production rate (STB/d)	Flowing pressure (psi)
289	312.0169	3310.1326	646	103.4845	2788.9117
290	245.9969	2968.9791	647	110.4803	2796.2370
291	249.1224	3193.6399	648	108.9255	2824.6700
292	257.3728	2950.7905	649	104.9955	2989.3220
293	261.3455	2945.4252	650	139.9979	2826.1514
294	262.3376	2955.3905	651	114.6031	2786.4808
295	260.2976	2950.6283	652	115.9697	2965.5909
296	243.3766	2971.5763	653	122.9176	2860.7798
297	262.6224	3105.5732	654	128.4169	2774.9982
298	240.5276	3000.7333	655	122.4628	2806.7057
299	244.0945	3019.9892	656	106.5169	2927.6619
300	247.3528	2940.2318	657	120.6193	2925.3218
301	233.9669	3088.2921	658	129.1928	2813.8881
302	246.3021	2936.4906	659	117.6572	2947.8863
303	139.5421	2943.2969	660	128.1462	2950.7056
304	236.8490	3039.9927	661	115.8976	2891.6768
305	250.6728	2932.0985	662	118.4676	2825.8730
306	236.8583	2936.4811	663	120.3331	2790.5055
307	246.7097	2816.2449	664	123.4531	2809.6809
308	242.7786	2935.7242	665	113.7845	2938.6308
309	257.5059	2930.6593	666	141.5983	2786.9679
310	239.3335	2934.8237	667	106.3645	2936.6901
311	231.1159	2928.5149	668	124.6345	2851.2559
312	228.0414	2936.6858	669	111.8310	2965.2109
313	232.7924	2958.7858	670	115.5476	2801.3183
314	230.4452	3069.0096	671	129.4221	2796.5580
315	214.5676	2911.8384	672	120.5472	2814.1854
316	126.8283	2918.2729	673	116.4441	2887.1805
317	228.5803	2974.3113	674	141.2507	2797.2692
318	230.3141	2940.7258	675	112.7103	2797.4786
319	237.1310	2979.2006	676	119.7776	2813.9405
320	231.5490	2975.4551	677	118.3014	2810.9523
321	220.1159	2822.4688	678	117.2490	2944.8747
322	242.8245	2926.9738	679	116.2038	2773.0848
323	184.3617	2932.9927	680	124.3562	2781.2573
324	220.5321	2984.5674	681	117.7452	2795.2283
325	227.2476	2933.2749	682	110.8741	2916.6625
326	229.8766	2922.6363	683	111.3893	2808.2015
327	223.7000	2919.6458	684	110.0093	2806.8068
328	231.2076	2921.8963	685	107.6776	2806.7969
329	224.9848	2917.3306	686	116.6262	2822.3130
330	225.9272	2923.5435	687	117.2800	2785.3452
331	213.8621	2913.6423	688	110.4748	2785.3502
332	215.4635	2961.8590	689	118.1962	2785.2998
333	178.0221	2969.6893	690	113.5810	2810.3585
334	188.4472	3032.1226	691	112.8221	2936.4563
335	179.8624	3214.4019	692	110.1328	2936.4508
336	86.2497	2976.8296	693	117.8728	2811.3500
337	1.0000	3268.2178	694	109.5266	2811.4073
338	173.6659	3274.4412	695	119.7890	2817.5405
339	231.9507	3065.3658	696	114.4548	2806.8697
340	230.2569	2985.4023	697	109.1266	2807.8806
341	217.1772	2957.7669	698	111.4766	2800.2475
342	218.3241	2920.1708	699	115.7917	2800.2643
343	224.7103	2944.0840	700	113.6897	2773.8908

Time (days)	Production rate (STB/d)	Flowing pressure (psi)	Time (days)	Production rate (STB/d)	Flowing pressure (psi)
344	214.7379	2925.0578	701	110.0466	2791.6333
345	227.0696	2943.2231	702	104.2524	2844.5099
346	223.4472	2902.8151	703	113.1690	2797.8755
347	217.9841	2903.9287	704	106.4500	2797.9389
348	223.5193	2904.0917	705	100.0897	2796.7265
349	203.3131	2903.3487	706	103.7228	2797.9707
350	212.6231	2913.0070	707	108.5214	2811.6622
351	215.3659	2904.1454	708	99.9334	2811.6956
352	213.9090	2885.0493	709	108.1779	2772.8398
353	231.4752	2901.3592	710	105.8003	2797.9028
354	208.9248	2850.2575	711	100.7879	2824.7487
355	229.7183	2885.3146	712	114.0659	2828.5726
356	220.8593	2877.5416	713	110.1783	2799.3543

References

Bourdet, D., Ayoub, J. A. and Pirard, Y. M. 1989. Use of Pressure Derivative in Well Test Interpretation. *SPEFE* (June 1989) 293-302.

APPENDIX E

SYNTHETIC DATA EVALUATION RESULT

This appendix presents the plots for every case of synthetic data analyzed in this study. There are three analytical solutions used to generate synthetic pressure response in this study which are

a. A vertical well in an infinite-acting reservoir with wellbore storage and skin (IARF)
b. A vertical well in an infinite-acting without wellbore storage and skin in naturally fractured reservoir system (dual porosity - DUAL)
c. A hydraulically fractured vertical well with an infinite fracture conductivity in an infinite-acting reservoir without wellbore storage and skin (HF).

For each analytical solution, we study three cases of noise including noise standard deviation at 0.1%, 1.0% and 5.0%. We calculate pressure derivative by Tikhonov regularization and Bourdet method for each case. Bourdet L values are value between 0.1, 0.2, 0.3 and 0.4 for each case. Therefore, there are total 36 cases of synthetic data evaluation in this study.

A vertical well in an infinite-acting reservoir with wellbore storage and skin (IARF)

The result for a vertical well in an infinite-acting reservoir with wellbore storage and skin is shown in **Fig. E. 1** to **Fig. E. 12**.

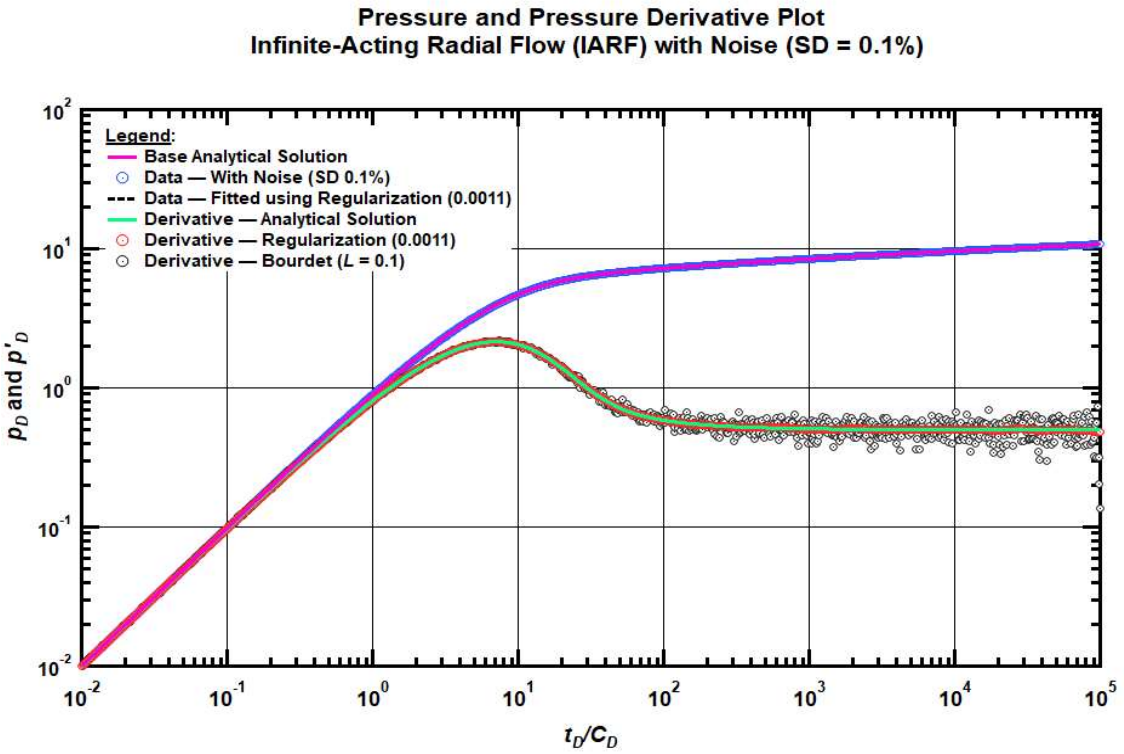

Fig. E. 1 — Pressure and pressure derivative plot for a vertical well in an infinite-acting reservoir with wellbore storage and skin case with noise standard deviation at 0.1%. Bourdet L value = 0.1.

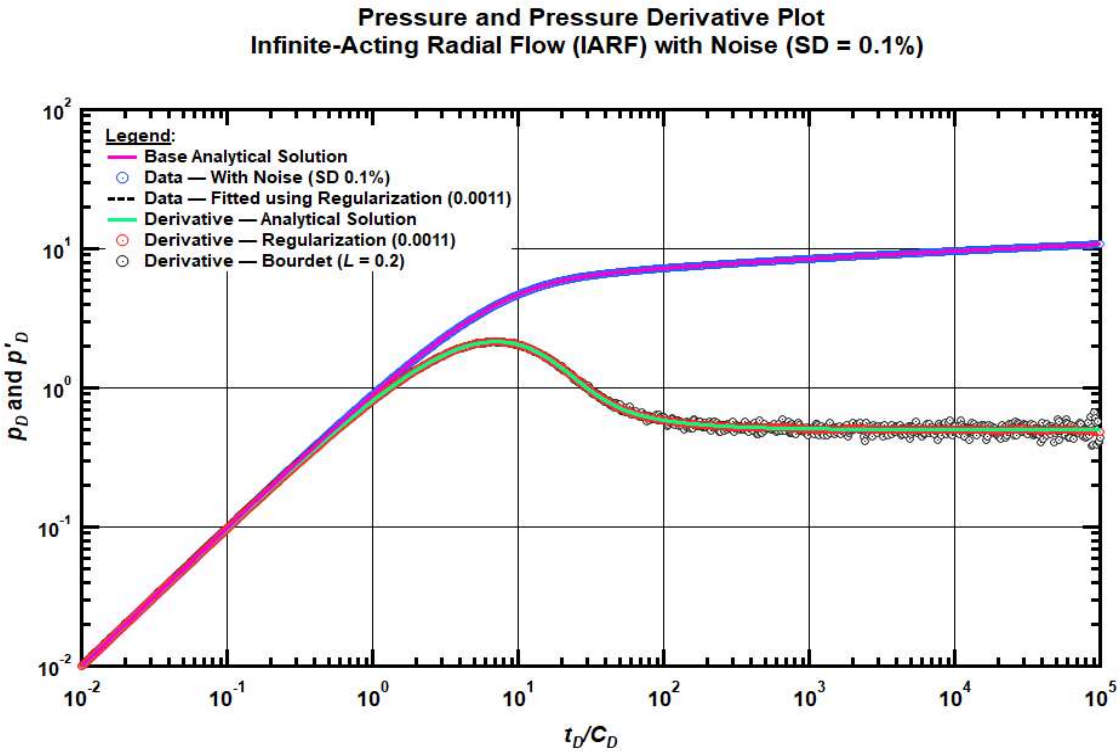

Fig. E. 2 — Pressure and pressure derivative plot for a vertical well in an infinite-acting reservoir with wellbore storage and skin case with noise standard deviation at 0.1%. Bourdet L value = 0.2.

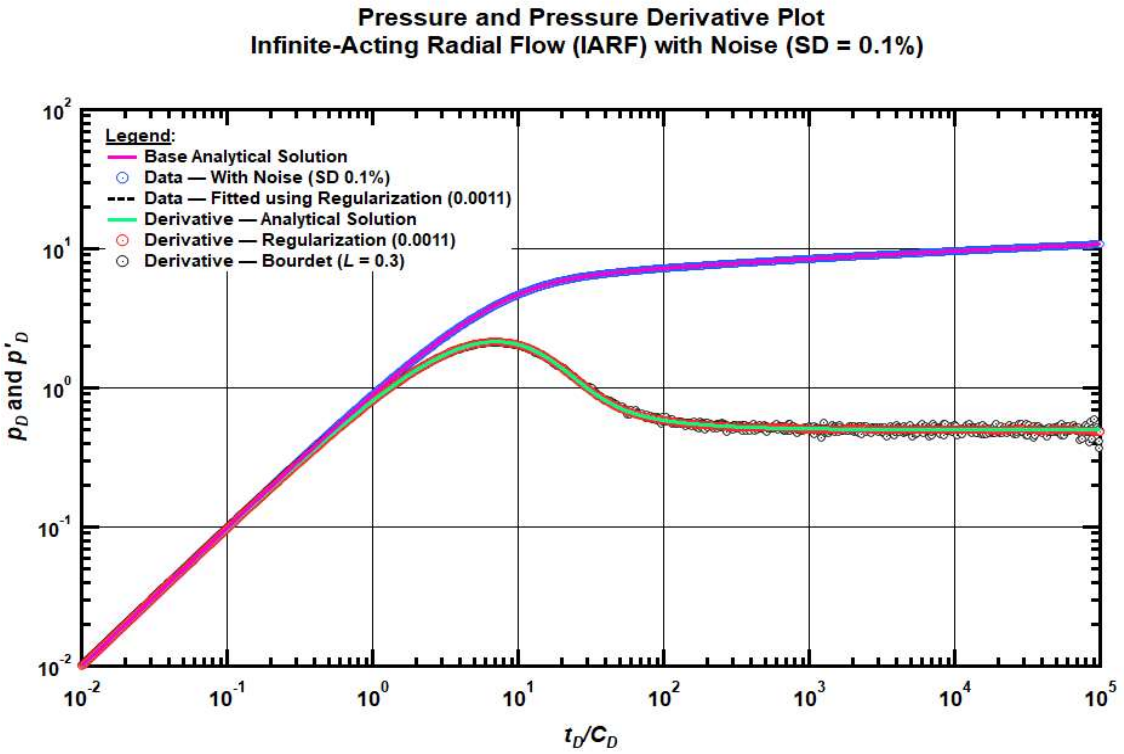

Fig. E. 3 — Pressure and pressure derivative plot for a vertical well in an infinite-acting reservoir with wellbore storage and skin case with noise standard deviation at 0.1%. Bourdet L value = 0.3.

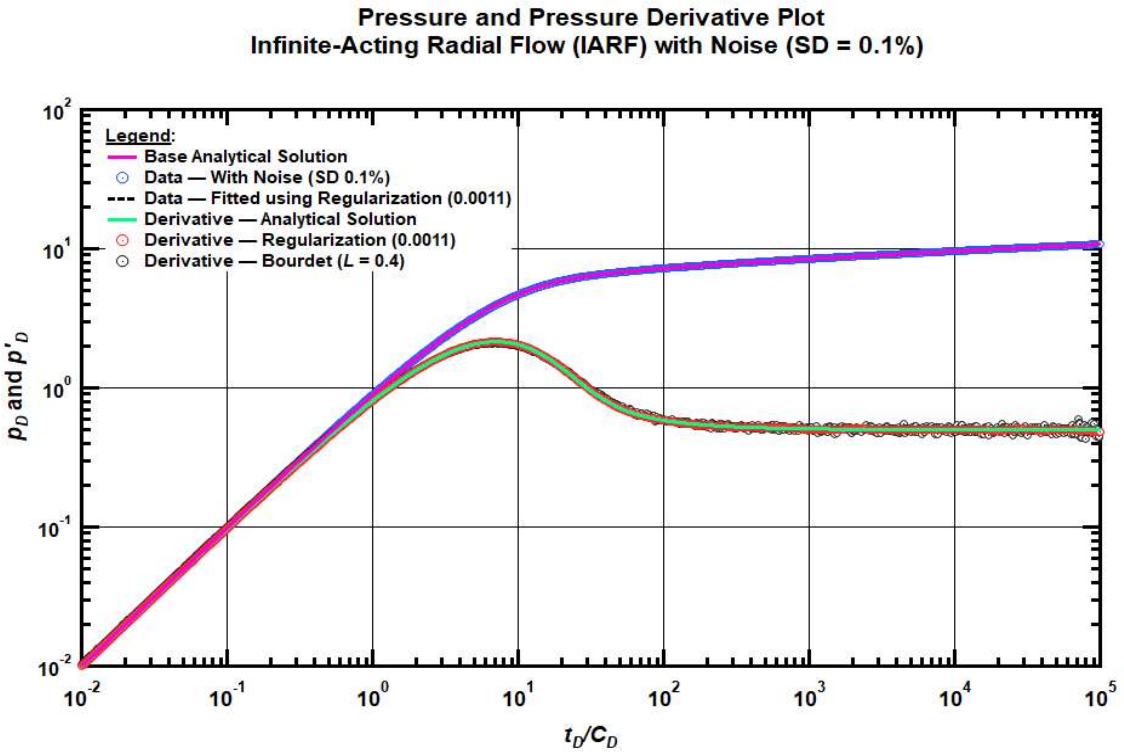

Fig. E. 4 — Pressure and pressure derivative plot for a vertical well in an infinite-acting reservoir with wellbore storage and skin case with noise standard deviation at 0.1%. Bourdet L value = 0.4.

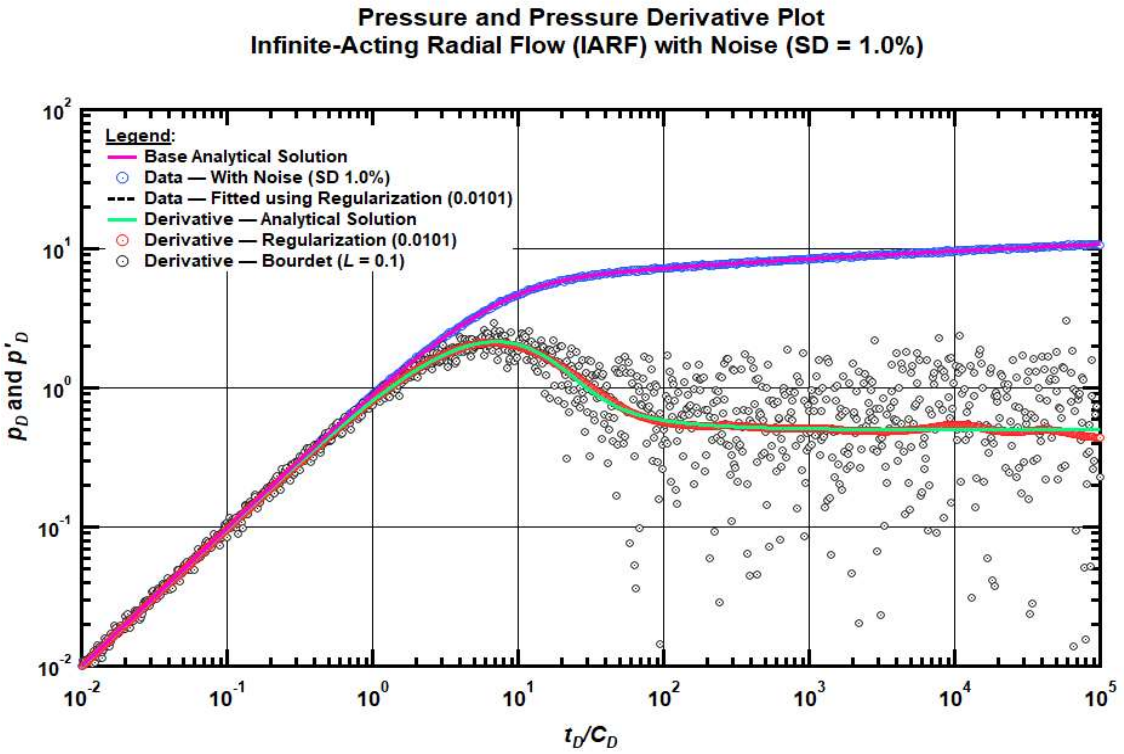

Fig. E. 5 — Pressure and pressure derivative plot for a vertical well in an infinite-acting reservoir with wellbore storage and skin case with noise standard deviation at 1.0%. Bourdet L value = 0.1.

.

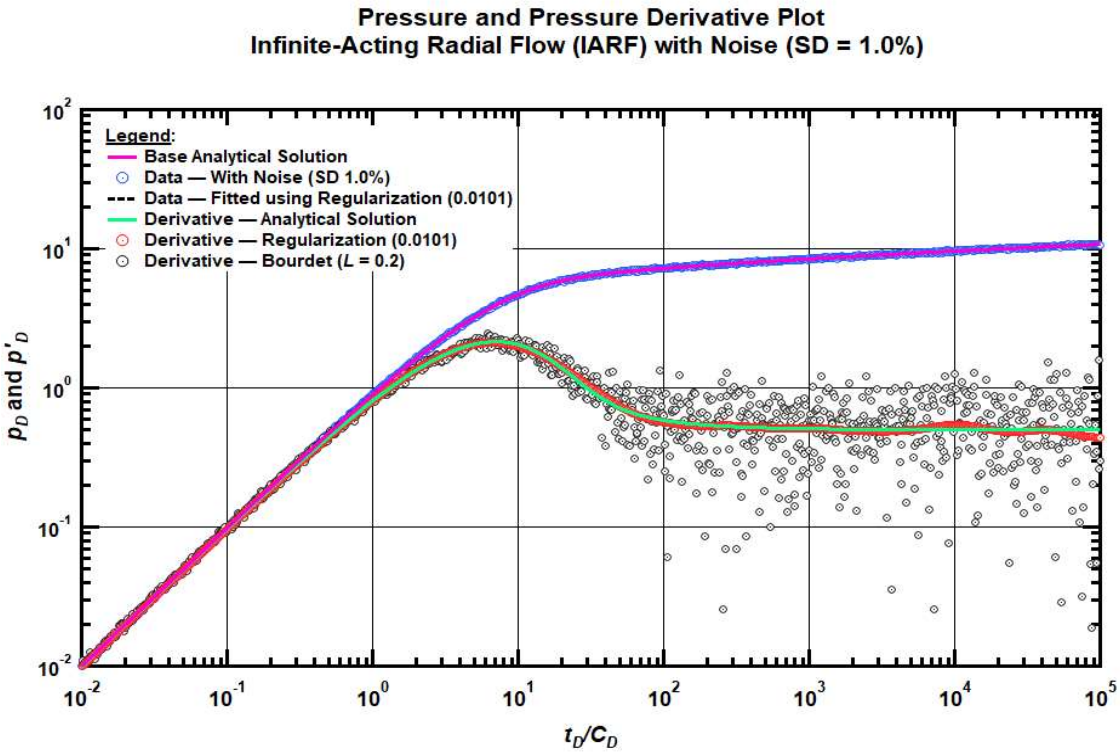

Fig. E. 6 — Pressure and pressure derivative plot for a vertical well in an infinite-acting reservoir with wellbore storage and skin case with noise standard deviation at 1.0%. Bourdet L value = 0.2.

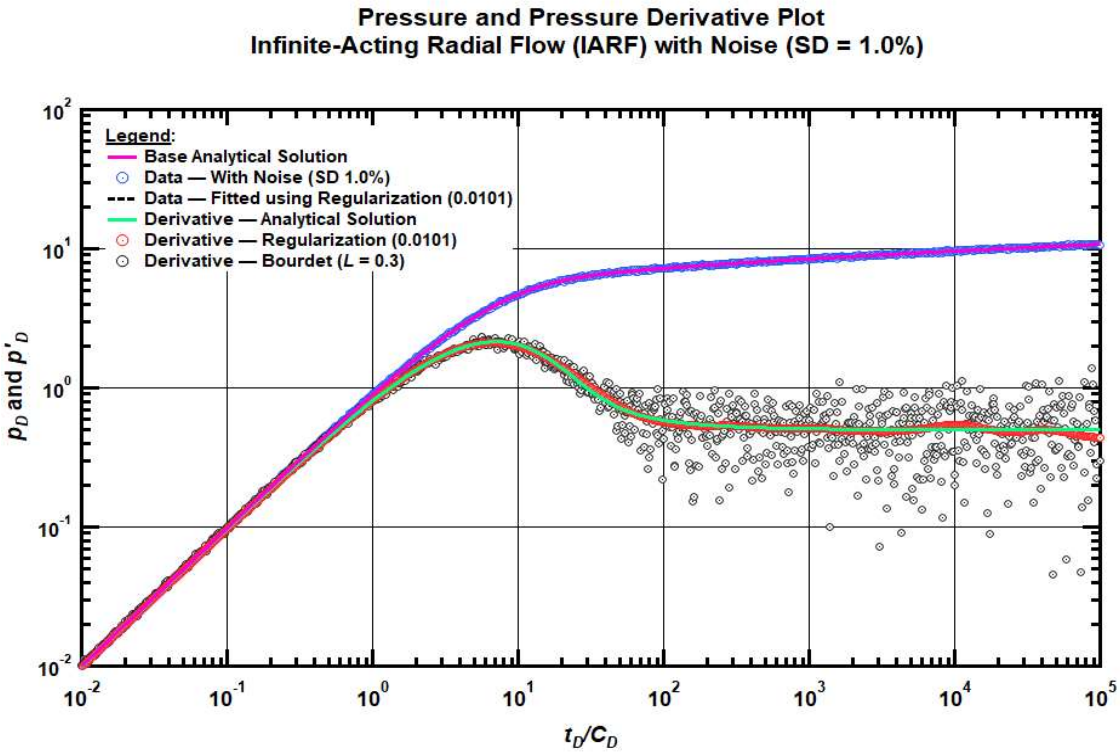

Fig. E. 7 — Pressure and pressure derivative plot for a vertical well in an infinite-acting reservoir with wellbore storage and skin case with noise standard deviation at 1.0%. Bourdet L value = 0.3.

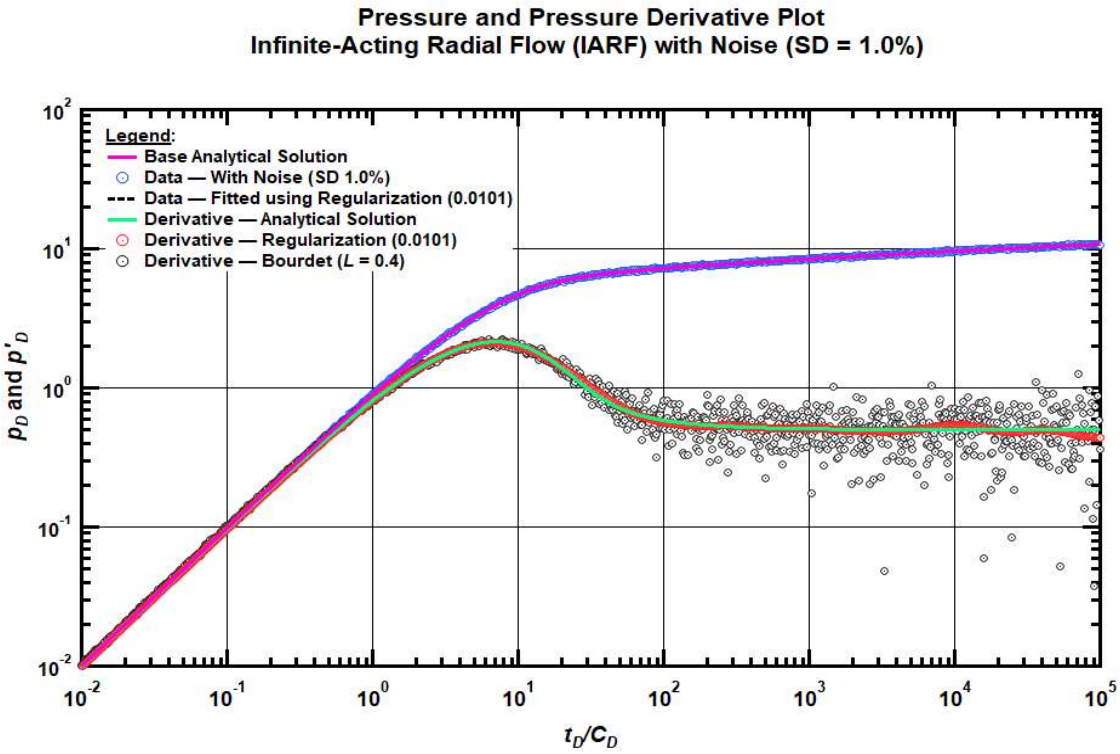

Fig. E. 8 — Pressure and pressure derivative plot for a vertical well in an infinite-acting reservoir with wellbore storage and skin case with noise standard deviation at 1.0%. Bourdet L value = 0.4.

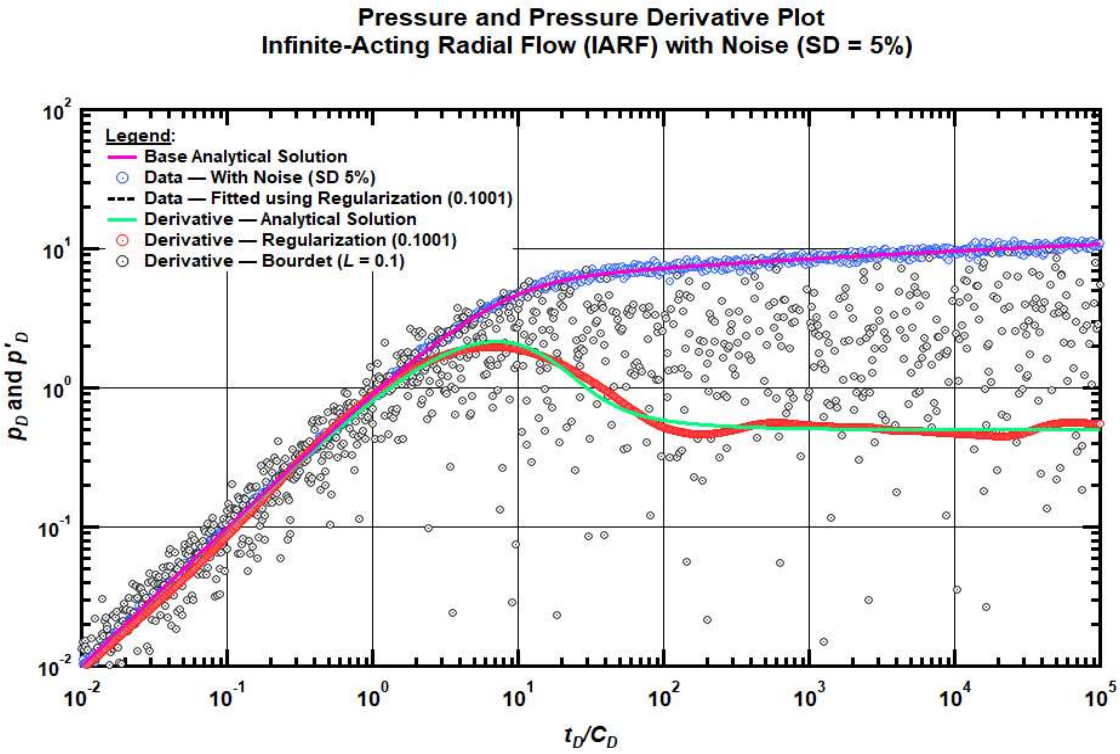

Fig. E. 9 — Pressure and pressure derivative plot for a vertical well in an infinite-acting reservoir with wellbore storage and skin case with noise standard deviation at 5.0%. Bourdet L value = 0.1.

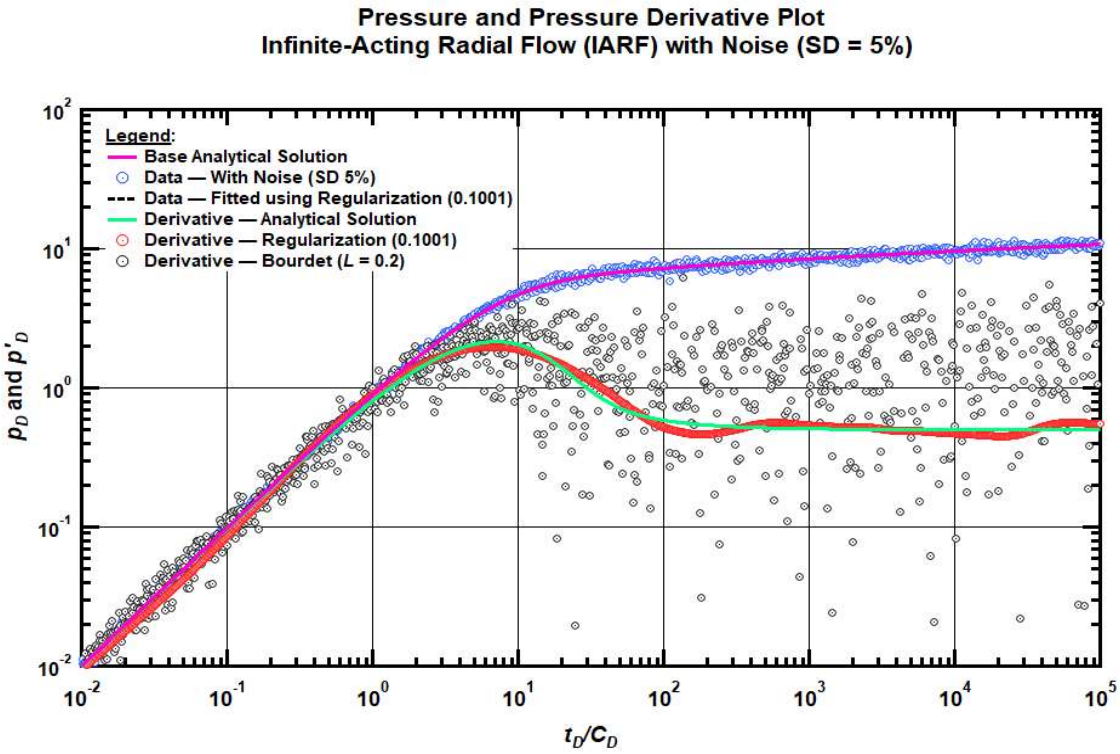

Fig. E. 10 — Pressure and pressure derivative plot for a vertical well in an infinite-acting reservoir with wellbore storage and skin case with noise standard deviation at 5.0%. Bourdet L value = 0.2.

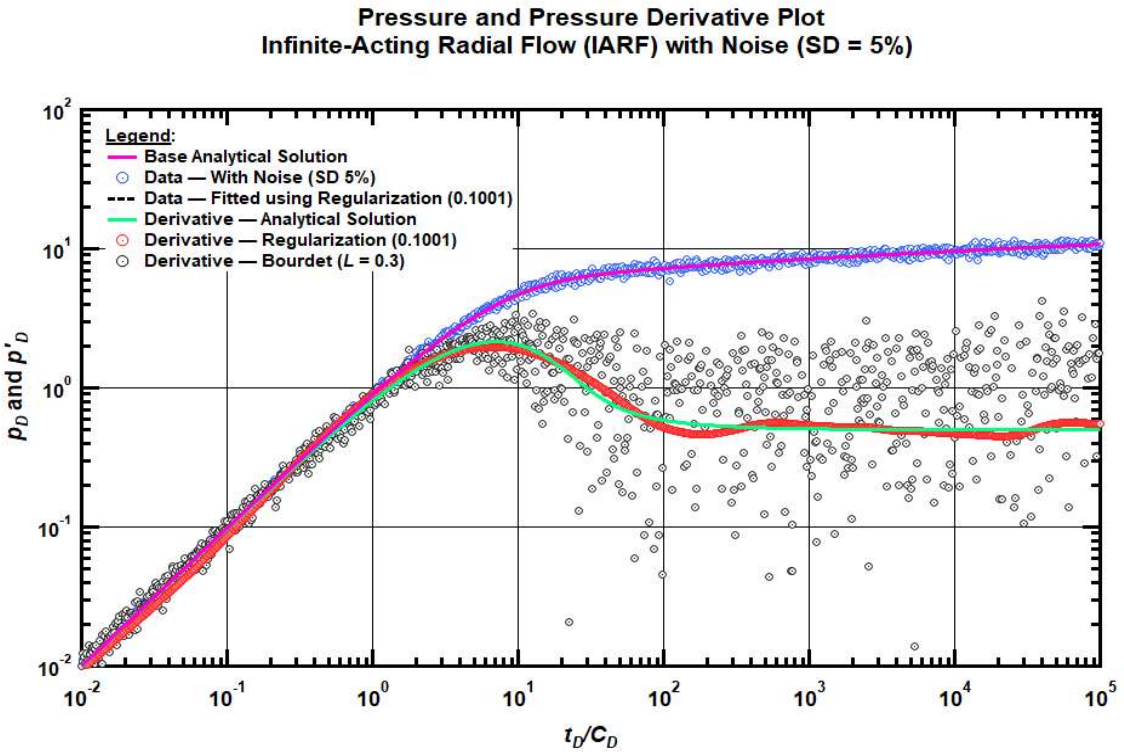

Fig. E. 11 — Pressure and pressure derivative plot for a vertical well in an infinite-acting reservoir with wellbore storage and skin case with noise standard deviation at 5.0%. Bourdet L value = 0.3.

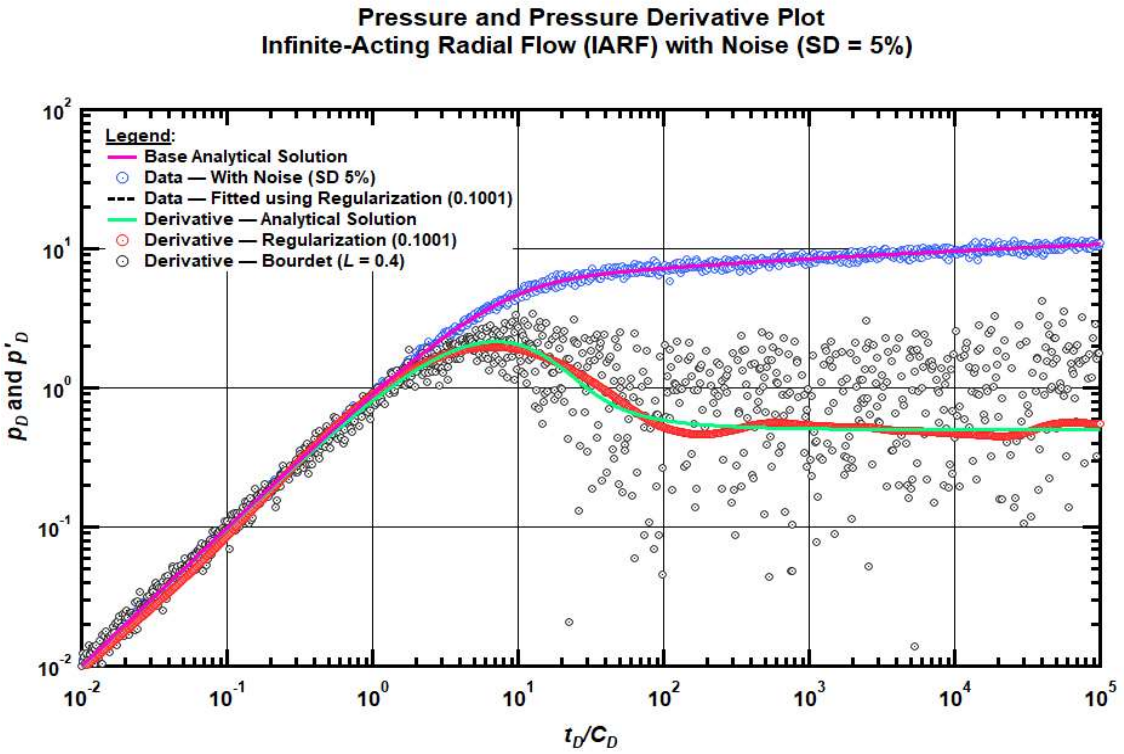

Fig. E. 12 — Pressure and pressure derivative plot for a vertical well in an infinite-acting reservoir with wellbore storage and skin case with noise standard deviation at 5.0%. Bourdet L value = 0.4.

A vertical well in an infinite-acting without wellbore storage and skin in naturally fractured reservoir system (dual porosity - DUAL)

The result for a vertical well in an infinite-acting without wellbore storage and skin in naturally fractured reservoir system is shown in **Fig. E. 13** to **Fig. E. 24**.

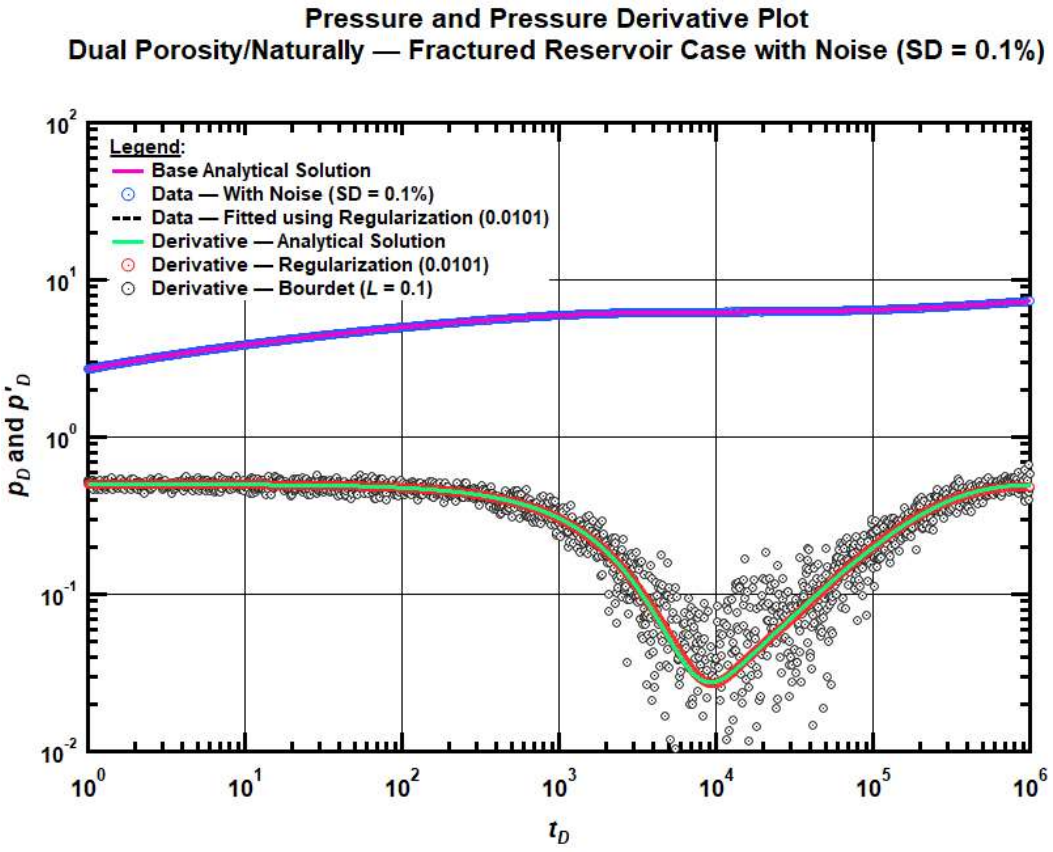

Fig. E. 13 — Pressure and pressure derivative plot for a vertical well in an infinite-acting without wellbore storage and skin in naturally fractured reservoir system case with noise standard deviation at 0.1%. Bourdet L value = 0.1.

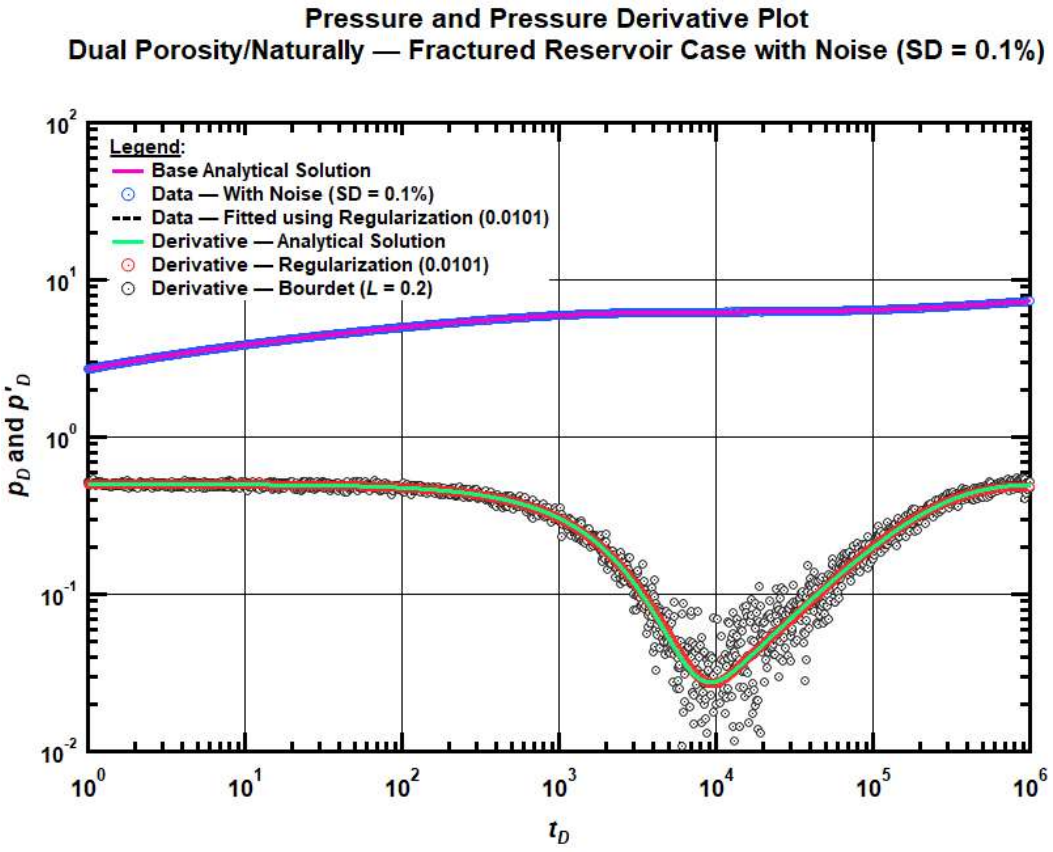

Fig. E. 14 — Pressure and pressure derivative plot for a vertical well in an infinite-acting without wellbore storage and skin in naturally fractured reservoir system case with noise standard deviation at 0.1%. Bourdet L value = 0.2.

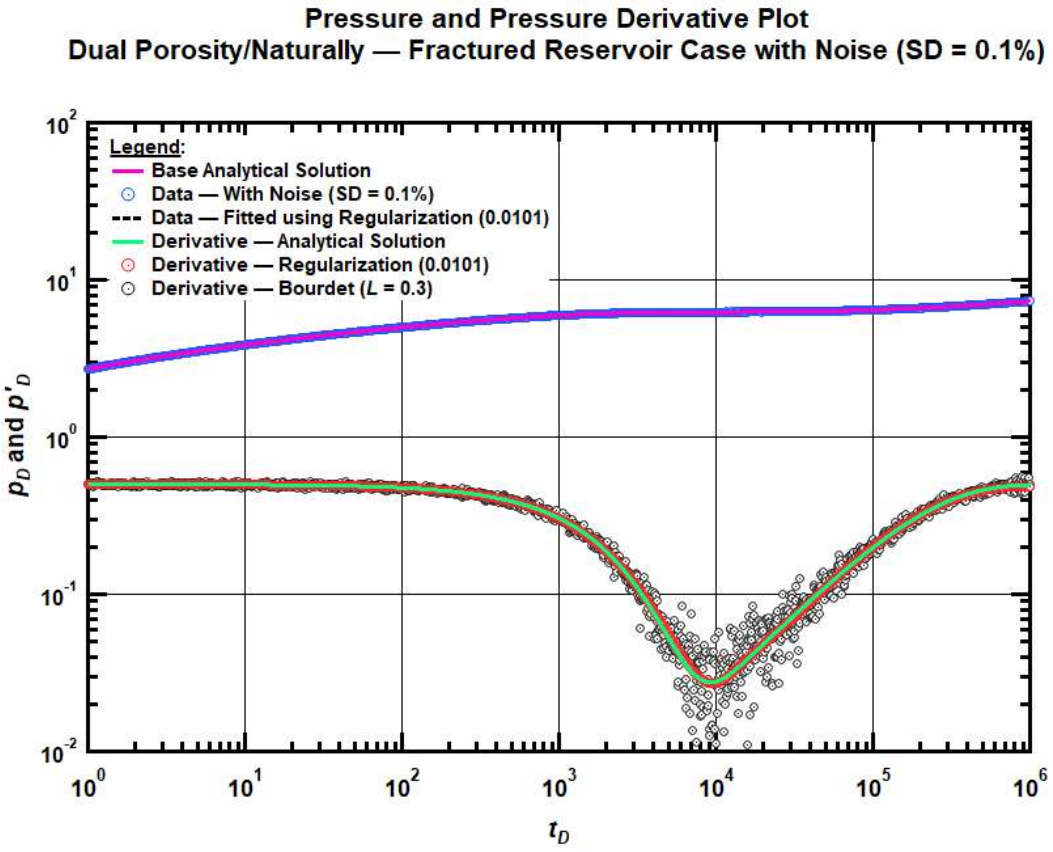

Fig. E. 15 — Pressure and pressure derivative plot for a vertical well in an infinite-acting without wellbore storage and skin in naturally fractured reservoir system case with noise standard deviation at 0.1%. Bourdet L value = 0.3.

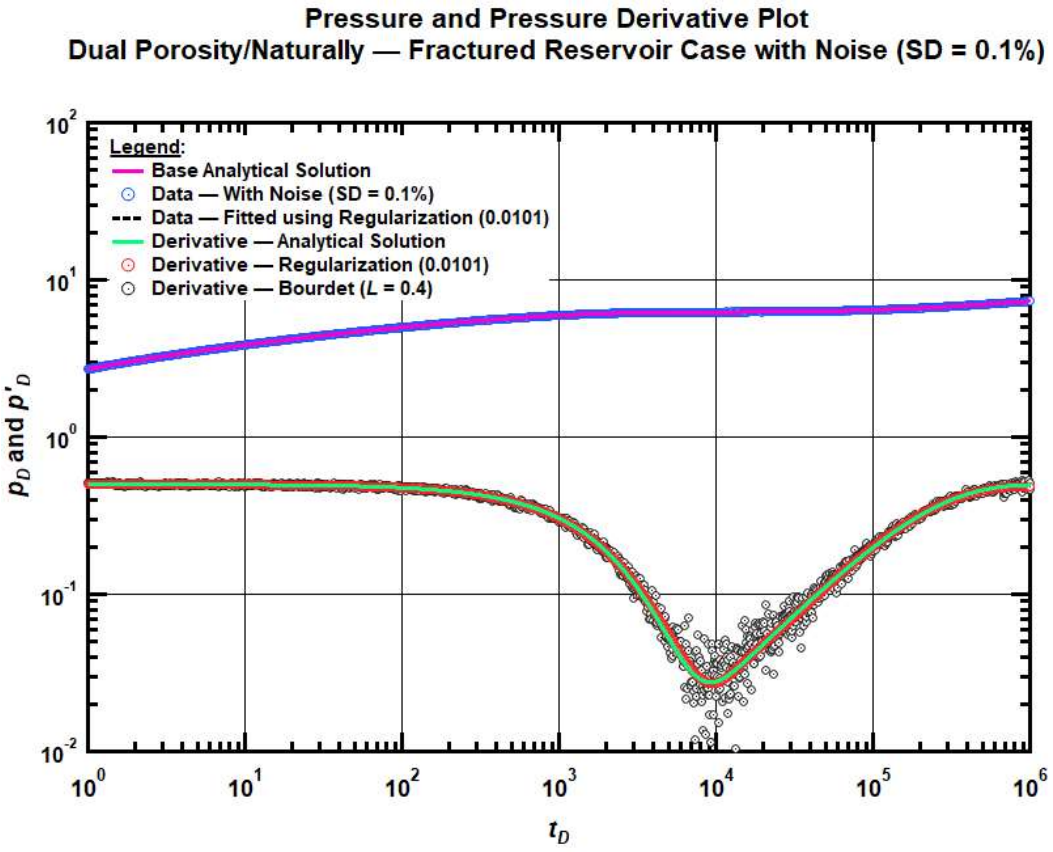

Fig. E. 16 — Pressure and pressure derivative plot for a vertical well in an infinite-acting without wellbore storage and skin in naturally fractured reservoir system case with noise standard deviation at 0.1%. Bourdet L value = 0.4.

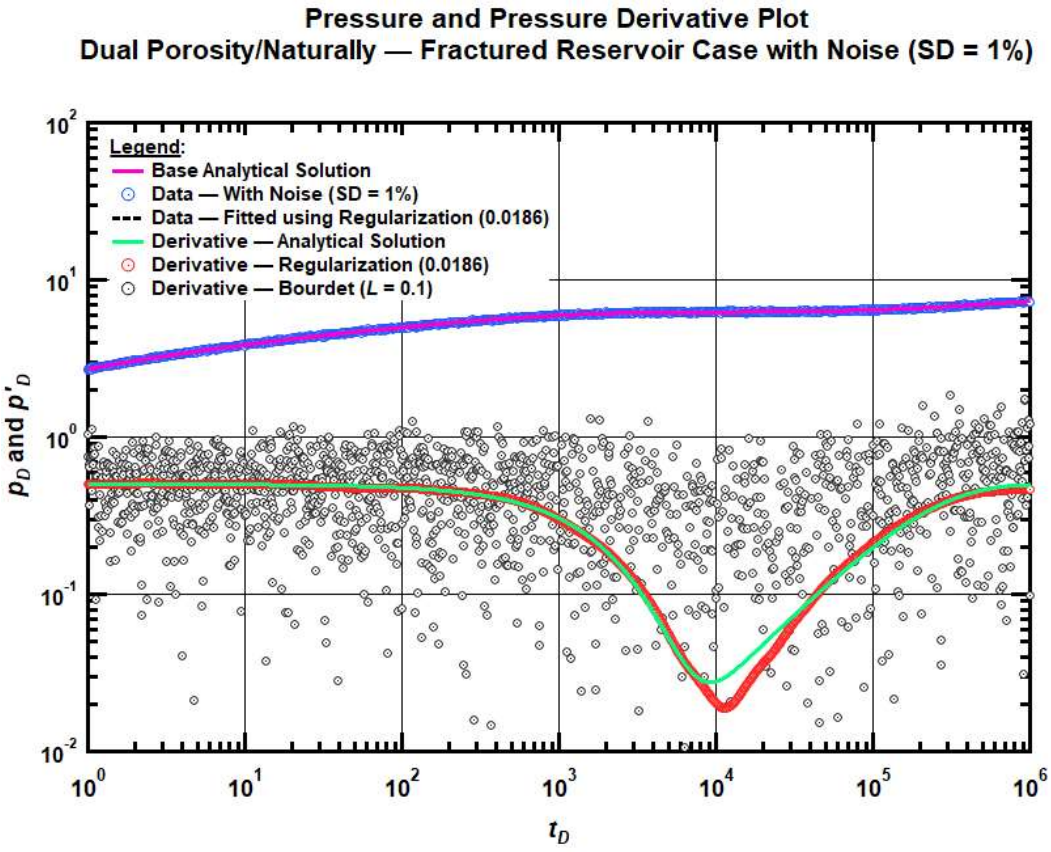

Fig. E. 17 — Pressure and pressure derivative plot for a vertical well in an infinite-acting without wellbore storage and skin in naturally fractured reservoir system case with noise standard deviation at 1.0%. Bourdet L value = 0.1.

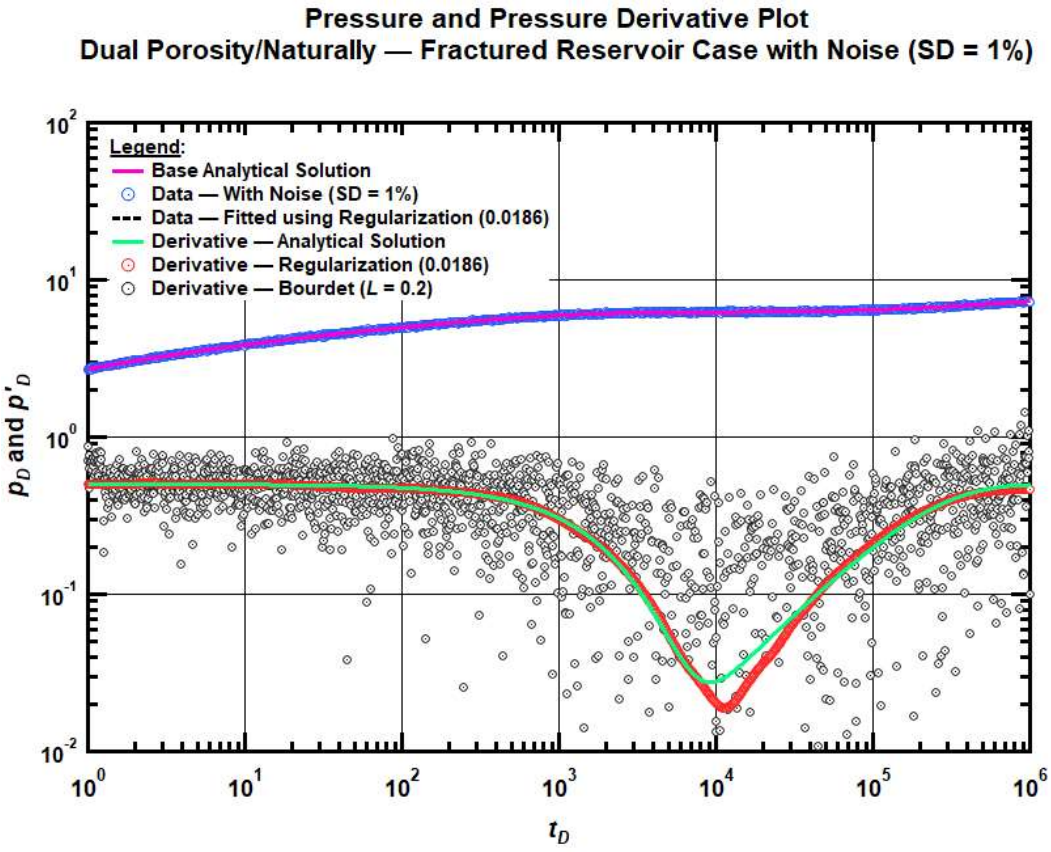

Fig. E. 18 — Pressure and pressure derivative plot for a vertical well in an infinite-acting without wellbore storage and skin in naturally fractured reservoir system case with noise standard deviation at 1.0%. Bourdet L value = 0.2.

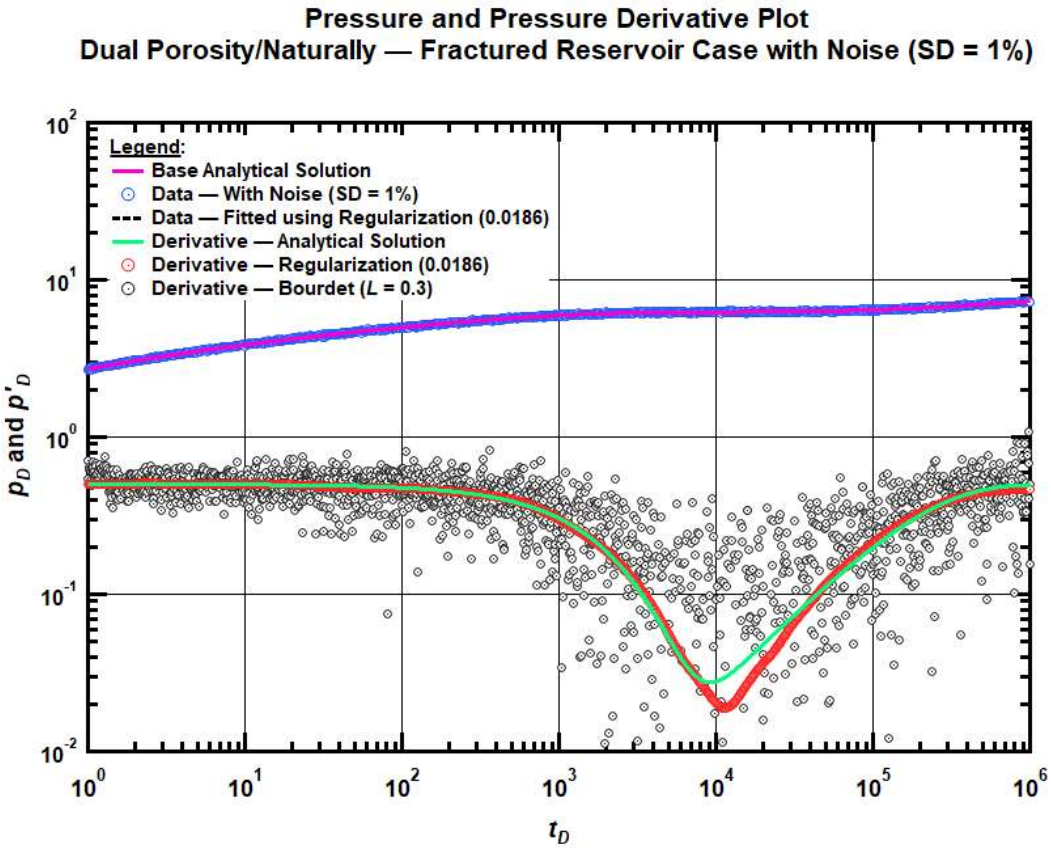

Fig. E. 19 — Pressure and pressure derivative plot for a vertical well in an infinite-acting without wellbore storage and skin in naturally fractured reservoir system case with noise standard deviation at 1.0%. Bourdet L value = 0.3.

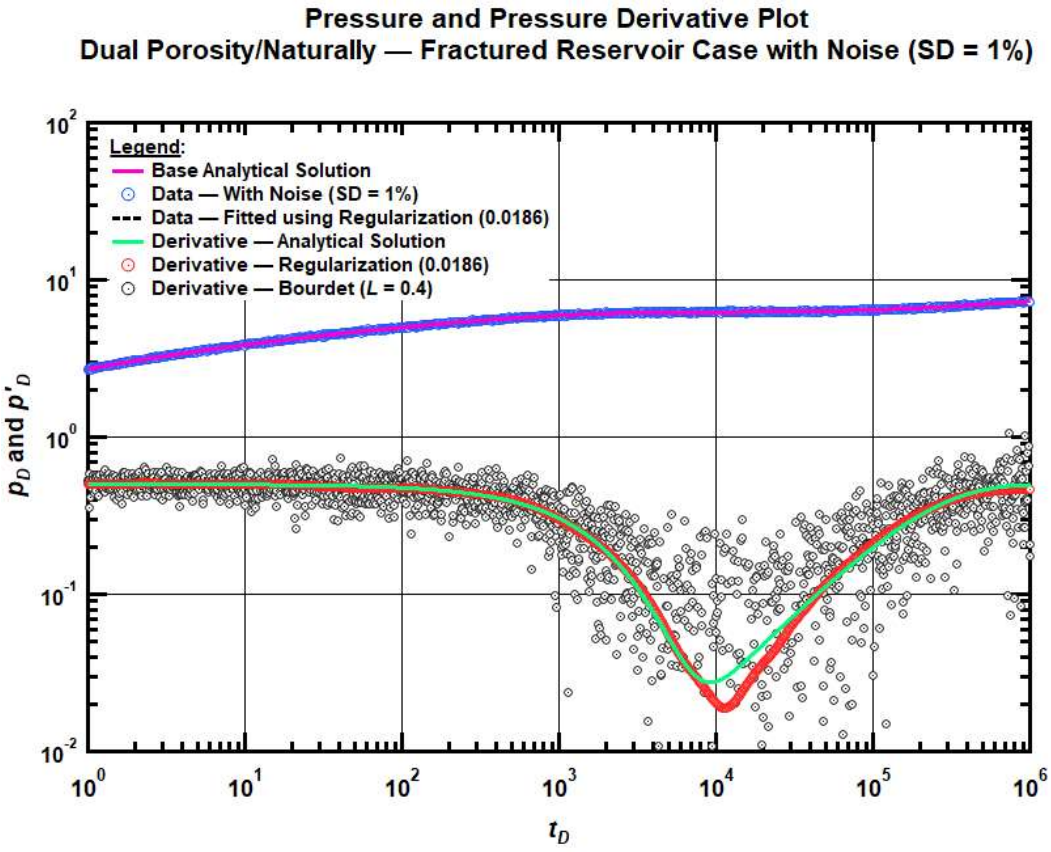

Fig. E. 20 — Pressure and pressure derivative plot for a vertical well in an infinite-acting without wellbore storage and skin in naturally fractured reservoir system case with noise standard deviation at 1.0%. Bourdet L value = 0.4.

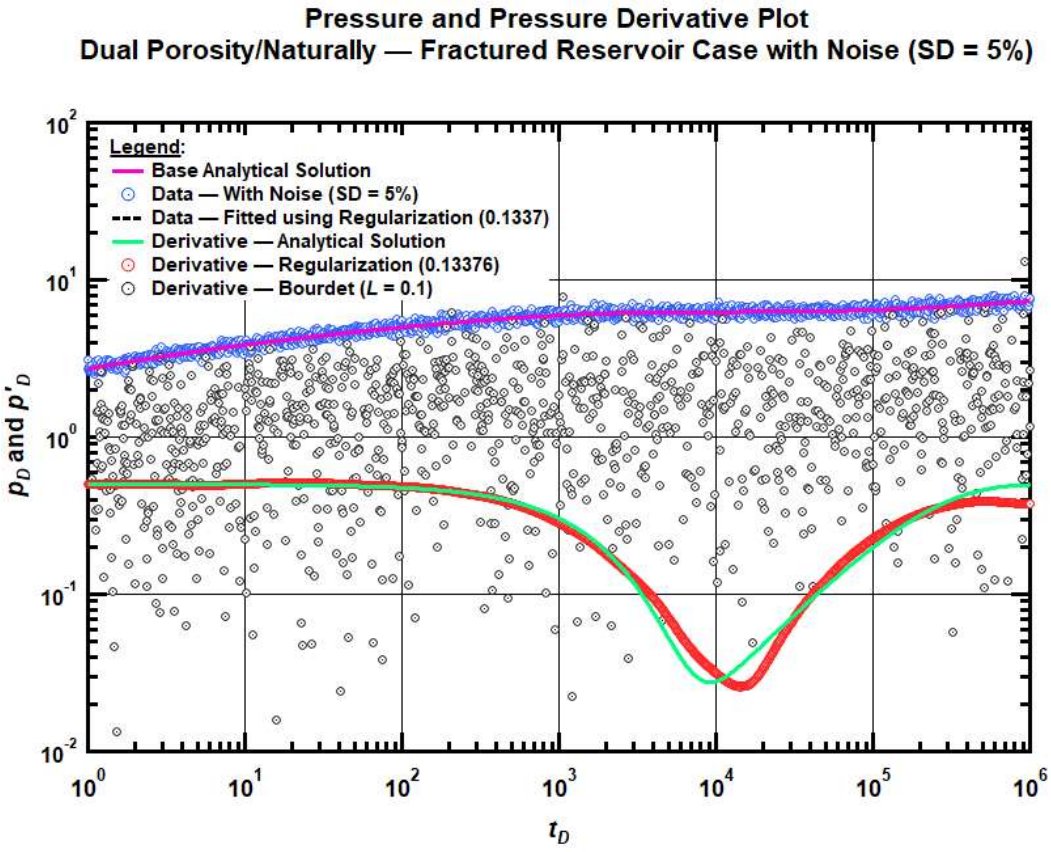

Fig. E. 21 — Pressure and pressure derivative plot for a vertical well in an infinite-acting without wellbore storage and skin in naturally fractured reservoir system case with noise standard deviation at 5.0%. Bourdet L value = 0.1.

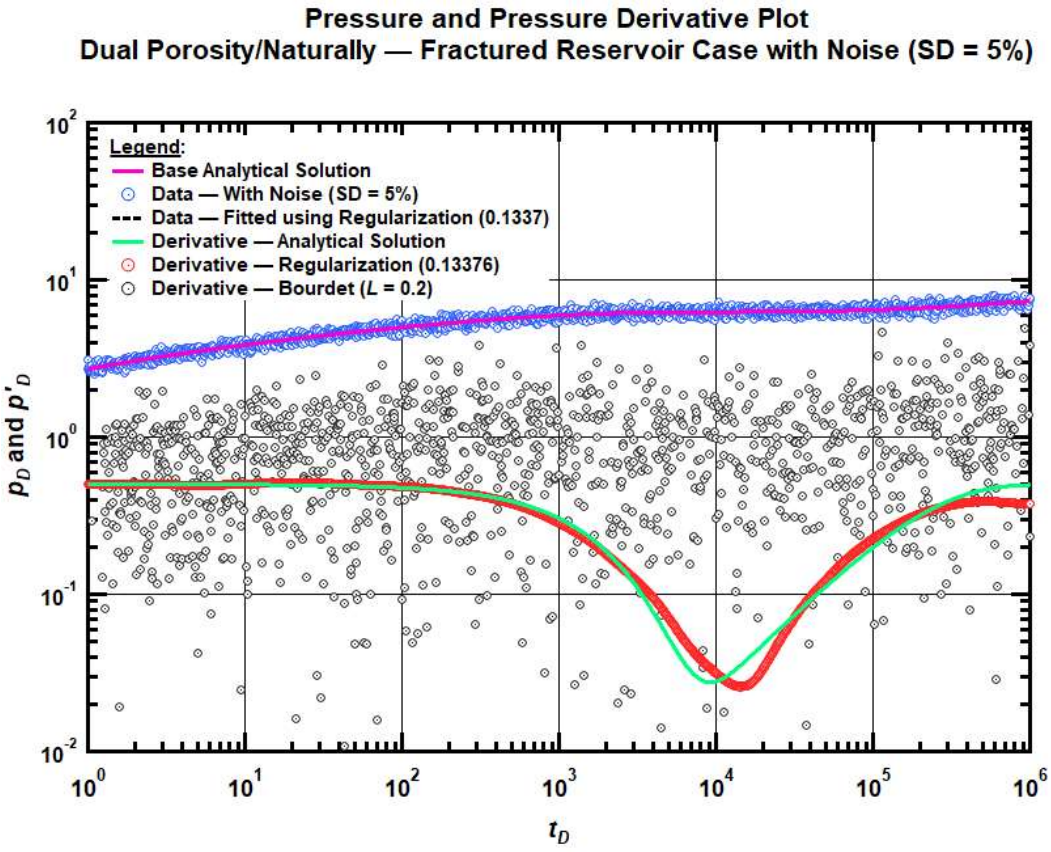

Fig. E. 22 — Pressure and pressure derivative plot for a vertical well in an infinite-acting without wellbore storage and skin in naturally fractured reservoir system case with noise standard deviation at 5.0%. Bourdet L value = 0.2.

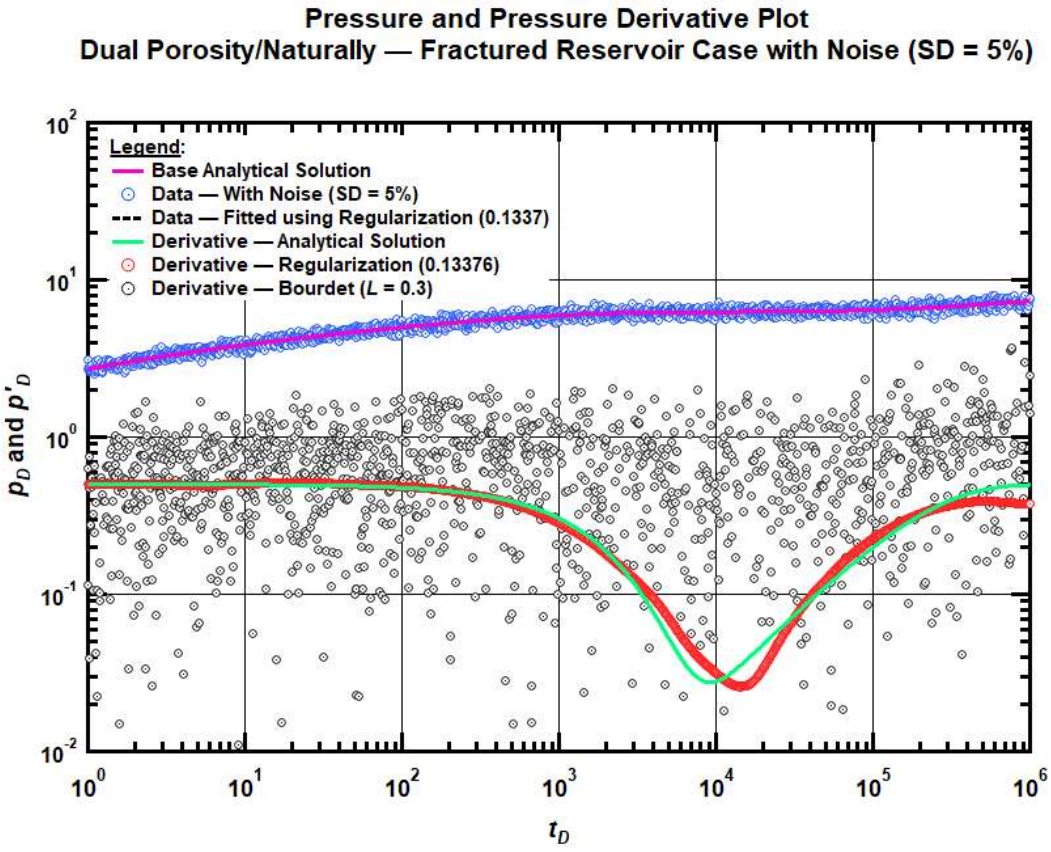

Fig. E. 23 — Pressure and pressure derivative plot for a vertical well in an infinite-acting without wellbore storage and skin in naturally fractured reservoir system case with noise standard deviation at 5.0%. Bourdet L value = 0.3.

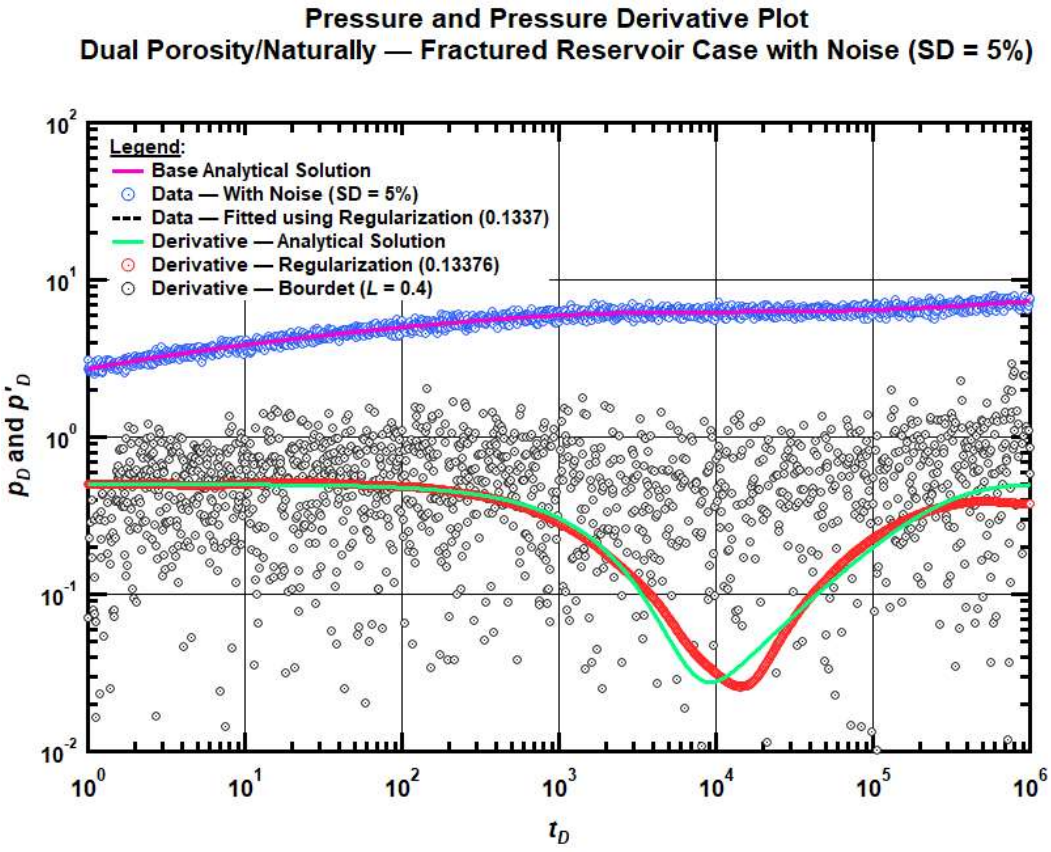

Fig. E. 24 — Pressure and pressure derivative plot for a vertical well in an infinite-acting without wellbore storage and skin in naturally fractured reservoir system case with noise standard deviation at 5.0%. Bourdet L value = 0.4.

A hydraulically fractured vertical well with an infinite fracture conductivity in an infinite-acting reservoir without wellbore storage and skin (HF)

The result for a hydraulically fractured vertical well with an infinite fracture conductivity in an infinite-acting reservoir without wellbore storage and skin is shown in **Fig. 25** to **Fig. E. 36**.

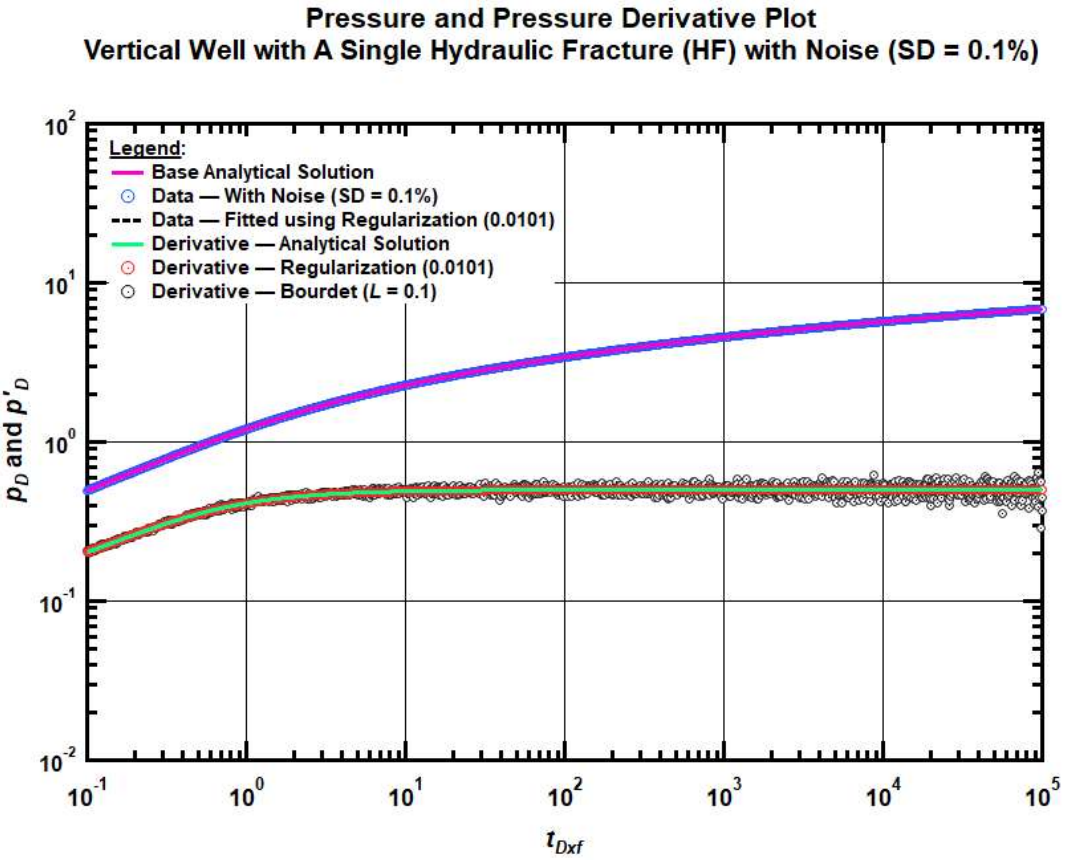

Fig. E. 25 — Pressure and pressure derivative plot for a hydraulically fractured vertical well with an infinite fracture conductivity in an infinite-acting reservoir without wellbore storage and skin case with noise standard deviation at 0.1%**.** Bourdet L value = 0.1.

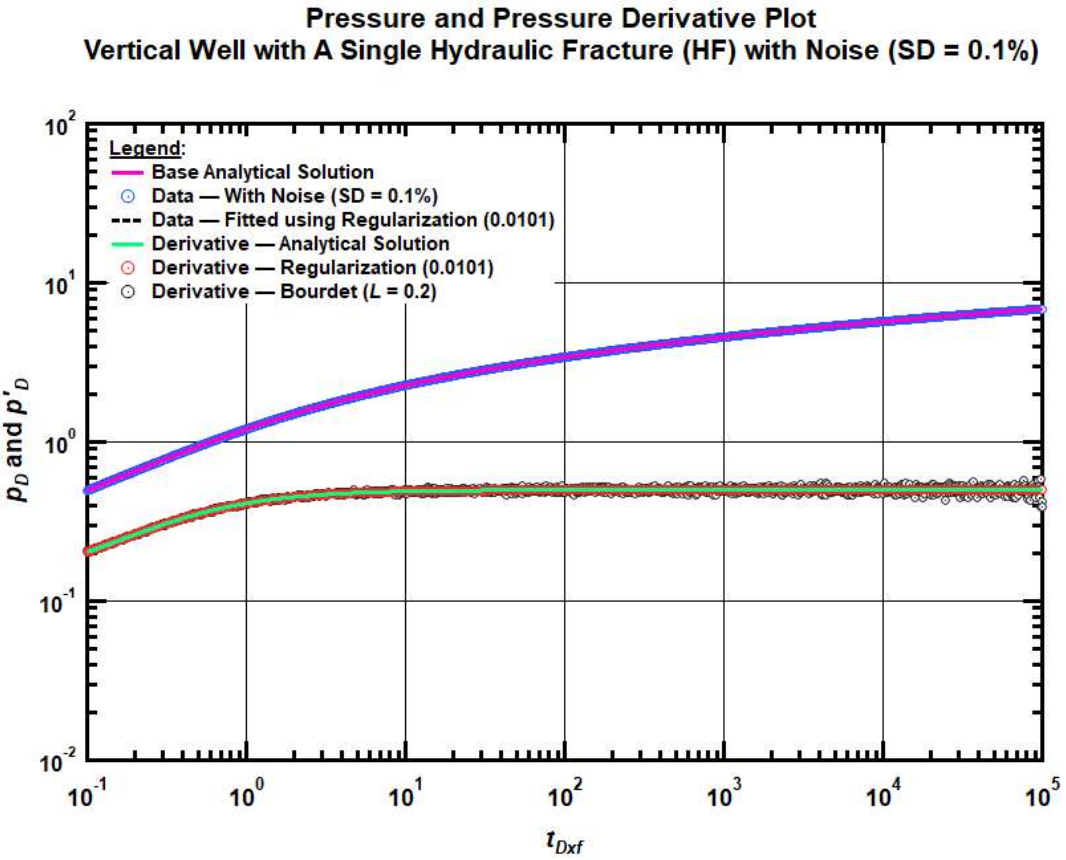

Fig. E. 26 — Pressure and pressure derivative plot for a hydraulically fractured vertical well with an infinite fracture conductivity in an infinite-acting reservoir without wellbore storage and skin case with noise standard deviation at 0.1%**.** Bourdet L value = 0.2.

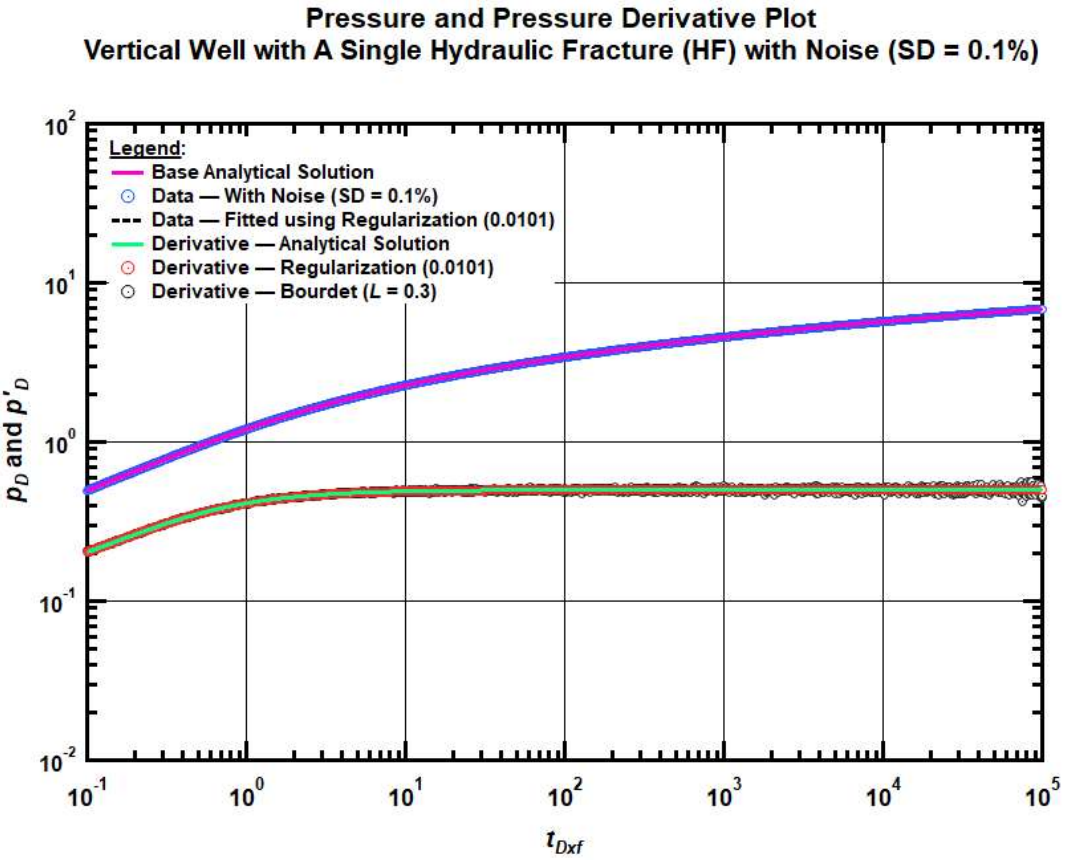

Fig. E. 27 — Pressure and pressure derivative plot for a hydraulically fractured vertical well with an infinite fracture conductivity in an infinite-acting reservoir without wellbore storage and skin case with noise standard deviation at 0.1%**.** Bourdet L value = 0.3.

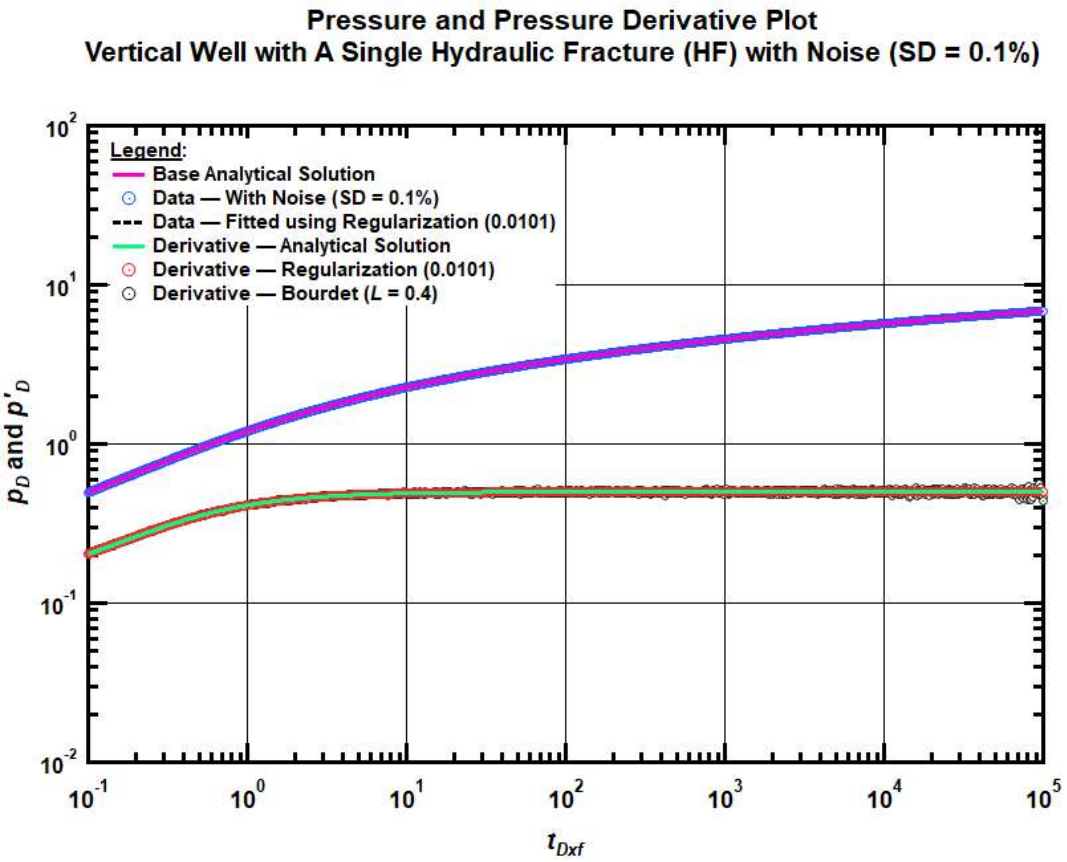

Fig. E. 28 — Pressure and pressure derivative plot for a hydraulically fractured vertical well with an infinite fracture conductivity in an infinite-acting reservoir without wellbore storage and skin case with noise standard deviation at 0.1%**.** Bourdet L value = 0.4.

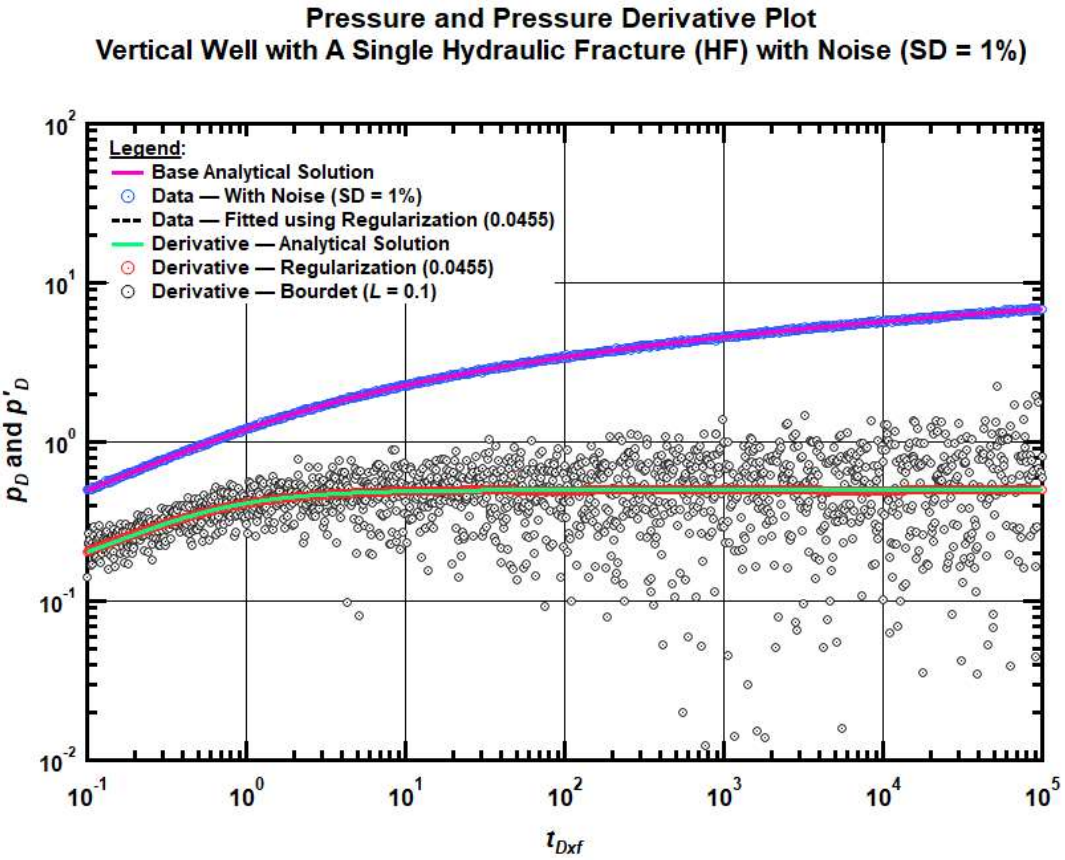

Fig. E. 29 — Pressure and pressure derivative plot for a hydraulically fractured vertical well with an infinite fracture conductivity in an infinite-acting reservoir without wellbore storage and skin case with noise standard deviation at 1.0%**.** Bourdet L value = 0.1.

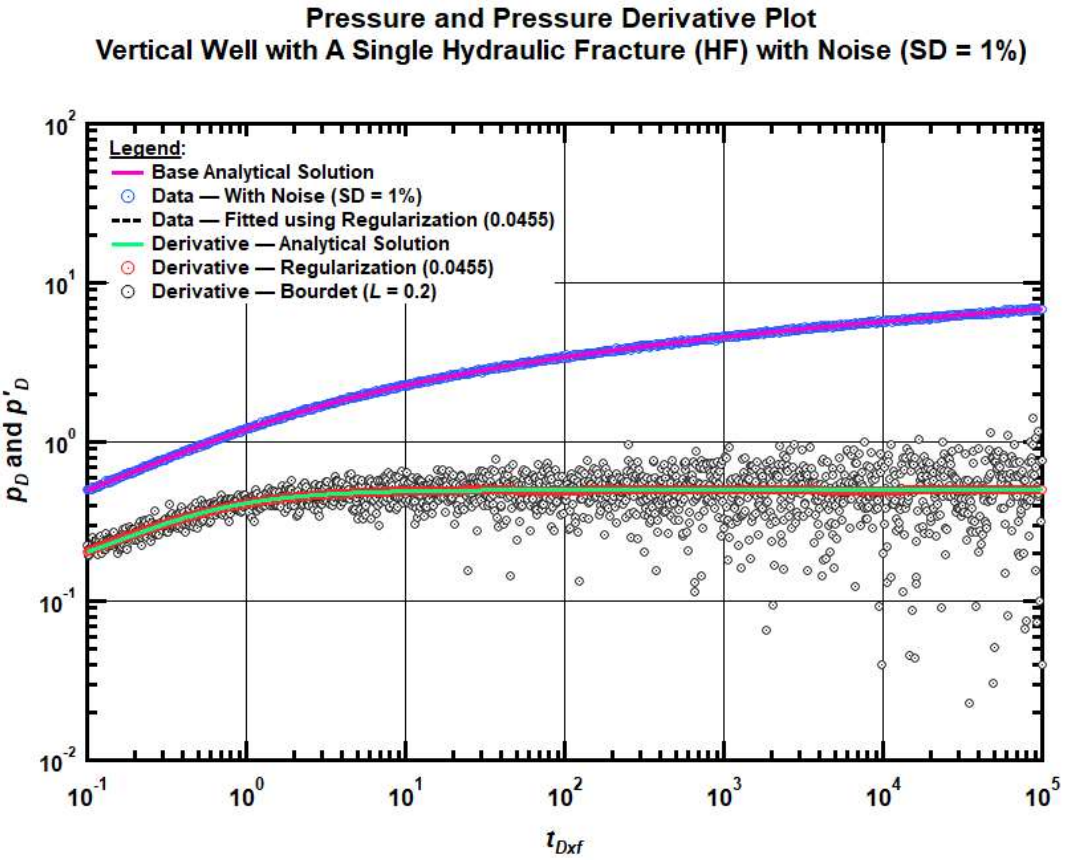

Fig. E. 30 — Pressure and pressure derivative plot for a hydraulically fractured vertical well with an infinite fracture conductivity in an infinite-acting reservoir without wellbore storage and skin case with noise standard deviation at 1.0%**.** Bourdet L value = 0.2.

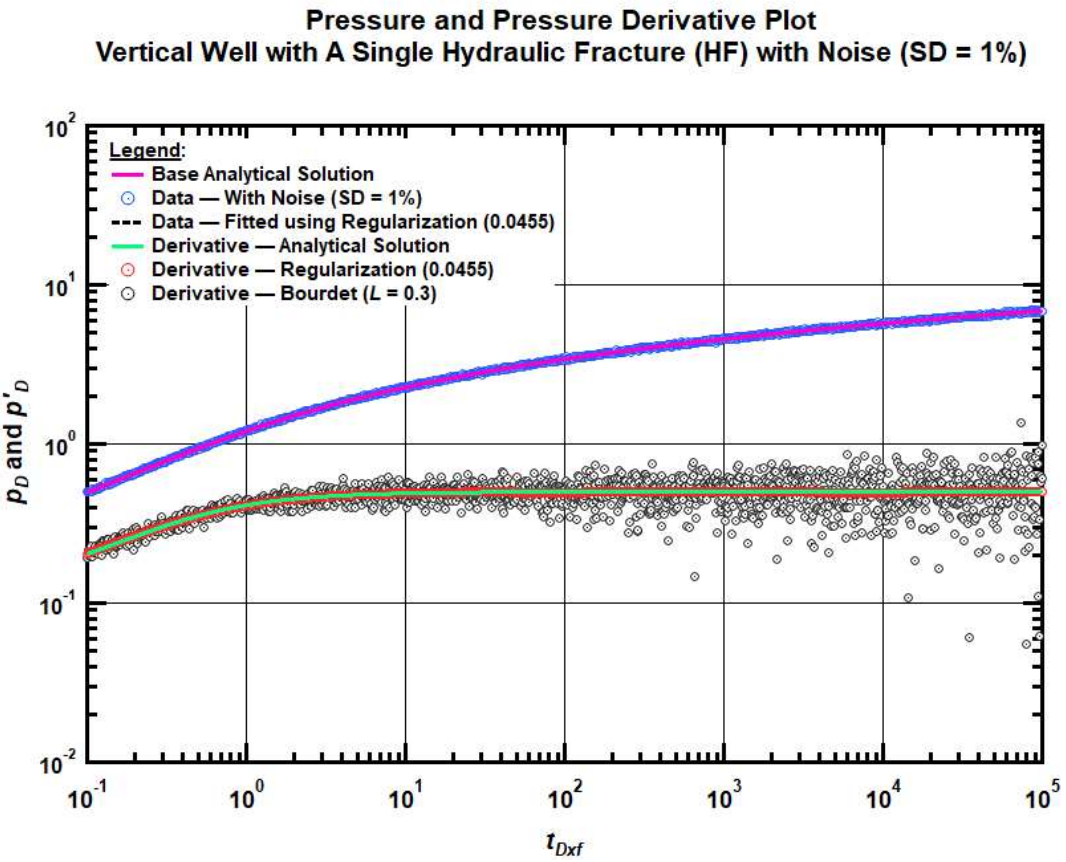

Fig. E. 31 — Pressure and pressure derivative plot for a hydraulically fractured vertical well with an infinite fracture conductivity in an infinite-acting reservoir without wellbore storage and skin case with noise standard deviation at 1.0%**.** Bourdet L value = 0.3.

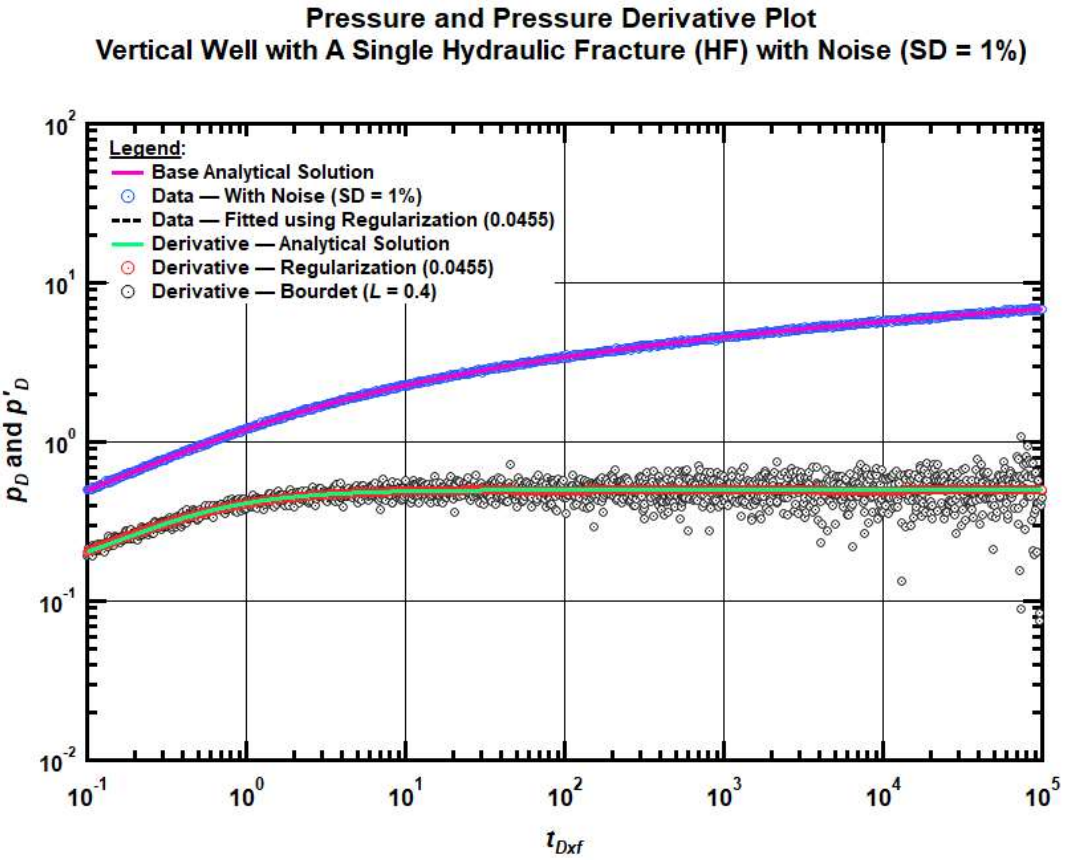

Fig. E. 32 — Pressure and pressure derivative plot for a hydraulically fractured vertical well with an infinite fracture conductivity in an infinite-acting reservoir without wellbore storage and skin case with noise standard deviation at 1.0%**.** Bourdet L value = 0.4.

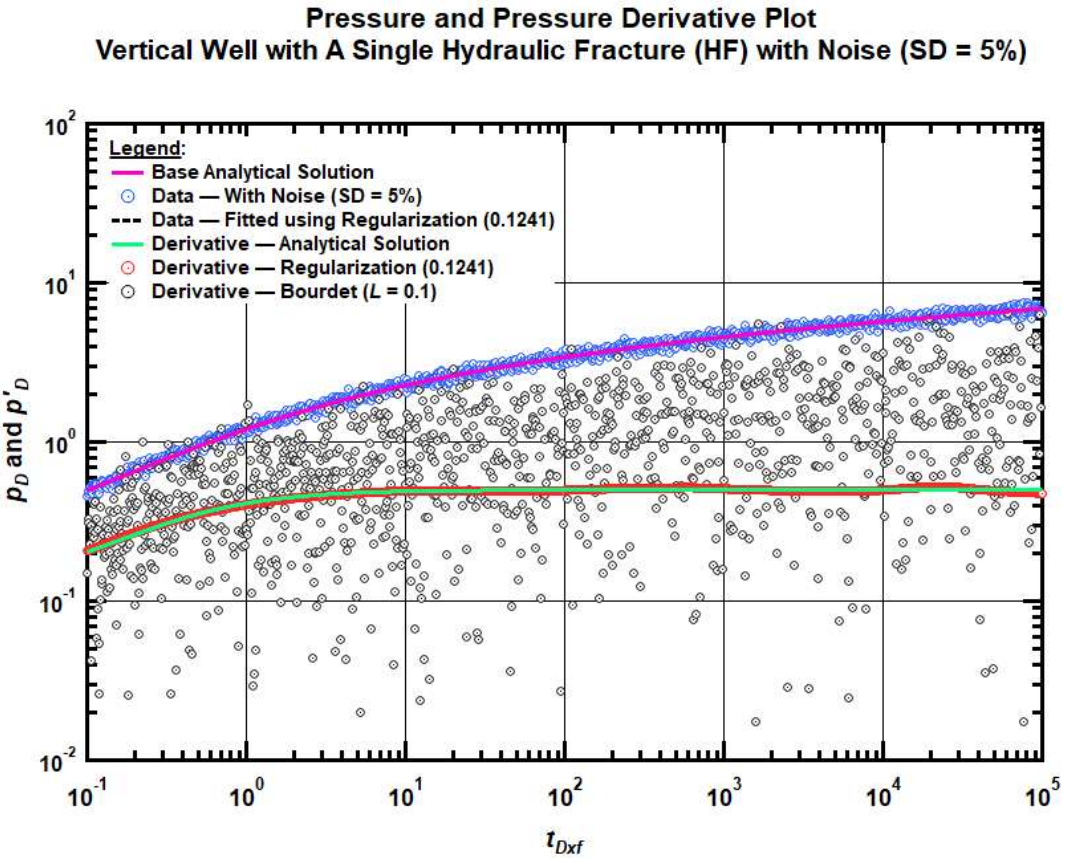

Fig. E. 33 — Pressure and pressure derivative plot for a hydraulically fractured vertical well with an infinite fracture conductivity in an infinite-acting reservoir without wellbore storage and skin case with noise standard deviation at 5.0%**.** Bourdet L value = 0.1.

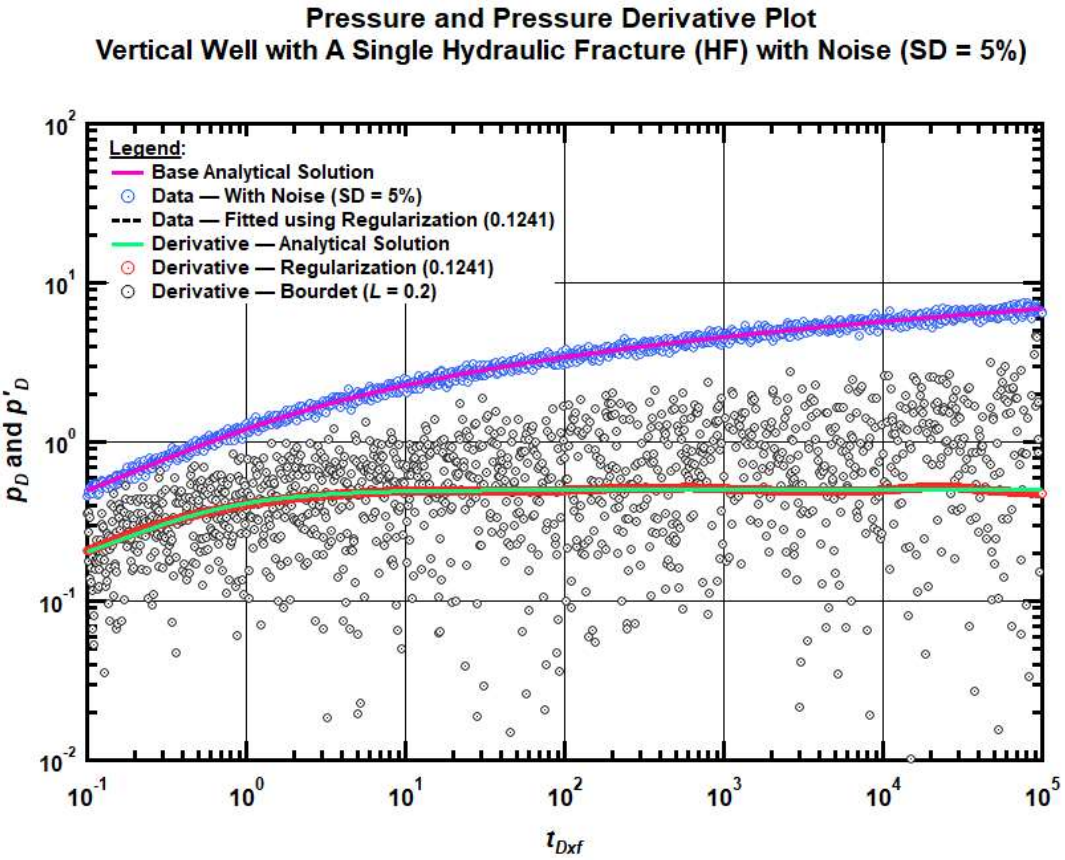

Fig. E. 34 — Pressure and pressure derivative plot for a hydraulically fractured vertical well with an infinite fracture conductivity in an infinite-acting reservoir without wellbore storage and skin case with noise standard deviation at 5.0%**.** Bourdet L value = 0.2.

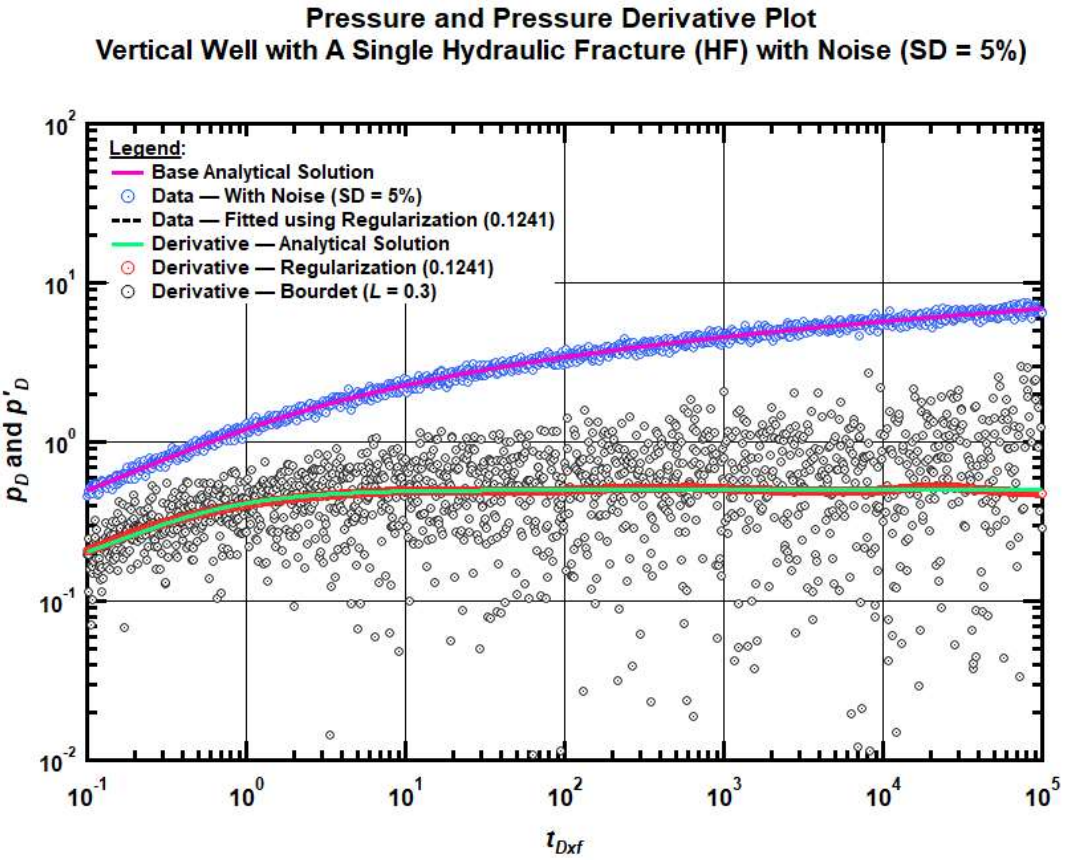

Fig. E. 35 — Pressure and pressure derivative plot for a hydraulically fractured vertical well with an infinite fracture conductivity in an infinite-acting reservoir without wellbore storage and skin case with noise standard deviation at 5.0%**.** Bourdet L value = 0.3.

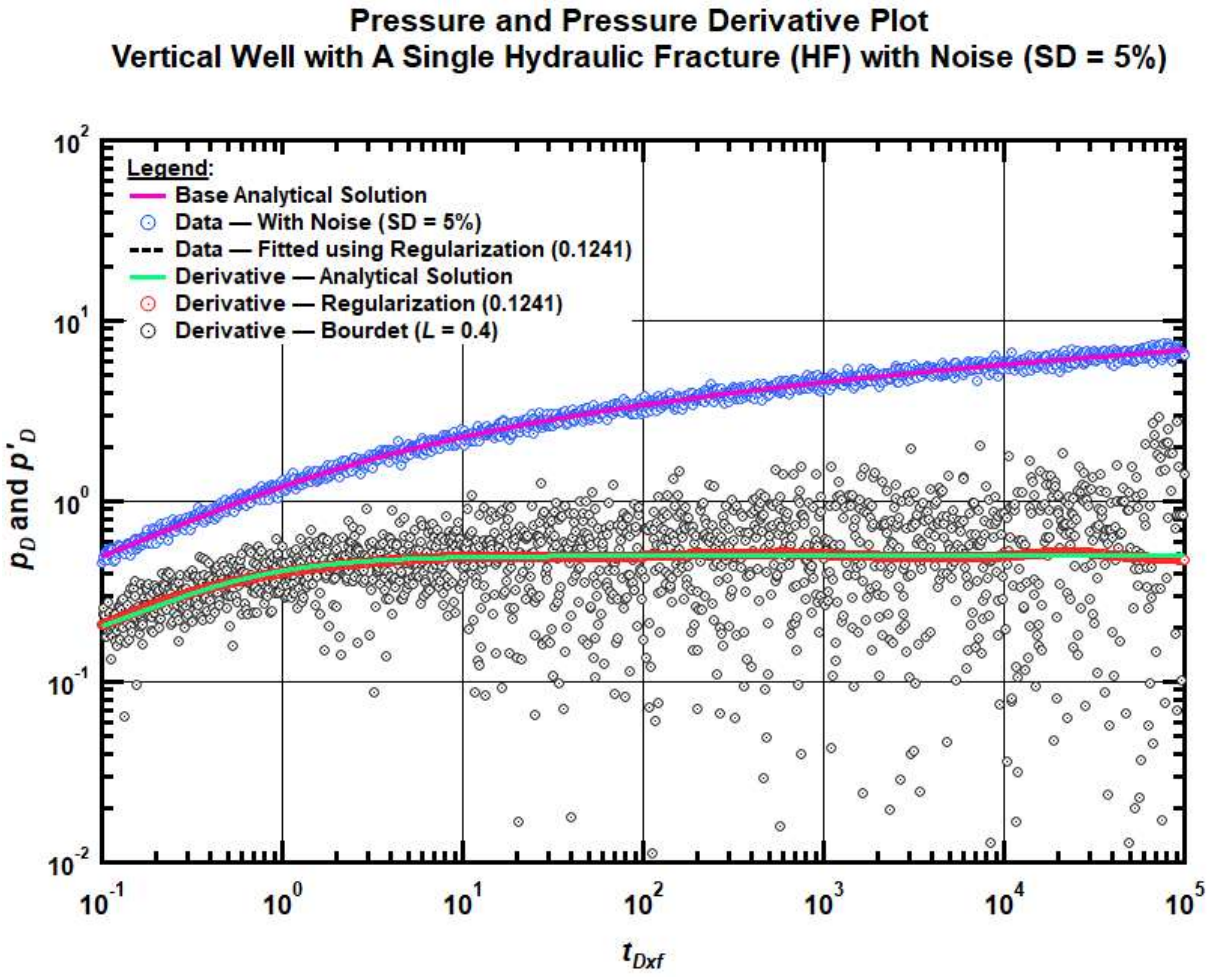

Fig. E. 36 — Pressure and pressure derivative plot for a hydraulically fractured vertical well with an infinite fracture conductivity in an infinite-acting reservoir without wellbore storage and skin case with noise standard deviation at 5.0%**.** Bourdet L value = 0.4.